CHARACTERIZATION OF FAM134B IN THE CONTEXT OF HEPATOCELLULAR CARCINOMA AND ENDOPLASMIC RETICULUM STRESS

A THESIS SUBMITTED TO
THE DEPARTMENT OF MOLECULAR BIOLOGY AND GENETICS
AND THE GRADUATE SCHOOL OF ENGINEERING AND SCIENCE OF
BILKENT UNIVERSITY
IN PARTIAL FULFILLMENT OF THE REQUIREMENTS
FOR THE DEGREE OF
MASTER OF SCIENCE

BY
MUSTAFA YILMAZ
AUGUST 2011

I certify that I have read this thesis and that in my opinion it is fully adequate, in scope and in quality, as a thesis for the degree of Master of Science.

Prof. Dr. Mehmet Öztürk

I certify that I have read this thesis and that in my opinion it is fully adequate, in scope and in quality, as a thesis for the degree of Master of Science.

Assist. Prof. Dr. Ebru Erbay

I certify that I have read this thesis and that in my opinion it is fully adequate, in scope and in quality, as a thesis for the degree of Master of Science.

Assist. Prof. Dr. Petek Ballar

Approved for the Graduate School of Engineering and Science

Director of Graduate School of
Engineering and Science
Prof. Dr. Levent Onural

ABSTRACT

CHARACTERIZATION OF FAM134B IN THE CONTEXT OF HEPATOCELLULAR CARCINOMA AND ENDOPLASMIC RETICULUM STRESS

Mustafa Yılmaz
M.Sc. in Molecular Biology and Genetics
Supervisor: Prof. Dr. Mehmet Öztürk
August 2011, 98 Pages

Family with sequence similarity 134, member B (FAM134B) is a replicative senescence associated gene, previously identified in studies of our group as a result of microarray analysis in spontaneously senescent clones of Huh7 hepatocellular carcinoma cell line and their immortal counterparts. Originating from this finding, this study primarily focused on characterization of FAM134B in the context of hepatocellular carcinoma and endoplasmic reticulum stress. At the beginning, the relationship between senescence and FAM134B was experimented by inducing premature senescence in Huh7 cells. Adriamycin or TGF-β induced premature senescence did not result in amplification of FAM134B gene expression, suggesting that upregulation of FAM134B expression in spontaneous replicative senescence is not directly associated with a senescence phenotype. Then, FAM134B mRNA and protein levels were analyzed in both well- and poorly-differentiated HCC cell lines. Results showed that FAM134B expression is greater in poorly-differentiated cell lines, which represent advanced and metastatic HCC in vitro. On the other hand, our studies on the relationship between FAM134B and endoplasmic reticulum (ER) stress showed that FAM134B is an ER stress response gene, whose expression is upregulated by induction of ER stress with chemicals, such as thapsigargin, tunicamycin or DTT. Therefore, high protein and mRNA levels of FAM134B in poorly-differentiated cell lines are linked to the presence of a basal level ER stress response in this group of cell lines. Furthermore, overexpression studies in Huh7 cells indicated that FAM134B cannot trigger an ER stress response or autophagic response in these cells. However, FAM134B was detected as an effector in cellular response, when ER stress is artificially induced by thapsigargin or tunicamycin treatments. FAM13B4 overexpression in Huh7 resulted in increased sensitivity to

thapsigargin or tunicamycin induced apoptosis. Moreover, increased FAM134B expression was also associated with decreased proliferative capacity in response to ER stress induction with the same chemicals. Consequently, FAM134B was suggested to affect the severity of stress in the ER when ER stress is started with an inducer. In addition, our tissue based experiments revealed that FAM134B is expressed in the brain and liver. Taken together, FAM134B might be an important protein contributing to the liver tissue damage and pathogenesis of HCC.

ÖZET

FAM134B'NİN KARACİĞER KANSERİ VE ENDOPLAZMİK RETİKULUM STRESİ KONULARINDAKi ÖZELLİKLERİNİN BELİRLENMESİ

Mustafa Yılmaz
Moleküler Biyoloji ve Genetik Yüksek Lisansı
Tez Yöneticisi: Prof. Dr. Mehmet Öztürk
Ağustos 2011, 98 Sayfa

FAM134B (Family with sequence similarity 134, member B)'nin daha önceki çalışmalarımızda Huh7 karaciğer kanseri hücre hattında kendiliğinden gelişen hücre yaşlanmasında yapılan gen ifade profilleri analizi sonucunda hücre yaşlanmasıyla ilgili olduğunu tespit ettik. Bu bilgiden yola çıkarak bu çalışmada özellikle FAM134B'nin karaciğer kanseri ve endoplazmik retikulum stresi konuları çerçevesinde niteliklerinin belirlenmesini amaçladık. İlk olarak, hücre yaşlanması ve FAM134B ilişkisi Huh7 hücrelerinde erken hücre yaşlanmasına neden olarak test ettik. Adriamisin ve TGF-β kullanılarak sebep olunan erken hücre yaşlanması FAM134B gen ifadesinde artışa neden olmadı. Bu nedenle, kendiliğinden gelişen hücre yaşlanmasında görülen gen ifade artışının doğrudan hücre yağlanma fenotipiyle alakalı olmadı sonucuna vardık. Daha sonra, FAM134B'nin iyi diferansiye ve kötü diferansiye karaciğer kanseri hücre hatlarındaki mRNA ve protein seviyelerini analiz ettik. Sonuçlara göre, FAM134B ifadesi karaciğer kanserinin daha ileri aşamasını ve metastatik karakteristiğini temsil eden kötü diferansiye hücre hatlarında daha yüksektir. Diğer taraftan, FAM134B ve endoplazmik retikulum stres ilişkisi üzerinde yaptığımız araştırmalar, FAM134B'nin tapsigargin, tunikamisin ve DTT gibi endoplazmik retikulum stresine neden olan kimyasallarla gen ifadesinde artışla yanıt verdiğini tespit ettik. Bu nedenle, FAM134B'nin endoplazmik retikulum stresine yanıt veren bir gen olduğunu gösterdik. Bu sonuçla birlikte, kötü diferansiye hücre hatlarındaki yüksek FAM134B protein ve mRNA miktarlarını bu hücrelerdeki bazal seviyede endoplazmik retikulum stres yanıtıyla ilişkilendirdik. Ayrıca, bu geni yüksek seviyede ifade eden Huh7 hücrelerinde yaptığımız deneyler sonucunda FAM134B'nin kendi başına endoplazmik retikulum stres yanıtı ve otofajiye neden olamayacağını gösterdik. Ancak, tapsigargin ve tunikamisin kullanarak yapılan yapay endoplazmik retikulum

stresi durumunda FAM134B'nin hücre yanıtında etkili olduğunu gördük. Huh7 hücrelerinde FAM134B geninin yüksek ifadesi tapsigargin ve tunikamisinin neden olduğu kontrollü hücre ölümü yanıtına duyarlılığı artırdığı sonucuna vardık. Ayrıca bu genin yüksek ifadesinin yine aynı şekilde endoplazmik retikulum stresi uygulandığı durumda hücrelerin çoğalma yeteneğini daha çok azalttığını gösterdik. Buna bağlı olarak, FAM134B, dışarıdan endoplazmik retikulum stresinin başlatıldığı durumlarda stresin şiddetinin artmasında rol oynadığını düşünmekteyiz. Bununla birlikte, dokular üzerinde yaptığımız çalışmada FAM134B ifadesinin beyin ve karaciğerde yoğun olduğunu gösterdik. Tüm bunlar göz önüne alındığında, FAM134B'nin karaciğer dokusunda biriken hasara ve böylece karaciğer kanserinin gelişimine etkili olma ihtimali vardır.

TO MY FAMILY

.

ACKNOWLEDGEMENTS

This thesis has been made possible thanks to the contributions of many people.

First of all, I would like to thank my thesis supervisor Prof. Dr. Mehmet Öztürk for his supervision throughout this project. He is an esteemed scientist with very high motivation and enthusiasm, as well as an extensive knowledge in molecular biology. It was a privilege for me to work in his laboratory as a M.Sc. student.

Secondly, I would like to thank Assist. Prof. Dr. Ebru Erbay for her guidance in designing experiments. She has always been supportive throughout this project. Besides, I definitely learned a lot from her about the endoplasmic reticulum biology.

All the past and present members of our group, especially Dilek Çevik and Ayşegül Örs, Eylül Harputlugil, Dr. Şerif Şentürk, Tülin Erşahin, Ebru Bilget Güven, İrem Durmaz, Gökhan Yıldız, Dr. Sevgi Bağışlar, Dr. Çiğdem Özen, Dr. Mine Mumcuoğlu have been wonderful colleagues and friends during my M.Sc. study.

I would also like to thank Füsun Elvan, Bilge Kılıç, Sevim Baran, and Abdullah Ünnü in the Department of Molecular Biology and Genetics for their invaluable help.

Finally, I would like to thank The Scientific and Technological Research Council of Turkey (TÜBİTAK). This master thesis work was financially supported by the grant from TÜBİTAK to Prof. Dr. Mehmet Öztürk (project number: 109S191). In addition, I have been personally supported by TÜBİTAK throughout my master study, through BİDEB 2210 scholarship.

TABLE OF CONTENTS

LIST OF TABLES

LIST OF FIGURES

1. INTRODUCTION

1.1 Hepatocellular carcinoma

1.1.1 Epidemiology of hepatocellular carcinoma

Hepatocellular carcinoma (HCC) is the most common liver cancer type with a percentage between 80-90% among all primary liver cancer types. Furthermore, if all cancers are taken into consideration, HCC is classified in a substantial percentage, around 6% of all cancers (Parkin et al., 2005). HCC affects many populations in the world, taking a place among the most lethal cancers (Farazi and DePinho, 2006). After lung and stomach cancers, HCC is the third leading cause of cancer related deaths. It causes 600,000 deaths every year with a new occurrence of 500,000 – 600,000 cases per year (Faloppi et al., 2011). Occurrence of HCC is directly related to age, having the highest frequency in the population of over age 65 (Gomaa et al., 2008). Apart from the relationship between age and HCC, there is a significant sex ratio of 2,4:1, more common in men (Parkin et al., 2005).

1.1.2 Aetiologies and risk factors of hepatocellular carcinoma

Hepatocellular carcinoma is a cancer type with high complexity in terms of the aetiological factors leading to the occurrence of the hepatocarcinogenesis. Among these risk factors, the most major are viral factors such as chronic Hepatitis B and Hepatitis C, metabolic factors such as non-alcoholic fatty liver disease and diabetes, toxic factors such as aflatoxins and alcohol, immune related factors such as autoimmune hepatitis, and additional factors such as cirrhosis and hereditary haemochromatosis (Badvie, 2000; Farazi and DePinho, 2006; Parikh and Hyman, 2007). Although all of these risk factors are associated with the incidence of HCC, effectiveness and the prevalence of these factors are highly dependent on the geographic condition over the world. For instance, the difference in the geographical

distribution of HCC is mainly due to the variable distribution of Hepatitis B virus (HBV) and Hepatitis C virus (HCV) infections (Liu and Kao, 2007). However, even though HBV and HCV infections are important factors, they are not that much prominent in the US. Instead, alcoholic cirrhosis and dietary related non-alcoholic fatty liver diseases are the major factors leading hepatocarcinogenesis in most western countries (Stickel and Hellerbrand, 2010).

1.1.2.1 Role of aflatoxin in hepatocarcinogenesis

Aflatoxin B1 (AFB1) is a toxic factor for the liver produced by *Aspergillus*, which contaminate some foods, such as corn, peanut, and grain (Groopman et al., 1996). Therefore, digestion of such contaminated foods causes aflatoxin exposure in the liver and trigger hepatocarcinogenesis. The affect of aflatoxin on hepatocarcinogenesis is associated with its role in causing specific codon 249 mutation on tumor suppressor p53 gene (Bressac et al., 1991; Ozturk, 1991). Interestingly, this mutation has also been detected in patients with a history of HBV infection (Yu et al., 2005). Hence, aflatoxin exposure is likely to trigger hepatocyte carcinogenesis by inducing a common mutation that is highly responsible for the lack of tumor suppression activity of p53.

1.1.2.2 Role of alcohol in hepatocarcinogenesis

Alcohol is metabolized mainly by activity of alcohol dehydrogenase enzyme in cytoplasm of hepatocytes, as well as by some other mechanisms in endoplasmic reticulum and peroxisomes (McKillop and Schrum, 2005). Ethanol metabolism results in products of free radicals and acetaldehyde. Release of these free radicals and acetaldehyde affects the cellular homeostasis by inducing oxidative stress and also preventing some cellular activities, such as DNA repair, by directly binding to the cellular components (Sun et al., 2001). On the other hand, ethanol directly affects the activities of some other key regulators of proliferation signaling and cell cycle, such as protein kinase C, adenylate cyclase, STAT, JNK, NF-κB, and MAPK (McKillop and Schrum, 2005) as well as increasing the activity of G protein inhibitor

which is associated with HCC through triggering p42/p44 MAPK signaling (Diehl, 2005)

1.1.2.3 Hepatitis B virus induced hepatocarcinogenesis

Three decades ago, it has been shown that hepatitis B carriers have an increased annual incidence of HCC with an average of 0,5%, and 1% for population with age over 70 (Beasley et al., 1981). Further studies pointed out that HBV associated hepatocarcinogenesis is directly related to the necro-inflammation and fibrosis effects of this viral infection. These effects further pave the way for hepatocyte regeneration (Waris and Siddiqui, 2003). In addition, HBV infection can contribute to hepatocellular carcinogenesis through host genome integration, triggering some oncogenic pathways and even endoplasmic reticulum interaction and upregulation of oxidative stress (Farazi and DePinho, 2006). In terms of HBV and cirrhosis relationship, in East Asian countries, the incidence rate of HCC in HBV-related cirrhosis was shown to be 2,7% (Michielsen et al., 2005). This suggests that underlying liver diseases are undoubtedly key factors of acquiring HCC. In fact, HBV infection may also result in HCC independent of cirrhotic contribution, showing that not merely HBV and cirrhosis co-contribution but co-contribution of HBV with some other factors lead to hepatocarcinogenesis (Waris and Siddiqui, 2003).

1.1.2.4 Hepatitis C virus induced hepatocarcinogenesis

Hepatitis C virus infection is associated with hepatocyte transformation in different ways. Firstly, studies showed that HCV infection is most likely to turn into chronic infection, because about 80% of the infected patients cannot be totally disinfected in the acute phase. Resulting chronic infection results in prevailing of the effects of viral infection, such as inflammation and regeneration in hepatocytes. These in advance lead to chronic hepatitis and cirrhosis, which finally brings out hepatocyte carcinogenesis with the accumulation of chromosomal abnormalities (Ahn and Flamm, 2004; Suruki et al., 2006). The percentage of cirrhosis development and hepatocellular carcinogenesis in the chronic infection cases are 20% and 2,5%,

respectively (Bowen and Walker, 2005). In addition, HCV induced hepatocarcinogenesis is found to involve some key viral proteins in promotion of carcinogenesis. Among these, NS5A is known to control transcription and mitogenic signal transduction as well as the regulation of cell cycle (Tellinghuisen and Rice, 2002). Besides, important cell regulatory mechanisms, such as proliferation, apoptosis, transcription and key signaling factors of these regulations, such as NF-κB and MAP kinase are modulated by HCV core protein (Block et al., 2003).

1.1.2.5 Other factors inducing hepatocarcinogenesis

Apart from the major risk factors of hepatocellular carcinogenesis, there are some other aspects contributing to the initiation or development of HCC.

Diabetes is considered as one of the key additional factors for the onset of HCC. Studies of Davila et al. showed that the ratio of HCC patients with diabetes is substantially greater than the patients with diabetes within the control group without cancer. Furthermore, independent of the other foremost risk factors, diabetes is regarded as a self-determining risk factor with an effect of 2-3 fold increase in occurrence of HCC (Davila et al., 2005). The link between diabetes and the hepatocellular carcinogenesis is possibly due to the accumulation of free fatty acids in liver and the acquisition of insulin resistance in the liver of diabetic patient (Maclaren et al., 2007). These results cause development of fibrosis through dysfunctional effects on hepatocyte homeostasis, such as hepatocyte injury and hepatocyte apoptosis (Farrell and Larter, 2006).

Apart from the effect of diabetes on HCC, other disorders affecting liver are also involved in the increased risk of hepatocarcinogenesis. Among these, non-alcoholic steatohepatitis and non-alcoholic fatty liver disease are likely to promote HCC development in a way that they contribute to advance of liver fibrosis and cirrhosis (Adams and Angulo, 2005). Furthermore, some other genetic disorders, such as hereditary haemochromatosis and alpha1-antitrypsin deficiency are associated with the higher risk of developing HCC (Badvie, 2000). Hereditary haemochromatosis is a disease related to the excess iron taking into hepatocytes. Such an iron overload in hepatocytes brings about a hepatocellular damage, finally leading to

hepatocarcinogenesis (Pietrangelo, 2009). Another inherited disease alpha1-antitrypsin deficiency comes up with the emergence of antitrypsin polymers in the liver cells. These antitrypsin polymers trigger hepatocyte fatality, and thereby, cirrhosis (Parfrey et al., 2003).

1.1.3 Molecular pathogenesis of hepatocellular carcinoma

It has been discussed that the molecular pathogenesis of hepatocellular carcinoma is a rather complex mechanism (Farazi and DePinho, 2006). Through the progress of HCC, different risk factors and modulations, such as mutation, altered pathways, genetic changes, epidgenetic changes, and chromosomal aberrations are involved. Accumulation of these changes through hepatocarcinogenesis paves the way for the development of neoplastic state in normal livers, non-cirrhotic livers and cirrhotic livers (Bruix and Sherman, 2005; Llovet et al., 2003). The basis of HCC originates initially from damaged hepatocytes which later on start proliferation and regeneration cycles. Increased regenerating activity of hepatocytes leads to the occurrence of cirrhosis and then dysplasia, finally to hepatocellular carcinoma with the help of addition effects and risk factors (Schlaeger et al., 2008). Nevertheless, details of the molecular events resulting in hepatocellular carcinoma are still not well known (Farazi and DePinho, 2006).

Normal liver to hepatocarcinogenic liver transition is a multistep mechanism mostly triggered by genetic changes resulting in firstly cirrhotic liver, and then cancer. This progress involves liver stem cells as well as hepatocytes (Llovet and Bruix, 2008). At the initial steps, HBV and HCV infections, amplified transforming growth factor alpha and insulin like growth factor 2 activities speeds up the early process of hepatocyte proliferation (Thorgeirsson and Grisham, 2002). During these stages, especially infection of HBV brings about oncogene activation, instable chromosomes and DNA rearrangements via integration of the viral genome (Ferber et al., 2003). On the other hand, DNA damage is further induced by occurrence of oxidative stress and chronic inflammation in hepatocytes (Hussain et al., 2007). At the preneoplastic stage of carcinogenesis, the process involves both genetic an epigenetic aberrations. In the mean time, dysplastic nodules are produced in a way that particular cell

populations with these aberrations are selected and grow up to form these dysplastic structures. This transformation is further supported by activation of survival and proliferation pathways, in addition to uncontrolled telomerase activity in order to serve for unlimited proliferative capacity of these cell populations (Llovet and Bruix, 2008). Dysplastic nodules are pre-malignant structures possessing abnormalities at the cellular level and are likely to transform into hepatocellular carcinoma thanks to the accumulation of genomic instability and loss of p53 function (Farazi and DePinho, 2006).

1.1.4 Genetics of hepatocellular carcinoma

As other cancer types, hepatocellular carcinoma is also highly associated with the genetic aberrations in the original cells. These aberrations involve changes in gene expression, somatic mutations, amplification or deletion of specific sites and epigenetic changes directly affecting the expression of key genes (Llovet and Bruix, 2008). Among these changes, genome wide alterations consisting of amplification or deletion of specific chromosomal sites have been detected in HCC cases. The most common amplification sites are 1q, 6p, 8q, 17q, and 20q, whereas deletion sites are 4q, 8p, 13q, 16q, and 17p (Chiang et al., 2008a; Thorgeirsson and Grisham, 2002). Besides, other critical amplification sites were detected at regions where cyclin D1 and VEGFA genes are located, at 11q13 and 6p21 sites, respectively (Chiang et al., 2008a). There are a few critical somatic mutations already found to be associated with hepatocarcinogenesis. One of the major tumor suppressors, TP53 gene, was found to be mutated with a frequency of 30% in HCC patients worldwide. And, this mutation at the codon 249 of TP53 gene was reported to be related to aflatoxin B1 exposure (Bressac et al., 1991). Besides, another cell cycle control gene Rb which is located at 13q site, which is a common loss of heterozygosity site, and inactivating mutations of Rb gene was reported to be at least 15% of HCC cases (Ozturk, 1999). In the aspect of genomic instability, the major alteration in the HCC cells is that hapatocarcinogenic cells have highly increased telomerase activity, approximately in 90% of HCC cases. Increased telomerase activity is most likely due to HBV genome integration into TERT locus, increased expression of telomerase RNA component

TERC, and loss of a chromosomal region involving telomerase repressor (Farazi et al., 2003). In addition to genetic alterations, epigenetic changes are also factors in promoting hepatocarcinogenesis. Expressions of some critical genes having tumor suppressor roles, such as p16INK4a, E-cadherin, BRCA1, and IGFR-II, are suppressed by hypermethylation of the promoter regions of these genes (Farazi and DePinho, 2006; Thorgeirsson and Grisham, 2002).

1.2 Senescence

1.2.1 Cellular senescence

Cellular senescence was first explained as a loss of proliferating ability of the cells in culture, resulting in the stop of population growth after an approximate number of passaging cells in vitro (Sherwood et al., 1988). Besides, cells with dividing and renewal ability can quit the cell cycle permanently due to various stress factors, such as DNA damage, mitogenic signals, change in the chromatin structure and dysfunctional telomeres (Campisi, 2005). Cellular senescence is a potential anti-cancer mechanism mainly regulated through p53 and RB proteins. Senescence response acts as a barrier for cancer in a way that damaged cells are prevented from aberrant proliferation which is a key factor of carcinogenesis (Campisi, 2005). However, senescent cells undergo significant changes at the cellular level, such as chromosomal aberrations, increased size and size heterogeneity (Sherwood et al., 1988). And, these changes at the cellular level may contribute to aging and some age related diseases (Campisi, 2005).

1.2.2 Replicative senescence

Replicative senescence refers to the induction of senescence response as a result of telomere shortening. Telomeres are repetitive hexamer units located at the ends of eukaryotic chromosomes. These structures act as caps for the linear end, having a length of a few to several kbs. Presence of telomeres at the end of chromosomes

provides protection against chromosomal degradation and chromosome end fusion (Reaper et al., 2004).

Telomere dependent senescence is associated with the telomere shortening. In the lack of adequate telomerase activity, a part of telomeres are lost during the replication process. Loss of telomeres in each replication results in drastically reduced telomere length, which is sensed as DNA damage signal (Ozturk et al., 2009). As a result of this DNA damage signal, key cell cycle regulators, such as p53, retinoblastoma protein, and p16INK4a are activated and cell cycle arrest occurs (Campisi, 2005).

1.2.3 Senescence in liver

Like other somatic cells, hepatocytes do not possess telomerase activity to compensate the telomeric loss at chromosome ends. Hence, during hepatocyte proliferation, shortening of telomeres is inevitable. Excess proliferation of hepatocytes results in progressive telomere shortening, eventually leading up to chronic liver diseases. Therefore, hepatocyte telomere shortening and resulting senescence phenotype are key features of liver cirrhosis (Wiemann et al., 2002). Cirrhosis is an important pathological factor for the development of HCC, and characterized by excessive collagen deposition. Collagen deposition in the liver causes the formation of nodules in the liver and acts as a key intermediate step for fibrosis (Farazi and DePinho, 2006).

Senescence response is a pathological condition in the liver, but development of hepatocarcinogenesis requires further factors at this step. In fact, senescence of hepatocytes is a barrier for carcinogenesis through which cells require additional aberrations to pass this barrier, regain proliferative ability, and trigger HCC (Paradis et al., 2001). The main aberrations required to overcome the senescence barrier are inactivation of pRb and p53 pathways (Ozturk et al., 2009). The most common of these are the inactivation mutation of p53 gene and silencing of p16INK4a at the epigenetic level (Ozturk et al., 2009; Soussi, 2007).

1.2.4 Spontaneous replicative senescence

Cancer cells have immortal characteristics. However, whether this characteristic is reversible or irreversible is still being questioned. In 2006, studies of Ozturk N. et al. showed that hepatocellular carcinoma cell line Huh7 derived cells can be reprogrammed into replicative senescence (Ozturk et al., 2006). In this study, Ozturk N. et al. made a long term culture of Huh7 cell line. After a long term culture, they obtained two sets of clones, namely C1/C3-Early/C3-Late and G11/G12-Early/G12-Late. The C3 clone stopped proliferation at 80 population doublings (PD), while C1 clone replicated over 150 PD. C3 clone was detected to be totally senescence-associated β-galactosidase (SABG) positive, and BrdU negative. C1 clone and C3-Early clones were similar. They showed normal Huh7 morphology, positive BrdU, and low percentage of SABG positive cells (Ozturk et al., 2006).

On the other hand, Ozturk N. et al. showed that while immortal clone of Huh7 had hTERT activity, the spontaneous senescent C3 clone did not possess hTERT activity. Besides, SIP1 gene (ZFHX1B, Zinc finger homeobox 1B) expression was detected to be inversely correlated with hTERT expression in C3 senescent clones. In order to further show the effect of SIP1 on hTERT activity, shRNA targeting of SIP1 was done. Results indicated that knockdown of SIP1 released hTERT expression and rescued spontaneous senescent C3 cells from senescence arrest (Ozturk et al., 2006).

This study was continued further in detailed with the expression profiling of the immortal and senescent Huh7 clones. Gene expression profiling was done using HU133Plus2 Affymetrix Chips and data was analyzed using R software. According to the results, the list of genes with statistically different expression between immortal and senescent clones involves 3073 genes. There is also a number of significant genes with differential expressions in other two-group comparisons, 2149 genes between immortal (C1) and early senescent (C3-Early), and 2023 genes between early senescent (C3-Early) and senescent (C3) (Ozturk M. et al., unpublished data).

1.2.5 FAM134B as a senescence-associated gene

Data analysis of gene expression profiling in senescent, pre-senescent and immortal clones of Huh7 resulted in detection of a number of differentially expressed genes in within three groups. Among these genes, there are some genes that have been and being studied extensively, while some are totally novel genes that were identified in whole genome sequencing but have not been studied and characterized yet. FAM134B (Family with sequence similarity 13, member B) was detected as a significant gene associated with senescence phenotype in this microarray study. FAM134B gene was represented with two different probes in the HU133Plus2 Affymetrix chip. Probe codes are 218532_s_at and 218510_x_at. According to the probe 218532_s_at, FAM134B gene was detected to be 6.5 fold up-regulated in senescent clones in comparison to immortal clones, and 2.6 fold up-regulated in senescent clones compared to pre-senescent clones. On the other hand, microarray results according to other probe 218510_x_at, 4.9 fold up-regulation was detected in senescent clones with respect to immortal clones, while 2.8 fold up-regulation detected in senescent clones with respect to pre-senescent clones. Consequently, FAM134B was identified as one of the most significant genes showing differential expression between senescent and immortal clones with a p-value of 1.097 E-06 (Ozturk M., unpublished data). According to these results, FAM134B is a senescence associated gene, and supposedly has a role in obtaining senescent phenotype or acquisition of senescence phenotype brings about increased expression of this gene. Therefore, the relationship between FAM134B gene and senescence is worth investigating in detail, especially because of the fact that it is a novel gene possibly having important functions in the cell context.

1.3 Endoplasmic reticulum stress

Endoplasmic reticulum (ER) is a key organelle in the cell functioning in the regulation and secretion of all proteins. After translation of linear proteins, these peptides enter into the ER and become mature in this organelle. The ER ensures proper folding and post-translational modifications of entered proteins before these proteins are transported to Golgi.

The lumen of ER is an environment with very high calcium ion concentration. Calcium ions are continuously transported into the ER by active transport through calcium ATPases. The lumen with high calcium ion concentration is a suitable environment for formation of disulfide bonds of proteins. Thanks to such oxidative environment and presence of calcium-dependent chaperone proteins in the ER, protein folding is done within the ER and folded proteins are transported out (Xu et al., 2005).

ER works in a dynamic fashion. The flux into the ER is not always at the same level, changing according to the cells' programs. Physiological state of the cell and environmental conditions are the main factors affecting the dynamic situation of the ER. ER always tries to keep protein mechanism well maintained. Therefore, protein folding capacity is adjusted in order to retain high fidelity. To maintain this homeostasis, ER requires sensors to determine the physiological conditions in the ER and signaling to regulate and maintain the homeostasis. However, homeostasis cannot be always well-maintained, resulting in an imbalance between the unfolded protein load in the ER and the effectiveness of ER machinery working on handling the situation. This imbalance is called endoplasmic reticulum stress (ER stress). The pathway reconciling the stress response and ER homeostasis is called unfolded protein response (UPR) (Ron and Walter, 2007). Presence of such a sensing mechanism and regulation was detected in a study showing that increasing the unfolded protein load of ER results in increased expression of ER lumen chaperones (Kozutsumi et al., 1988).

1.3.1 Handling mechanisms for endoplasmic reticulum stress

When an imbalance between accumulated unfolded proteins and the ER machinery occurs, the cell tries to overcome this situation by acquiring some adaptations. This intrinsic protection mechanism of cells is primarily focused on maintaining homeostasis at both cellular and tissue levels. Therefore, these adaptations may aim to relieve the stress or to remove the stressed cell from the tissue.

The first response against stressed ER is the reduction of unfolded protein load in the ER. This is a kind of transient solution for alleviating ER stress. The amount of accumulated unfolded proteins is reduced by some regulations, either aiming to decrease the amount of newly synthesized proteins or preventing entering of peptides into ER. Both of these regulations seek a solution for stressed ER by reducing the amount of proteins being processed in the ER. Secondly, apart from reducing the amount of proteins in the ER, cells acquire a further protection by increasing the working capacity of the ER machinery. This adaption is a long term response involving UPR target genes. Long term adaptation aims lessening ER stress by activating key UPR target genes encoding ER chaperone proteins. In this case, the more chaperones are produced and work in the ER, the faster ER stress is alleviated thanks to increased activity of these chaperones in proper folding of proteins. If both of these mechanisms do not result in alleviation of ER stress, cells activate a third mechanism, which is programmed cell death. This takes place in situations where ER homeostasis is no longer possible to be set up again. Hence, keeping homeostasis at organism level is preferred and stressed cell is programmed into controlled cell death (Ron and Walter, 2007).

1.3.2 Components of unfolded protein response

Unfolded protein response is the signal transduction response activated as a result of stress in the ER. So far, three different ER stress signal transducers have been identified in the ER. Each of these three initiates a signal transduction through a particular branch of UPR. These three elements are Inositol requiring protein 1 (IRE1), activating transcription factor 6 (ATF6), and PKR-like ER kinase (PERK) (Ron and Walter, 2007).

Inositol requiring protein 1 is the highly conserved arm of UPR. This element was firstly identified in yeast and found to be encoded by *IRE1* gene. This gene encodes a ER transmembrane protein with a luminal and a cytoplasmic domain (Cox et al., 1993). Cytoplasmic domain of IRE1 consists of a kinase activity, which is triggered by activation of ER stress signal coming from the luminal part. Following the activation signal, IRE1 activates itself by oligomerization and trans-

autophosphorylation of the kinase domains (Credle et al., 2005; Zhou et al., 2006). Activation of the kinase domain of IRE1 also activates its other functional response, endonucleolytic cleavage. The substrate of this endonucleolytic activity is a transcription factor Hac1 in yeast (Cox and Walter, 1996; Mori et al., 1996), and X-box binding protein 1 (XBP1) in metazoans (Calfon et al., 2002). IRE1 dependent transcriptional regulation works through its endonucleolytic activity to cleave and remove an intron from XBP1 mRNA. This cleavage makes XBP1 transcription factor active by leading spliced XBP1 mRNA to translation (Lee et al., 2002; Yoshida et al., 2001). Apart from activation of XBP1 by endonucleolytic cleavage, XBP1 expression is also controlled at the transcription level during UPR. XBP1 mRNA levels are increased as UPR is induced (Yoshida et al., 2006). Functional XBP1 protein works as a transcription factor at the promoter sites of some genes having role in endoplasmic reticulum associated protein degradation and transport of unfolded proteins out of ER (Rao and Bredesen, 2004). Furthermore, with accompany of NF-Y, XBP1 binds to two different types of cis-acting elements, which are ER stress enhancer and UPR element (Yoshida et al., 2001). On the other hand, IRE1 is responsible for activation of kinases having role in inflammation and cell death machinery in association with TRAF2. Downstream of IRE1, TRAF2 activates kinase Ask1 and stress induced Jun N-terminal kinase (JNK) (Urano et al., 2000), as well as caspase-12 of apoptotic pathway (Yoneda et al., 2001).

Other arm of the UPR signals through activating transcription factor 6. ATF6 was firstly identified as a new class of UPR signal transducer specifically in metazoans (Haze et al., 1999). ATF6 is found tethered to ER membrane as an inactive precursor. Upon activation of UPR, ATF6 is transported from ER membrane to Golgi apparatus. In Golgi, ATF6 undergoes two protease cleavages, which are processed by site 1 protease (S1P) and by site 2 protease (S2P), respectively. After cleavage, remaining active ATF6 fragment translocates into the nucleus to activate expression of target genes (Haze et al., 1999; Ye et al., 2000). ATF6 activates expression of a set of UPR genes including XBP1 (Yoshida et al., 2001). When UPR signal is activated, IRE1 and ATF6 arms of UPR act cooperatively in a way that while ATF6 increases the transcription of XBP1, IRE1 undertakes endonucleolytic cleavage and activating role of XBP1 to trigger expression of target alarm genes.

The third arm of UPR involves PKR-like ER kinase. PERK is activated similar to IRE1 by oligomerization of PERK and trans-autophosphorylation of its cytoplasmic domain (Bertolotti et al., 2000). In addition to its autophosphorlyation function, PERK also phosphorylates eukaryotic translation initiation factor-2-alpha (eIF2α) at Ser51 site. Ser51 phosphorylation of eIF2α results in inhibition of eIF2α re-cycling by guanine nucleotide exchange factor eIF2B. Lack of eIF2B functioning on eIF2α decreases the amount of active GTP-bound form of eIF2α. As a result of less active eIF2α, general translation initiation is halted, thereby reducing the amount of newly synthesized proteins (Harding et al., 1999). Activation of the PERK arm not only signals through reduction of translation, but also regulates activation of some downstream targets. For instance, activating transcription factor-4 (ATF4) and nuclear factor κB (NF-κB) are activated at translational and post-translational levels via PERK signaling (Ron and Walter, 2007). ATF4 activated another important transcription factor C/EBP homologous protein (CHOP). Signaling cascade continues with the targets of CHOP, which are growth arrest and DNA damage-inducible protein-34 (GADD34) and ER oxidase-1 (ERO1) (Marciniak et al., 2004).

1.3.3 Sensing the stress

Activation of UPR is dependent on sensing stressed ER. Because ER is stressed due to the accumulation of unfolded proteins, heavy unfolded protein load must be sensed in order to start a signal transduction through three main arms of UPR. The most common chaperone protein BiP is the key sensor for ER stress (Rutkowski and Kaufman, 2004). One of the three main elements of UPR, ATF6, is held in the ER via protein-protein interaction with BiP (Shen et al., 2002). Other UPR element, IRE1 is also retained associated with BiP via its lumenal domain (Liu et al., 2003). And, the last arm of UPR, PERK, is also located on ER membrane and bound to BiP through hydrophobic regions on its lumenal domain (Ma et al., 2002).

Sensing stress via BiP relies on the ability of BiP to bind peptide binding regions of proteins. BiP binds to both these three UPR elements and unfolded proteins thanks to this region. In the unstressed ER, the most abundant chaperone in the ER, BiP, binds to lumenal domains of PERK and IRE1, preventing dimerization of these UPR

elements to become active. In the stressed ER, due to excess unfolded proteins, BiP starts binding to unfolded proteins, decreasing its affinity to PERK, IRE1 and ATF6. Dissociation of BiP from PERK and IRE1 allows homodimerization and autophosphorylation of these proteins, which activates these two arms of UPR. On the other hand, dissociation of BiP from ATF6 releases ATF6 to transport into Golgi and become activated by proteolytic cleavage (Rutkowski and Kaufman, 2004).

1.3.4 Deciding survival or death during ER stress

Accumulation of excess unfolded proteins in the ER triggers UPR to somehow overcome this unfavorable situation. Three main elements of UPR control activities of some key regulators functioning in the cell death response. While the decision of cells' survival or death relies on the activities of these key UPR elements, actual factor behind this scenario is dependent on how severe the cell experiences a stress in the ER and how persistent the stress is.

ER associated cell death is likely to be controlled by the level of calcium ions in the ER. Calcium ions might take a role in activation of proteases in cytoplasm to induce cell death (Nakagawa and Yuan, 2000). However, there is no detected relationship between the ER stress and release of calcium from the ER so far. ER stress might contribute to apoptosis through some key apoptotic regulator, such as BAX and BAK. These death factors normally reside in the ER, but translocating onto mitochondria membrane, where they can function upon ER stress (Scorrano et al., 2003; Wei et al., 2001). ER stress mediated cell death might also signal through IRE1 branch of UPR. In this case, caspase-12 activation with the help of TRAF2 triggers death in mice (Nakagawa et al., 2000). Paralog of mice caspase-12 in human, caspase-4 is also associated with the ER functioning, possibly performing a similar role of its paralog in mice (Hitomi et al., 2004). Furthermore, IRE1 mediated Ask1 activation leads to JNK activation, resulting in the phosphorylation of JNK targets. Among these targets, phosphorylation of Bcl-2 inhibits its anti-apoptotic activity (Yamamoto et al., 1999), whereas phosphorylation of Bim results in activation of its pro-apoptotic function (Lei and Davis, 2003). At the transcription factor level, ER stress induced apoptosis is regulated by CHOP (GADD153). CHOP can repress the

expression of anti-apoptotic Bcl-2, resulting in the promotion of cell death (McCullough et al., 2001). In brief, at least two of the three branches of UPR have already been detected as factors in ER stress induced cell death. Therefore, cell death response is likely to be resulted from the cooperative role of different UPR signaling elements. Even though the primary goal of UPR is to alleviate the stress level in the ER, if the improper folding process in the ER is excessive or persistent, UPR response aims directing cells to death, typically apoptosis (Xu et al., 2005).

1.4 Liver and ER stress

The major cell type in the liver, hepatocytes, is a type of cell specialized in metabolic activities. Hepatocytes are responsible for high amount of protein synthesis and secretion in the body. Since the endoplasmic reticulum is the site where post translation control of synthesized proteins is done, ER in hepatocytes has to work at maximum capacity. Under normal circumstances, hepatocytes can handle this massive work of protein synthesis, folding and port-translational modification, and secretion in a routine way thanks to presence of abundant endoplasmic reticulum. However, hepatocyte ER might be stressed upon emergence of some internal and external factors. Viral infections to hepatocytes, alcohol and drug usage, metabolic disorders, and mutations in ER protein encoding genes are the main causes of stressed ER in the liver (Ji and Kaplowitz, 2006).

Stressed ER in hepatocytes can be overcome by common adaptive stress response, UPR. When ER stress is induced by the abovementioned factors, UPR is activated and tries to overcome the stress by inducing ER resident proteins having role in protein folding, triggering degradation of unfolded proteins, and decreasing the total protein synthesis in ribosomes. In a case that ER stress cannot be assuaged by these adaptations, continual stress brings about pathological outcomes in the liver. Hepatocyte death, inflammation and accumulation of hepatic fat are among these pathological consequences or uncontrolled ER stress. These conditions may lead to liver diseases and contribute to the occurrence of liver injury and exacerbate the prevailing liver disease of other aetiological factors, such as viral infection or diabetes associated liver disease (Ji and Kaplowitz, 2006).

1.5 FAM134B in the literature

Family with sequence similarity 134, member B (FAM134B) is a novel gene belonging to the same family with FAM134A and FAM134C. Even though there is a few publications related to this gene, its function is still not known. All the information that has been identified so far is summarized below.

In 2007, the studies of Tang et al. were published in an article titled 'Oncogenic properties of a novel gene JK-1 located in chromosome 5p and its overexpression in human esophageal squamous cell carcinoma.' This research showed that novel gene JK-1, which is the name of FAM134B isoform number 2, is associated with esophageal squamous cell carcinoma (ESCC) and has a transforming capacity in normal cells. Firstly, their results indicated that JK-1 is overexpressed in 69% (9/13) of ESCC cell lines and 30% (9/30) of ESCC patient samples. Furthermore, when they overexpressed JK-1 in normal cell types, NIH3T3 and HEK293, these cells possessed anchorage dependent and anchorage independent growth. And also, Tang et al. reported that subcutaneous injection of JK-1 overexpressing NIH3T3 cells created subcutaneous sarcomas in all (3/3) three mice. In brief, this study provided the first evidence for JK-1's transforming capacity and JK-1 may be associated with the pathogenesis of ESCC (Tang et al., 2007).

In 2009, Kurth et al. published an important article, titled 'Mutations in FAM134B, encoding a newly identified Golgi protein, cause severe sensory and autonomic neuropathy', indicating the first evidence that FAM134B mutation is associated with a neurodegenerative disease. In their study, genome-wide homozyosity mapping in the sample family having hereditary sensory and autonomic neuropathy type II (HSANII) disease resulted in focusing on a candidate region of 5p15.1. Further analysis pointed out a homozygous nonsense mutation in the FAM134B gene. In order to detect the specific tissues expressing this gene, they performed an in situ hybridization assay. The results showed that FAM134B is predominantly expressed in sensory and autonomic ganglia, while other family members FAM134A and FAM134C are strongly expressed in central nervous system as wells as organs like liver, lung and kidney. Their localization studies resulted in the detection of FAM134B protein co-localized with cis-Golgi marker giantin in N2a cells,

autonomic ganglion neurons related tumor cell line. In order to test the role of FAM134B in the structure of Golgi, they knocked down FAM134B with a lentiviral approach in N2a cells. Knock down of FAM13B4 resulted in a significant reduction in the cis-Golgi size, with a reduction rate of 38% and 40% for two different RNAi. On the other hand, they noticed induction of apoptosis in cultured dorsal root ganglia (DRG) neurons when they are infected with lentiviral approach to knock down FAM134B. However, unlike DRG neurons, when mouse hippocampal pyramidal neurons were infected with the same RNAi approach, these cells were not affected. This might point out that nociception neurons are specifically sensitive to FAM134B depletion. In brief, this study indicated that FAM13B4 has an important role in survival of sensory and autonomic ganglia neurons. Because other members of the same family, family with sequence similarity 134, were also detected to be predominantly expressed in the nervous system, it is likely to state that this family of proteins might have a general role in the maintenance of neurons (Kurth et al., 2009).

Previous studies in our group detected FAM134B as a spontaneous replicative senescence-associated gene (Ozturk et al., unpublished data). Therefore, our group aimed to find out the relationship between FAM134B and senescence. To do that, firstly, its association with senescence, which was previously detected in the microarray study, was tested with semi-quantitative RT-PCR. Results showed that FAM134B is indeed over expressed in C3 senescent clone of Huh7 cells in comparison with parental Huh7 and C1 immortal Huh7 clone. Furthermore, localization immunofluorescence studies resulted in the detection of FAM134B colocalization with endoplasmic reticulum protein calnexin. On the other hand, because Huh7 HCC cells have low level of FAM134B, FAM134B overexpressing stable Huh7 cells were created. FAM134B is associated with replicative senescence. However, it was not known whether this is the cause or the result of senescence. To test this, senescence-associated β-galactosidase experiments were performed. Results showed that FAM134B overexpression does not induce senescence in Huh7 cells. Besides, further BrdU incorporation studies indicated that FAM134B does not induce or repress Huh7 cell proliferation (Tasdemir et al, unpublished data).

Studies on FAM134B so far come up briefly with the following information: its possible relationship with ESCC, its role in survival of specific neurons and neurodegenerative disease, its localization to endoplasmic reticulum or cis-Golgi, and its structural function in cis-Golgi. However, we still do not know much about the function of this protein in the contexts of general cell biology and hepatocellular carcinoma.

2. OBJECTIVES AND RATIONALE

Being one of the most common and lethal cancer types in the human population worldwide, hepatocellular carcinoma is a significant cancer type that awaits a cure. However, the molecular pathogenesis of hepatocellular carcinoma is a rather complex mechanism (Farazi and DePinho, 2006). Indeed, through the progress of HCC, different risk factors and modulations, such as mutation, altered pathways, genetic changes, epigenetic changes, and chromosomal aberrations are involved (Bruix and Sherman, 2005).

Studies of Ozturk et al. showed that immortal HCC cell line Huh7 can be reprogrammed into replicative senescence, resulting in the loss of tumorigenic capacity of parental immortal cells (Ozturk et al., 2006). Acquisition of such a non-proliferative capacity of immortal cells came up with the idea that directing immortal cells into senescence might be a potential therapeutic approach to tumorigenesis.

Designing promising therapies relies on the characterization of the features of immortal and replicative senescent cells in detail. As being one of the most significantly upregulated gene in senescent clones, FAM134B might undertake a critical function in the context of HCC.

On the other hand, Studies of Kurth et al. indicated that mutation in FAM134B is associated with HSANII neurodegenerative disease. Knock down of FAM134B in neural cells results in decreased cis-Golgi size, and induction of apoptosis in some neurons (Kurth et al., 2009). Therefore, FAM134B gene might have a significant role in the survival of neurons. Because senescence is also a survival but non-proliferative response, increased FAM134B expression in senescent cells is also correlated with its survival function in neuron.

Lastly, FAM134B seems to have a structural function in the cis-Golgi and/or ER. Apart from its structural function, it might possess other critical functions related to the survival of the cells, cellular homeostasis and pathogenesis of diseases.

3. MATERIALS AND METHODS

3.1 MATERIALS

3.1.1 General Laboratory Reagents

The reagents used in this research were bought from major biochemical companies such as Sigma-Aldrich (St. Louis, MO, USA) and Merck (Darmstadt, Germany). X-gal was purchased from MBI Fermentas GmbH (Germany). Ethanol, methanol, haematoxylene and Bradford reagents were from Sigma-Aldrich (St. Louis, MO, USA). DMSO and Ponceau S were purchased from Applied Biochemia (Darmstadt, Germany). Plasmid maxi-prep kit used for plasmid extraction was purchased from Quiagen (Chatsworth, CA, USA). Nucleospin RNA II total RNA isolation kit was from Macherey-Nagel (Duren, Germany). Agarose was purchased from Sigma Biosciences (St. Louis, MO, USA). ECL+ blot detection kit and western blot membranes were purchased from Amersham Pharmacia Biotech Company. Yeast extract, agar and tryptone were from Gibco (Carlsbad, CA, USA) and BRL Life Technology Inc. (Gaithersburgs, MD, USA). TGF-β1 was purchased from R&D Systems (Minneapolis, USA).

3.1.2 Tissue culture materials and reagents

All plastic materials used in cell culture, such as petri dishes, plates, flask were purchased from Corning Life Sciences Inc. (USA). Dulbecco's modified Eagle's medium (DMEM) and Roswell Park Memorial Institute (RPMI) cell culture mediums were bought from GIBCO (Invitrogen, Carlsbad, CA, USA). Optimem transfection medium and lipofectamine 2000 transfection reagents were from GIBCO and Invitrogen, respectively. Furthermore, other cell culture reagents such as trypsin

EDTA, fetal bovise serum (FCS), penicillin/strepromycin antibiotics, and L-glutamine were also purchased from GIBCO.

3.1.3 Bacterial Strains

The bacteria strain used in this research was E. coli DH5α strain.

3.1.4 cDNA synthesis

Fermentas RevertAid First strand cDNA synthesis kit (MBI Fermentas, Germany) was used for preparation of cDNAs for expression analysis.

3.1.5 Polymerase chain reaction

Semi quantitative polymerase chain reaction (PCR) reagents, 10X Taq DNA polymerase Buffer (+(NH4)2SO4 – MgCl2), Taq DNA polymerase, 2 mM dNTPs, 25 mM MgCl2 were bought from MBI Fermentas. Quantitative RT-PCR reaction reagents DyNAmo HS SYBR Green qPCR Kit F-410 was purchased from Finnzymes.

3.1.6 Nucleic acids

DNA molecular weight markers were purchased from MBI Fermentas (Germany). pCMV10-FLAG and pCMV14-FLAG plasmids were from Sigma-Aldrich (St.Louis, MO, USA). pGIPZ and pGIPZ-shFAM134B plasmids were purchased from Open Biosystems.

3.1.7 Oligonucleotides

Primer	Sequence	Tm
hFAM134B isoform 1 For.	CAAGAGGTGCACAGTTGTGGAGAA	58
hFAM134B isoform 1 Rev.	GCAACCGTGAGGCTAATCTTAGGA	58

hFAM134B isoform 2 For.	CTCGAGAAGCTTATGCCTGAAGGTGAAGACTT	58
hFAM134B isoform 2 Rev.	GCAACCGTGAGGCTAATCTTAGGA	58
hXBP-1 For.	TTACGAGAGAAAACTCATGGCC	58
hXBP-1 Rev.	GGGTCCAAGTTGTCCAGAATGC	62
hGAPDH For.	GGCTGAGAACGGGAAGCTTGTCAT	60
hGAPDH Rev.	CAGCCTTCTCCATGGTGGTGAAGA	60
hVimentin For.	CGTCACCTTCGTGAATACCA	60
hVimentin Rev.	CCAGAGGGAGTGAATCCAGA	60
hFAM134B isoform 1 For.	TTGGGCGTGTTATTATGCAA	53
hFAM134B isoform 1 Rev.	GCCAGGGCTCTGCTGTTTA	58
hFAM134B isoform 2 For.	CACATTAGCCGTGGTTAGCA	57
hFAM134B isoform 2 Rev.	TTCTGCAATACAGTGGCTGAG	58
hFAM134B common For.	TGGGACCTTCAACCTTTCAG	57
hFAM134B common Rev.	ATTGCGTCTCTTTGCTTGGT	55

Table 3.1 : Primer list, sequences and Tm values

3.1.8 Electrophoresis, photography and spectrophotometry

Agarose used for gel electrophoresis was purchased from Sigma Biosciences Chemical Company (St. Louis, MO, USA). Electrophoresis apparatus was from Thermo Electron Corporation. Power supplies PAC-200 and PAC-300 were bought from Bio Rad Laboratories (CA, USA). Nucleic acid concentration were measured by using NanoDrop from Thermo Scientific (Wilmington, USA). Bradford based protein concentration measurements were done using spectrophotometer Beckman Du640 from Beckman Instruments Inc. (CA, USA).

3.1.9 Antibodies

Antibodies used in this study, their catalog numbers, and working dilutions are given below.

Antibody	Company and catalog number	Dilution
FAM134B	Sigma, HPA026906	1:2500
FAM134B	Sigma, AV44827	1:1000
Calnexin	Sigma, C4731	1:5000
α-tubulin	Calbiochem, CP06	1:4000
Phospho-eIF2α	Invitrogen, 44728G	1:1000
Phospho-PERK	Cell Signaling, 3179	1:1000
Phospho-Rb	Cell Signaling, 9398	1:1000
BrdU	DAKO, M0744	1:500
Anti-mouse-HRP	Sigma, A0168	1:5000
Anti-rabbit-HRP	Sigma, 6154	1:5000
Anti-mouse/rabbit-Alexa Fluor 488	Invitrogen, A11034	1:750
Flag M2	Sigma, F1804	1:5000
PARP	Santa Cruz, sc8007	1:250
Cleaved caspase 3(Asp 175)	Cell signaling, 9664	1:500
Vimentin	Dako, M7020	1:500

Table 3.2: Antibody list, catalog numbers and working dilutions

3.2 SOLUTIONS AND MEDIA

3.2.1 General solutions

50X Tris Acetate EDTA (TAE)	242 g Tris base, 57.1 ml glacial acetic acid, 18.6 EDTA were dissolved in 1 liter ddH20 Working dilution is 1X
10X Phosphate Buffered Saline (PBS)	80 g NaCL, 2 g KCl, 14.4 g Na2HPO4, 2.4 g KH2PO4 in 1 litre ddH2O Working dilution is 1X
Ethidium bromide	10 mg/ml dissolved in ddH2O (stock) Working concentration is 30 µg/ml

3.2.2 Bacteria solutions

Luria-Bertani medium (LB medium)	10g bacto-tryptone, 5 g bacto-yeast extract and 10g NaCl for 1 litre. Additionally, 15 g/L bacto agar for LB agar plates
Glycerol stock solution	Final concentration of glycerol is 25% in LB
Ampicillin	100 mg/ml stock solution in ddH2O Working solution is 100 µg/ml

3.2.3 Tissue culture solutions

DMEM/RPMI media	Complete medium contains 10% Fetal bovine serum, 1% penicillin/streptomycin, 1% non-essential amino acids, stored at 4℃

10X Phosphate buffered saline (PBS)	80 g NaCL, 2 g KCl, 14.4 g Na2HPO4, 2.4 g KH2PO4 in 1 litre ddH2O Working dilution is 1X, stored at 4℃

3.2.4 Senescence associated β-galactosidase (SABG) solutions

SABG solution	1 mg/ml X-gal, 2 mM MgCl2, 150 mM NaCl, 5 mM potassium ferricyanide, 5 mM potassium ferrocyanide, 40 mM citric acid/ sodium phosphate buffer (pH 6)

3.2.5 BrdU incorporation assay solutions

BrdU	10 mg/ml BrdU in ddH2O stock Working dilution is 30 μM
2N HCl	8.62 ml of 37% HCl, 16.36 ml H2O
PBS-TritonX 100	0.1% TritonX-100 in PBS

3.2.6 Immunofluorescence assay solutions

Immunofluorescence blocking solution	10% FCS in 0.2% PBS-Tween 20
Washing solution	0.2% PBS-Tween 20
Antibody dissolved in	2% FCS in 0.2% PBS-Tween 20
DAPI (4',6-diamino-2-phenylindole)	0.1-1 μg/ml working solution in PBS or ddH2O

3.2.7 Propidum iodide cell cyle analysis solution

Propiduim iodide solution	50 μg/ml propidium iodide, 0.1 mg/ml RNase A and 0.05% TritonX-100 in PBS

3.2.8 Sodium Deodecyl Sulphate (SDS) – Polyacrylamide Gel Electrophoresis (PAGE) and immunoblotting solution

In this study, NuPAGE NOVEX pre-cast western blotting system (Invitrogen, CA, USA) was used for the immunoblotting experiments. Pre-cast gels used were 4-12% gradient, 10% and 12% Bis-Tris gels. Furthermore, for the detection of high weight proteins 3-8% Tris-acetate pre-cast gels were used, all from Invitrogen. Running buffers were also purchased from Invitrogen. MES and MOPS ready to use 20X stock running buffers used according to the weight of the protein of interest. Wet transfers were done to either PVDF membrane or nitrocellulose. 20X transfer buffer for wet transfer, 4X sample loading buffer, antioxidant and 10X denaturing reagent (500 mM DTT) were also purchased from Invitrogen.

Running buffers MES and MOPS	20X stock, working solution is 1X
Transfer buffer (Invitrogen)	20X stock, working solution is 1X with 10% methanol
Blocking solution	5% (w/v) non-fat dry milk was dissolved in 0.2% TBS-Tween 20, or 2.5% Quick Blocker (Calbiochem) was dissolved in 0.2% TBS-Tween 20
10X Tris buffered saline (TBS)	12.9 g Trisma base, 87.76 g NaCl in 1 litre of ddH2O, working dilution is 1X and pH 8
TBS-Tween 20	0.2% Tween 20 in 1X TBS
Ponceau S	0.1% (w/v) Ponceau S and 5% (v/v) acetic

	acid was dissolved in 0.2 % TBS-Tween 20
Coomassie brilliant blue solution	100 mg coomassie brilliant blue G-250, 50 ml 95% ethanol, 100 ml 85% phosphoric acid. Filtered using whatman paper
NP-40 lysis buffer	50 mM Tris HCl, 150 mM NaCl, 1% NP-40, 0.1% SDS, 1X protease inhibitor cocktail

3.3 METHODS

3.3.1 Tissue culture methods

3.3.1.1 Cell lines and growth conditions of cells

Hepatocellular carcinoma cell lines used in this study were cultured in either DMEM or RPMI media. Well-differentiated cell lines Huh-7, Hep40, HepG2, Hep3B, Hep3B-TR, PLC and also Mahlavu, Focus, SK-HEP-1 cell lines were cultured in complete DMEM medium. Other HCC cell lines Snu-182, Snu-387, Snu-398, Snu-423, Snu-449, and Snu-475 were cultured in complete RPMI medium.

DMEM and RPMI mediums used for culturing cells were complete mediums containing 10% fetal bovine serum, 1% penicillin/streptomycin antibiotics and 1% non-essential amino acids. All the cells were kept in incubators at 37 °C with 5% carbon dioxide concentration in the air. All the cells kept in incubators were checked regularly. Cells were passaged into new dishes or plates before they reached high confluency in the dish.

3.3.1.2 Passaging the cells

For passaging cells, firstly, the medium was aspirated using sterile pipettes and the cells were washed at least once with PBS. Thereafter, trypsin-EDTA was added in the dish or flask. The amount of trypsin-EDTA was between 0,5 ml- 2ml, depending on the surface area of the dish or plate. Trypsinized cells were kept in the incubator

for 1-2 minutes. Then, detached cells were collected in a complete medium in 15 or 50 ml falcon tubes, using serological pipettes. Cells were mixed by pipetting up and down. Desired portion of the collected cells were reseeded on petri dishes or flasks depending on the requirements.

3.3.1.3 Thawing the cells

For thawing the cells, stock cryovial of a cell line of interest was taken from either from nitrogen tank stocks or from – 80 °C freezer stocks and put on ice immediately. Thereafter, the vial was put in the 37 C water bath in order to thaw in a few minutes. Before thawing completely, cells were pipetted using a several milliliters of completes medium and transferred into 15 ml tubes. Resuspended cells were centrifuges for 4 minutes at 1500 rpm. Supernatant containing DMSO was removed and cell pellet was resuspended in a complete medium and transferred into petri dish or flask. Flasks and dishes were chosen depending on the amount of pellet, smaller flask or dish for less amount of cell pellet. Cells were distributed in the flask or dish evenly by moving the flask or the dish back-forth and right-left. Cells were kept in incubators, at 37 C and 5% carbon dioxide conditions. The day after, cells were washed and unattached cells were removed and the mediums were refreshed.

3.3.1.4 Cryopreservation of the cells

Cell stocks were prepared from the cell in culture with around 60-70% confluency. These cells were washed with PBS and collected by adding trypsin-EDTA and medium afterwards. Cells were centrifuged for 4 minutes at 1500 rpm. Thereafter, freezing medium, containing 7% DMSO and 20% FSB in complete medium, was used for resuspending the cells. Cells in freezing medium were transferred into cryotubes and kept at -20 °C for about 1 hour. Afterwards, cryovials were stored at – 80 °C overnight and transferred into nitrogen tanks.

3.3.1.5 Transient transfection of cells using Lipofectamine 2000

Transfection of plasmid DNA into cells was done by using Lipofectamine 2000 transfection reagent (Invitrogen, CA, USA). Firstly, cells were seeded in 6 well or 12 well plates one day before the transfection. Transfection was done when cells have high confluency. OPTI-MEM and Lipofectamine 2000 mixture and OPTI-MEM and DNA mixtures were prepared. Thereafter, these mixtures were mixed and let to stay at room temperature for 30 minutes. Thereafter, cells were washed with PBS and transfection mixture was added on cells. After 6-8 hours, Lipofectamine containing transfection mixture was removed, cells were washed and fresh growth medium was added on cells. For determining transfection efficiency, a control GFP vector was also transfected into control cells and efficiency was checked under fluorescent inverted microscope. Cells were collected about 48h after transfection for western blot experiment. In this protocol, DNA:Lipofectamine 2000 ratio was 1:2,5. The transfection medium used was OPTI-MEM serum medium from GIBCO.

3.3.1.6 Treatment of the cells

Firstly, cells were seeded in appropriate dishes, flasks or plates according to the experiment type. One day after the seeding, the mediums were removed. Cells were washed with PBS. Treatments were done in complete DMEM or RPMI mediums. Treatment mediums containing chemicals, such as thapsigargin, tunicamycin etc. were prepared freshly. For the control samples, complete mediums containing same amount of solvents were prepared, such as water or DMSO.

3.3.2 Total RNA extraction from cultured cells

For RNA extraction from the cultured cells, first of all, cells were collected by adding trypsin-EDTA and growth medium. Then, cells were centrifuged and the pellets were used for RNA extraction using NucleoSpin RNA II Kit (MN Macherey-Nagel, Duren, Germany) according to the manufacturer's protocol.

3.3.3 First strand cDNA synthesis

First strand cDNAs were synthesized by using Fermentas RevertAid cDNA synthesis Kit (MBI Fermentas, Germany). 1-2 ug RNA was used for cDNA synthesis according to the manufacturer's instruction. Firstly, Oligo(dT)18 primers were added into RNA and this provided reverse transcription of only mRNAs with polyA tails. After addition of reaction buffer and dNTPs, RevertAid M-MuLV RT reverse transcriptase enzyme did the reverse transcription at 42 °C. All these steps with different temperatures were done in thermocycler machine. Total final volume of 20 cDNA was diluted to 1:1 in DEPC-treated water.

3.3.4 Primer designing for semi-quantitaive and real time RT-PCR analysis

In order to obtain efficient results from expression analysis, primers for semi-quantitative and quantitative RT-PCR were designed carefully. Designed forward and reverse primers were arranged in a way that they anneal on different exons. Thereby, amplification from the genomic DNA was not expected. Even if so, primers were designed in a way that amplification from genomic DNA would give a greater product which could be detected on the gel. Furthermore, primers were designed in a way that they contain low GC content, especially at the ends of the primers and also forward and reverse primers have approximately the same melting temperatures.

3.3.5 Detection of genomic DNA contamination in cDNA synthesis

For the detection of any unexpected amplification from genomic DNA cDNA synthesis was done using a reverse transcriptase control samples. In this control experiment, all the RNA samples were prepared exactly the same according to the cDNA synthesis kit protocol except the addition of RevertAid reverse transcriptase enzyme. In lack of this enzyme, cDNAs were not expected to be synthesized. Therefore, if the PCR gives a product, this was expected to be amplified from genomic DNA. When each cDNA set was prepared, these RT – control samples were checked at least once by RT-PCR and run on the agarose gel. On the other hand, control PCR was done using glyceraldehyde-3-phosphate dehydrogenase primers in a

way that these primers were designed to give a product of 151 bp from cDNA but 250 bp product from genomic DNA.

3.3.6 Expression analysis of a gene by semi-quantitative RT-PCR

3.3.6.1 GAPDH normalization

When a cDNA set was synthesized, first of all GAPDH RT-PCR was done in order to normalize the amounts of cDNAs to use in PCR reactions. GAPDH RT-PCR was run on the agarose gel to detect the band intensities. According to the band intensities GAPDH normalization was done aiming to equalize the GAPDH intensity, thereby, providing an efficient comparison of the expression of the gene of interest in the samples. After relative GAPDH PCR product intensities were detected on the gel, the amount of cDNAs for the next RT-PCR were estimated and the other RT-PCRs were done using these amounts of cDNAs from the same cDNA samples.

3.3.6.2 Choosing optimum cycle for RT-PCR

Optimum cycles for a particular RT-PCR analysis may vary according to the gene of interest, primer efficiency and cell line of the sample. Therefore, for each set of primers and cell line combinations, optimum cycle numbers were aimed to be detected. To do this, different cycle numbers were tested on run on the gel. The optimum cycle number in which bands can be seen clearly but the product amounts are not so high that the differences between the band intensities cannot be noticed, was chosen as an optimum cycle and the following PCR reactions were done with this cycle number.

3.3.7 Agarose gel electrophoresis

DNA samples and PCR products were detected on agarose gel using horizontal gel electrophoresis. Gels were prepared and run in 1X TAE buffers with different agarose concentrations between 1-3% depending on the size of the DNA fragment. Smaller DNA fragments were run on 2% agarose gels, while larger ones were run on

1% agarose gels. RT-PCR products of XBP-1 gene were run on 3% agarose gels because of the reason that the transcript variant 1 and variant 2 of the XBP-1 gene has only 26 base difference in length. It was possible to detect the change between unspliced and 26 bases shorter spliced form of this gene on 3% agarose gel. During preparation of the gel, corresponding amount of agarose was dissolved in 1X TAE buffer and boiled in microwave. Then, the solution was left to cool down for a while and ethidium bromide was added on with a final concentration of 30 µg/ml before pouring the gel. DNA samples were mixed with 6X bromophenol blue or xylene cyanol loading dyes before loading into the gel. Agarose gels were run at room temperature under around 100-120 V voltage. 100 bp or 1 kb ladders were used as a reference point on the gels when the gels were visualized under UV light.

3.3.8 Expression analysis of a gene by quantitative RT-PCR

Quantitative PCR analysis was done using Stratagene Mx 3005P. DyNAmo HS SYBR Green qPCR Kit F-410 from Finnzymes was used for the quantitative RT-PCR experiments, according to the manufacturer's protocol. Real time PCR reactions were prepared in 20 µl total volume containing 1 µl cDNA sample. Reactions started with initial denaturation step at 95 °C for 10 minutes. Then, 40-45 cycles of amplification reaction was performed at 95 °C 30 seconds, at 58-60 °C 30 seconds, at 72 °C 30 seconds. Expression levels of the genes were calculated according to the Ct value of the amplification of the gene of interest, Ct value of the reference gene (GAPDH) and efficiency of the primer used. Efficiencies of the primers were calculated before the actually expression analysis by making a serial dilution of a cDNA pool. All real time RT-PCR experiments were performed in at least duplicates of each sample.

3.3.9 Bromodeoxyuridine (BrdU) assay

In order to detect the ratio of proliferating cells, cells were incubated with 30 µM bromodeoxyuridine for 2 hours after particular treatments. Thereafter, cells were fixed with ice-cold 70% ethanol for 10 minutes. Then, cells were exposed to 2 N HCl

for 20 minutes to denature their DNA. Incorporated BrdU was detected using anti-BrdU monoclonal antibody (1:500 dilution) for 1 hour. As a secondary antibody, Alexa Flour 488 anti-mouse (1:750 dilution) was used and cells were counter stained with DAPI (1/10000 in water) for 1 minute. Then, cover slips were covered on slides using fluorescence mounting medium and observed under fluorescence microscope.

3.3.10 Cell cycle analysis using flow cytometry

In order to test the cell cycle distribution of the cells after treatment, cells were rinsed with 1X PBS and trypsinized. Then, cells were collected by centrifugation and resuspended in 1ml of 1X PBS. Cells in PBS solution was fixed by adding 2,5 ml absolute ethanol for 15 minutes or kept at 4 °C in ethanol if the experiment continued later on. After fixation of the cells, cells were pelleted again and propidium iodide solution (50 µl/ml propidium iodide, 0.1 mg/ml RNase A, and 0.05 % TritonX-100) was added to resuspend the pellet. Cells were incubated with this solution for 45 minutes at 37 °C. Then, cells were centrifuged to remove PI solution at 1500 rpm for 4 minutes and were transfer into polystyrene tubes by resuspending with corresponding amount of PBS depending on the pellet size. Analysis was done using FACSCalibur Flow Cytometer (BD Biosciences) and the results were analyzed and figured using Cell Quest 3.2 software.

3.3.11 Senescence associated β-galactosidase (SA-β-Gal) assay

SA-β-Gal assay was performed by seeding cells on circular or square cover slips put in 6-well or 12-well plates. After treatments are finished, cells were washed with 1X PBS and fixed with 4% formaldehyde for 10 minutes at room temperature. Then, SA-β-Gal buffer was added on the cells and the plates were covered with aluminum foil. Plates were kept at 37 °C in a CO2-free incubator for 12-16 hours or until the blue-green staining was detected in the cells.

3.3.12 Immunofluorescence staining assay

For immunofluorescence staining, first of all, cells were fixed with 4% formaldehyde for 10 minutes at room temperature. After fixation, cell permeabilization was done using 0.5% saponin, 0.3% TritonX-100 in 1X PBS solution for 10 minutes at room temperature. Permeabilized cells were blocked with 10% fetal calf serum (FCS), and 0.1 TritonX-100 in 1X PBS for 1 hour at room temperature. After blocking, primary antibody incubation was done using a specific antibody prepared in 2% fetal calf serum and 0,1% TritonX-100 in 1X PBS for 1 hour at room temperature. Primary antibodies were removed and cells were washed with PBS-TritonX-100. Then, secondary fluorescent antibodies, anti-rabbit or anti-mouse Alexa Fluor 488 were used for the detection of the primary antibody. After secondary antibody incubation, cells were counter stained with DAPI (1:10000 dilution in ddH2O) for 1 minute. Finally, cover slips were mounted on slides using fluorescent mounting medium and visualized and photographed under fluorescence microscope.

3.3.13 Total protein extraction from cultured cells

Cells in flasks of dishes were collected either by trypsinization or by scraping. Then, appropriate and sufficient amount of lysis buffer (RIPA buffer in general) was added on the cell pellet and cells were mixed with the lysis buffer properly by pipetting up and down and vortexing every 5 minutes for 30 minutes. Thereafter, lyzed cells were centrifuged at 11000 g for 30 minutes and the supernatants were collected in pre-chilled new eppendorf tubes. Protein concentrations were measured using Bradford reagent. Already known BSA measurements were used as a reference. All the measurements were done with spectrophotometer.

3.3.14 Total protein extraction from tissues

Mouse (Mus musculus) and rat (Rattus norvegicus) organs were taken from Animal Facility in the Department of Molecular Biology and Genetics at Bilkent University. Organs were immediately frozen in liquid nitrogen and stored at -80 °C freezers. 50-100 mg of each tissue were homogenized with pestle and mortar in liquid nitrogen.

Then, powders of the tissues were transferred into glass tubes in an adequate amount of lysis buffer and further pressed under homogenizer. After this further homogenization and lysis step, samples were kept on ice and vortexed every 5 minutes for 30 minutes. Then, samples were centrifuged at 11000 rpm for 30 minutes and supernatants were transferred into new eppendorf tubes. Protein concentrations were measured by conventional Bradford assay with a spectrophotometer measurement at 595 nm.

3.3.15 Western blotting

Firstly, concentrations of the proteins were measured using conventional Bradford assay. All the absorbance values were taken using spectrophotometer at 595 nm wavelength. At the same time with the samples, different dilutions of already known protein concentration of bovine serum albumin (BSA) were measured with Bradford and the respective standard curve was calculated. This was used as a reference for the proteins with unknown concentration and thereby their concentrations were estimated by putting the absorbance values in the equation.

After quantification of the protein concentrations of the samples, equal amounts of proteins were used to prepare loading mixtures. 25 to 40 µg of proteins were loaded into the gel according to the type of experiment. Loading samples were prepared by adding 4X NuPAGE LDS sample buffer, 10X denaturing agent (or 1M DTT), and ddH2O up to the final volume of 25 or 30 µl per well. Then, prepared loading mixtures were heated at 70 °C for 10 minutes before loading into the gel.

In this study, NOVEX NuPAGE western blotting system was used for running the gels and transferring the proteins onto membrane. Gel concentrations and type of running buffers were chosen mainly according to size of the protein of interest. 10%, 12% and 4-12% gradient Bis-tris precast gels were the type of gels used. And also, precast 3-8% gradient Tris-acetate gels were used for the detection of proteins with very high kDa values. Tris-acetate gels were run in the Tris-acetate running buffer. Furthermore, type of running buffer, either MES or MOPS, was also chosen depending on the size of the protein of interest. After running, proteins were

transferred onto Amersham HyBond ECL nitrocellulose or PVDF membranes with wet transfer protocol. Transfer buffer was prepared 1X (from 20X stock) with 10% methanol in ddH2O. Before preparation of wet transfer sandwich, all of the materials were soaked into transfer buffer, and especially PVDF membranes were extra activated in absolute methanol before soaked into transfer buffer. Transfer was done for 90-100 minutes (longer for proteins with very high kDa) under 30 V voltage applied. During the transfer, western blot tank was either kept in cold room or covered with ice.

When the transfer was completed, the efficiency of transfer was tested by putting membrane into Ponceau S solution for 30 seconds. Then, Ponceau S solution was removed by washing membrane in ddH2O for a few minutes. Membranes were blocked with 5% non fat dry milk, 5% BSA or 2.5% QuickBlocker (Calbiochem, USA) in 0.2% TBS-Tween for 1 hour, 1 hour or 30 minutes, respectively. Short time blockings were done at room temperature, whereas over night blockings at +4 °C. After blocking, primary antibodies were prepared in non fat dry milk solution or BSA solutions and incubated for 1-2 hour(s) at room temperature or over night at +4 °C. After primary antibody incubation, membranes were washed with 0.2% TBS-T three times for 5, 10, 10 minutes at room temperature. Then, horseradish peroxidase conjugated secondary antibodies; anti-mouse, anti-rabbit or anti-goat, were used as secondary antibodies according to the type of primary antibody used. Secondary antibody incubation was performed at room temperature for 1 hour. After this incubation, membranes were again washed three times for 5, 10, 10 minutes at room temperature on a shaker. Then, detections were done using chemiluminescent detection kits, ECL+ (Amersham, UK), West DURA (Thermo, USA), and West FEMTO (Thermo, USA), according to the manufacturer's protocols, and depending on the intensity of signal expected on the membrane. Finally, X-ray films were exposed to the emitted chemiluminescent light from the reaction of horseradish peroxidase and developed in X-ray developer. Time of exposure was chosen depending on the detection reagent and the specific antibody used against the protein of interest.

3.3.16 Real-time cell proliferation rate analysis with Roche xCELLigence system

Real-time cell proliferation analysis was performed using Roche xCELLigence system. In order to detect proliferation, equal numbers of cells (4000) were seeded in E-96 96 well plates in a total volume of 200 µl. After 18 hours, real-time measurement was stopped and treatments were done immediately. Measurements were taken again in every 20 minutes for up to total 110 hours. Then, the corresponding cell index and proliferation curve data were saved.

4. RESULTS

4.1 FAM134B

4.1.1 FAM134B at NCBI

Family with sequence similarity 134, member B (FAM134B) is a protein coding gene in a family of family with sequence similarity 134. In addition to its first name, this gene is also known as JK1; FLJ20152; FLJ22155; FLJ22179. FAM134B has a NCBI gene ID 54463. Its location on the genome is chromosome 5, NC_000005.9. It is mapped to the region of 5p15.1 with the neighboring ZNF622 gene at upstream and MYO10 gene at downstream. FAM134B gene has two transcripts.

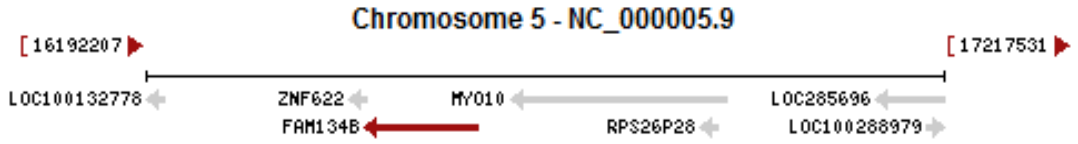

Figure 4.1: Genomic context of FAM134B gene

NM_001034850.1 transcript is the transcript number 1, which represents the longer transcript and encodes the longer isoform. NM_019000.3 is the transcript variant number 2. Transcript 2 differs in the 5' UTR and coding sequence compared to transcript 1. Isoform 2 encoded by transcript 2 has a shorter and distinct N-terminus compared to isoform 1. These two transcripts are produced by alternative splicing.

Figure 4.2: Genomic region and transcripts of FAM134B

Longer transcript, variant 1, consists of 9 exons while shorter transcript, variant 2, consists of 7 exons. Among these exons, the last 6 exons are identical in both variants while the first 3 exons of transcript 1 and the first exon of transcript 2 are unique for those transcripts.

These two transcripts of FAM134B code for two different protein isoforms of FAM134B protein. Protein isoform 1 with accession number of NP_001030022 is the longer protein form consisting of 497 amino acids. Protein isoform 2 with accession number of NP_061873 is the shorter form consisting of 356 amino acids.

4.1.2 Domains of FAM134B

In the 'ensemble' database, information for the domains of FAMN134B is given as the followings. FAM134B protein isoform 1 consists of one coiled coil domain at the C-terminal end of the protein, and two transmembrane domains located close to the N-terminal end of the protein. Similar to isoform 1, isoform 2 also has a coiled coil domain at the C-terminal end of the protein; whereas, isoform 2 consists of only one transmembrane domain close to the N-terminal end of the protein. Difference in the number of transmembrane domains of two isoforms is due to the fact that longer form has extra 3 exons at the 5' end of the transcript encoding for amino acids representing an extra transmembrane domain for this isoform. Besides, isoform 1 has three low complexity regions on the protein, while shorter form has two of them.

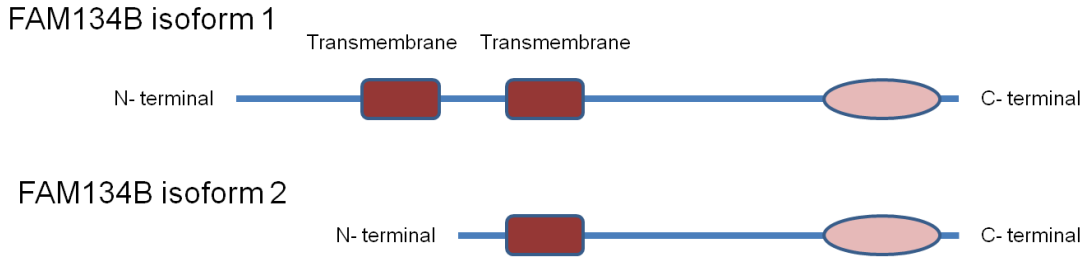

Figure 4.3: Domain representations of two isoforms of FAM134B

4.2 FAM134B in premature senescence

Our group identified FAM134B gene as a replicative senescence associated gene. Previous studies on the relationship between FAM134B and replicative senescence came up with the results showing that FAM134B is not a cause of senescence; because its overexpression does not induce senescence in Huh7 cells (Tasdemir et al. unpublished data). However, increased FAM134B expression was detected in the replicative senescent clones in comparison with the immortal counterparts. A next question waiting to be answered was whether such an increase in FAM134B expression also takes place in premature senescence.

4.2.1 FAM134B expression is not affected in adriamycin-induced premature senescence in Huh7 cells

Adriamycin, also known as doxorubicin, is a drug used mainly in chemotherapy. Adriamycin is an inhibitor of topoisomerase II, and topoisomerase II inhibition results in the prevention of DNA synthesis. Adriamycin is also able to induce DNA strand breaks, leading to the activation of DNA damage response (Fornari et al., 1994). Adriamycin treatment to Huh7 cells results in induction of premature senescence due to the accumulation of DNA damage leading to arrest in cell cycle. As seen in Figure 4.4, 72h 50ng/ml Adriamycin treatment to Huh7 cell causes cell cycle arrest, enlargement of the cytoplasm, and senescence-associated β-galactosidase (SABG) positive phenotype in Huh7 cells.

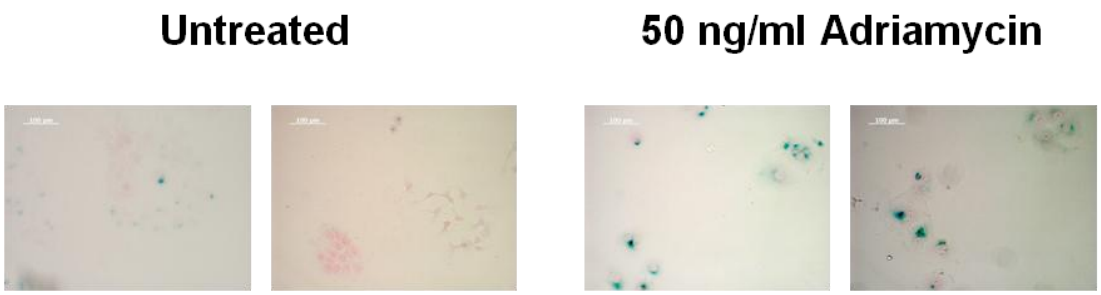

Figure 4.4: Adriamycin induces senescence in Huh7 cells, detected by SABG

In order to test whether there is a change in FAM134B expression in adriamycin induced premature senescence, Huh7 cells were treated with different concentrations of adriamycin for 3 days. Semi-quantitative RT-PCR result showing FAM134B expressions in each sample is given below.

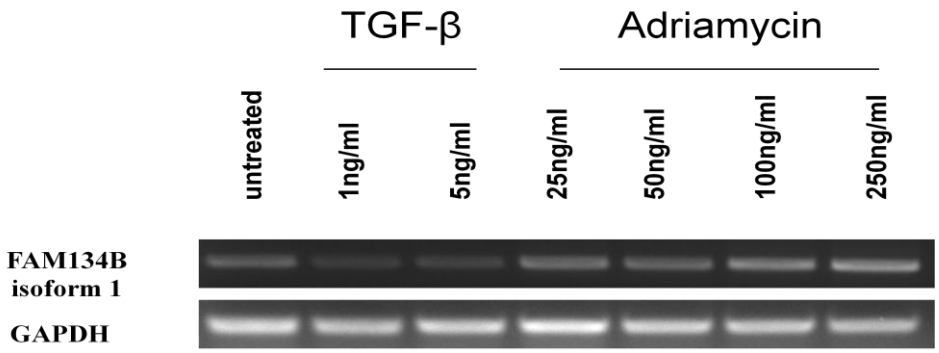

Figure 4.5: Adriamycin treatment does not change FAM134B expression in Huh7 cells.

According to this result, expression of FAM134B isoform 1 is not affected by adriamycin treatment in Huh7 cells, regardless of the adriamycin concentration ranging from 50 ng/ml to 250 ng/ml. This result indicates that increased FAM134B expression in replicative senescent is not observed under another senescence condition, premature senescence induced by adriamycin.

4.2.2 TGF-β treatment decreases FAM134B expression in Huh7 cells

In addition to adriamycin, TGF-β is also used for induction of senescence in Huh7 cells. TGF-β1 can induce senescence in HCC cell lines by activating p21(Cip1) and p15(Ink4b), resulting in the arrest of cells at G1 phase, independent of p53 status (Senturk et al., 2010). Therefore, in order to test if TGF-β induced senescence response is associated with increased expression of FAM134B, Huh7 cells were treated with 1 ng/ml and 5 ng/ml concentrations of TGF-β, which is sufficient for induction of premature senescence in Huh7 cells (Senturk et al., 2010).

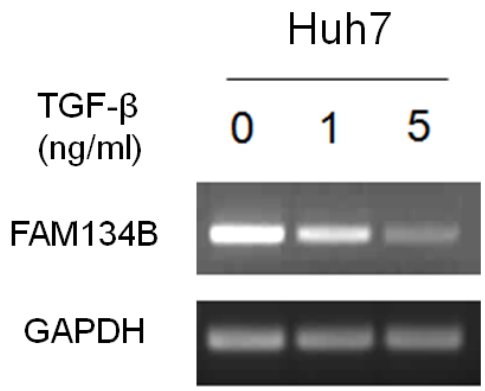

Figure 4.6: TGF-β treatment decreases FAM134B expression in Huh7 cells

Figure 4.6 shows the result of semi-quantitative RT-PCR experiment of FAM134B isoform 1 expression. According to this result, TGF-β treatment with different concentrations (1ng/ml or 5ng/ml) significantly decreases the expression of FAM134B isoform 1. Here, decrease in the expression is proportional to the concentration of the TGF-β treatment, indicating that decrease in FAM134B expression is possible not due to the induction of senescence phenotype but instead, FAM134B is somehow under a direct or indirect control of TGF-β pathway, because 1 ng/ml TGF-β treatment for 3 days is sufficient to induce senescence in Huh7 cells (Senturk et al., 2010).

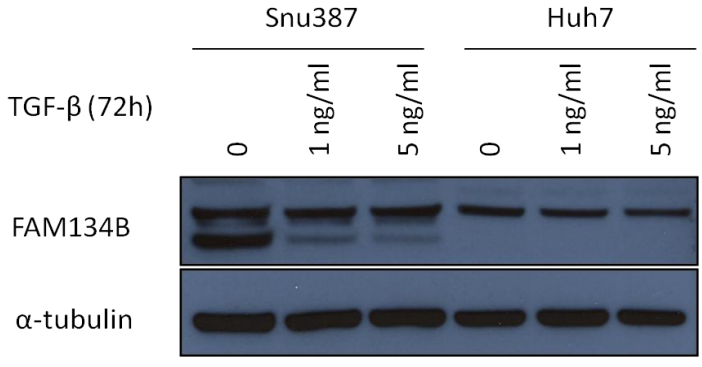

Figure 4.7: TGF-β treatment causes a decrease in protein levels of FAM134B in HCC cells

Figure 4.7 shows a western blot result of change in FAM134B protein levels in response to 3 days TGF-β treatment in Huh7 and Snu387 HCC cell lines. According to these results, TGF-β treatment notably causes a decrease at protein levels of FAM134B in Snu387 poorly-differentiated HCC cell line. However, such a notable decrease cannot be seen in Huh7 cells, even though there is still a slight decrease at protein level in Huh7 cells.

Together with the results of adriamycin treatment, these results briefly indicated that induction of premature senescence in distinct ways, either with adriamycin or with TGF-β, does not result in an increased FAM134B expression, unlike it has been detected in spontaneous replicative senescent model of Huh7 cells.

4.3 FAM134B expression in HCC cell lines and tissues

FAM134B is a newly identified gene and therefore there is not many published research referring to its expression in distinct cell types and tissues. Studies of Kurth et al. showed that FAM134B is predominantly expressed in mouse sensory and autonomic ganglia cells, while its other family members are predominantly expressed in central nervous system as well as liver, lung, and kidney (Kurth et al., 2009). These might present a clue about a tissue specific expression pattern of this gene in the organism. However, in order to obtain further information about the function of this gene at the tissue and cellular levels, cell line and tissue expression analysis of our laboratory models were performed at both mRNA level and protein levels.

4.3.1 Detection of FAM134B mRNA levels in HCC cell lines

FAM134B was firstly identified in a microarray study on a HCC cell line Huh7. Huh7 is one of the most commonly used HCC cell line model. However, there are other HCC cell lines with distinct mutations leading immortality or with different status of differentiation. In order to find out whether FAM134B expression is associated with any characteristics of these distinct hepatocellular carcinoma cell lines, FAM134B expression and protein level detection experiments were performed.

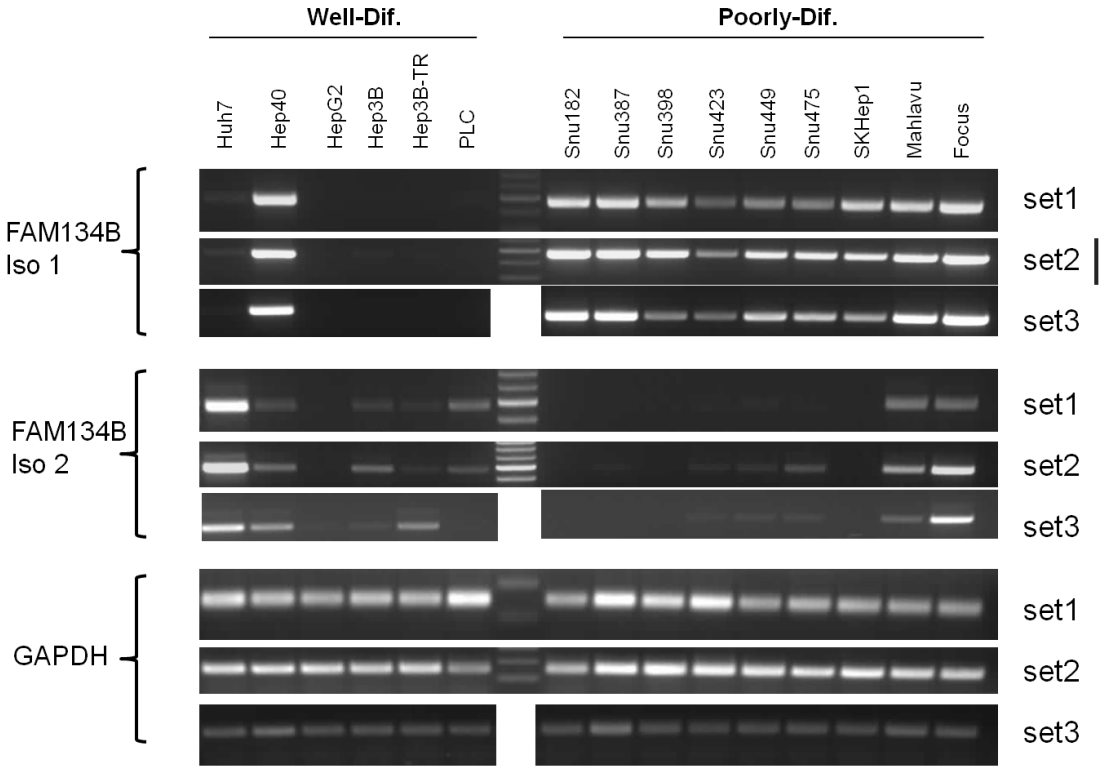

Figure 4.8: FAM134B mRNA levels in HCC cell lines

Semi-quantitave RT-PCR results of FAM134B expression is shown in Figure 4.8. In this experiment, 15 different HCC cell lines were tested for both FAM134B isoform 1 and isoform 2 mRNA levels in these cells. At the differentiation level, these 15 cell lines are grouped into two, namely well- and poorly-differentiated HCC cell lines. These subtypes of HCC were classified according to the markers of hepatocyte lineage and epithelial or mesenchymal characteristics. For instance, compared to well-differentiated cell lines, poorly-differentiated cell lines lost their hepatocyte characteristics and epithelial markers. Unlike poorly-differentiated cell lines, well-differentiated ones remain their hepatocyte characteristics and they are not invasive (Yuzugullu et al., 2009). According to the results of this RT-PCR experiments from three different sets of HCC panel, FAM134B isoform 1 is predominantly expressed in poorly-differentiated cell lines in comparison to well-differentiated ones. Only exception is Hep40 well-differentiated cell line with high isoform 1 expression. On the other hand, isoform 2 is more likely to be expressed in well-differentiated HCC

cell lines, especially in Huh7, while most of the poorly differentiated cell lines are negative for isoform 2 expression, except Mahlavu and Focus.

4.3.2 Detection of FAM134B protein levels in HCC cell lines

In order to test whether distinct expression pattern of FAM13B isoform 1 is also represented at the protein level, western blot analysis of all 15 HCC cell lines was done.

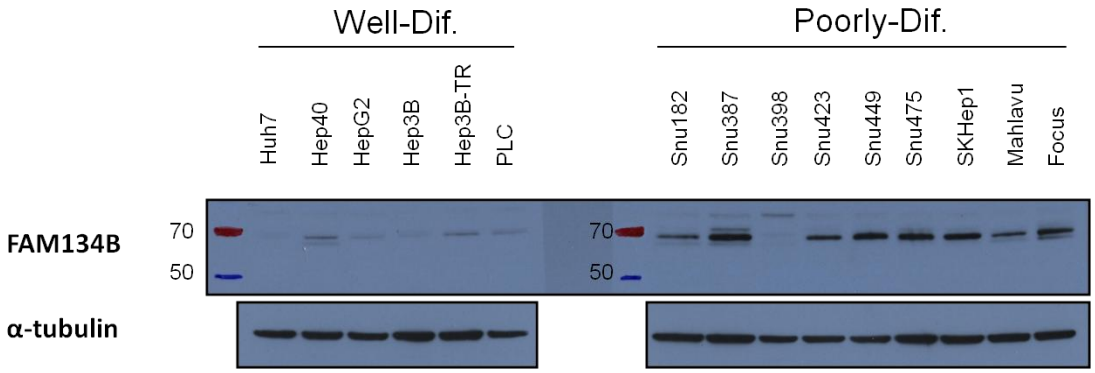

Figure 4.9: FAM134B protein levels in HCC cell lines

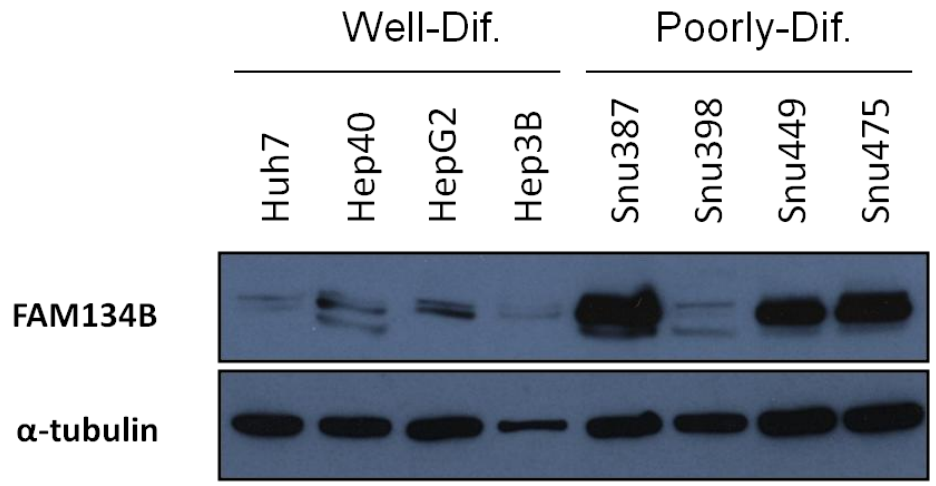

Figure 4.10: Comparison of FAM134 protein levels in well- and poorly-differentiated HCC cell lines

According to the results shown in Figures 4.9 and 4.10, FAM134B protein levels are in a good correlation with the mRNA levels shown in Figure 4.8. FAM134B protein isoform 1 is detected at around 70 kDa marker. However, even though isoform 2 mRNA was detected in some of HCC cell lines in RT-PCR experiment, protein isoform 2 cannot be detected in western blot experiment. Most of poorly differentiated cell lines, except Snu398, have substantial levels of FAM134B isoform 1 protein, while all well-differentiated HCC cell lines, except Hep40, have low FAM134B isoform 1 protein. Figure 4.10 gives a better understanding of the relative protein levels in some well- and poorly-differentiated cell lines, loaded into the same gel. According to this result, FAM134B protein isoform 1 levels in poorly-differentiated cells are considerably greater than that of well differentiated cells. In these western blot experiments, α-tubulin was used as a loading control.

4.3.3 Detection of FAM134B protein levels in tissues

In addition to detection of FAM134B in a group of HCC cell lines, FAM134B protein levels in distinct tissues were tested with western blot technique. These tissues were isolated from rat (Rattus norvegicus), homogenized and total cell lysates were collected using RIPA lysis buffer.

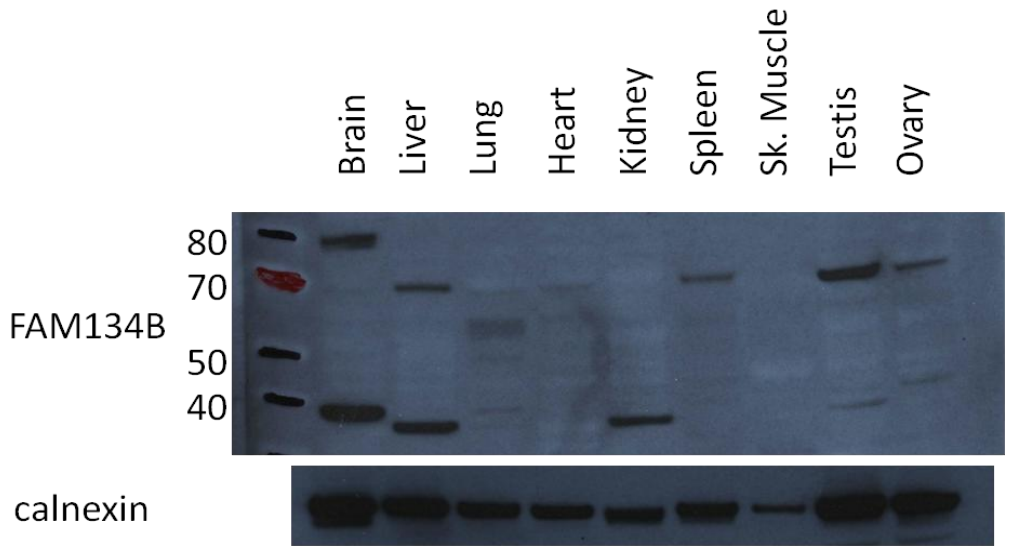

Figure 4.11: FAM134B protein levels in rat tissues

Western blot result showed that FAM134B is mainly expressed in brain, testis, and liver. However, low FAM134B protein levels were also detected in spleen, kidney and ovary. On the other hand, FAM134B protein detected in the rat tissues consists of more than one form. Protein isoform 1, similar to human FAM134B isoform 1, has a protein weight of around 70 kDa, while another form, possibly a rat specific form, is below 40 kDa.

4.4 FAM134B expression is down-regulated in cancer

4.4.1 FAM134B in Chen liver data

In 2002, studies of Chen et al. were published in an article titled 'Gene expression patterns in human liver cancers.' Liver tumor and non-tumor liver sample were collected and microarray gene expression analysis was done on 197 samples (Chen et al., 2002). Results of this expression analysis are publically available at 'Oncomine' database. Previous western blot experiment showed that FAM134B is expressed in normal liver of rat. To test if FAM134B expression varies in normal liver and HCC conditions, FAM134B expression was searched in Chen liver gene expression data. The box plot figure of FAM134B expression in normal liver and HCC samples, and calculated fold changes at 'oncomine' database are given below.

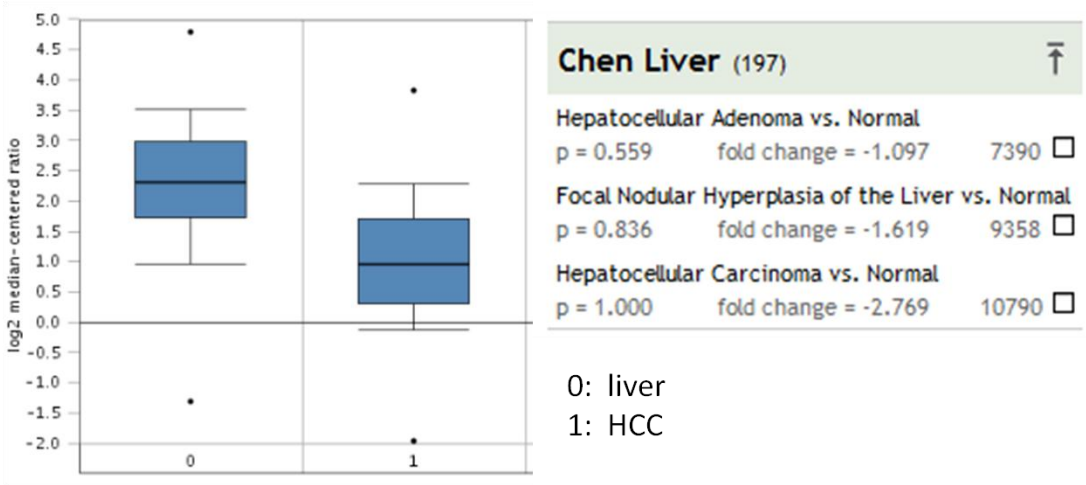

Figure 4.12: FAM134B expression in Chen liver data

According to the Chen liver data, FAM134B expression is down-regulated in hepatocellular carcinoma samples in comparison with the normal liver samples. The fold change between HCC and normal is -2.769 fold, indicating that FAM134B expression is decreased more than 2 fold in HCC.

4.4.2 FAM134B in Wurmbach liver data

Studies of Wurmbach et al. was published in an article titled 'Genome-wide molecular profiles of HCV-induced dysplasia and hepatocellular carcinoma.' Gene expression profiles of 75 samples were analyzed. Among these 75 tissues, there were tissues representing each stem of liver carcinogenic process, including cirrhosis, dysplasia and HCC (Wurmbach et al., 2007). In order to check changes in FAM134B expression during different stages of molecular pathogenesis of HCC, FAM134B expression was searched on Wurmbach liver data at 'oncomine' database.

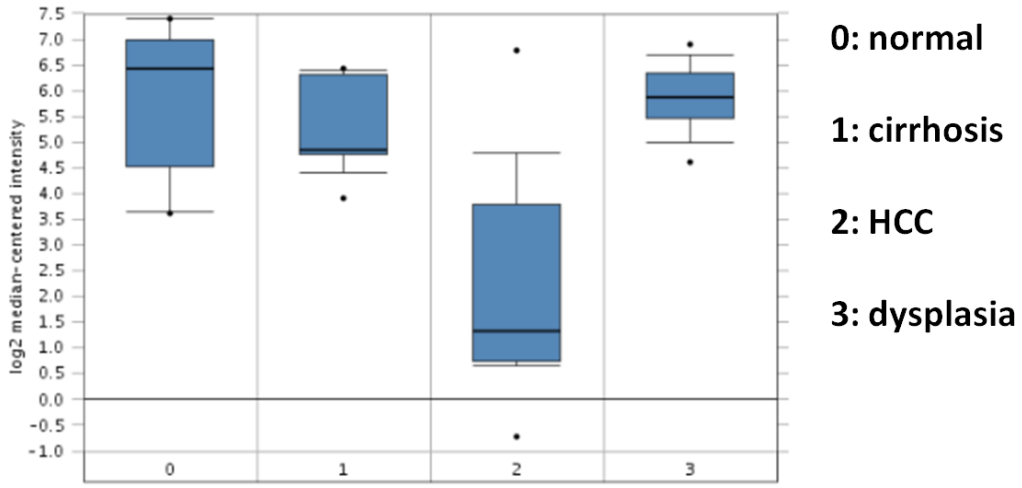

Figure 4.13: FAM134B expression in Wurmbach liver data

According to the analysis of FAM13B4 expression in Wurmbach liver data, FAM134B expression varies between different stages of HCC pathogenesis. Expression is high in normal liver samples, while being decreased in the initial stages of pathogenesis, namely cirrhosis and dysplasia. And, FAM134B expression is decreased far more in HCC. On the other hand, FAM134B expression is inversely

proportional to the grading of HCC cases, done in this study. According to the grading system of hepatocarcinogenesis, FAM134B expression is further decreased as going from grade 1 to grade 3 of HCC samples (data not shown).

4.5 FAM134B expression is increased in response to ER stress

Previous studies showed that FAM134B protein is localized onto cis-Golgi membrane (Kurth et al., 2009), or endoplasmic reticulum membrane (Tasdemir et al. unpublished data). In addition to its localization on ER membrane, FAM134B was firstly identified as senescence associated gene by our group (Ozturk et al. unpublished data). Because senescent cells starts secreting substantial amount of cytokines and growth factors, ER is forced to work at maximum capacity, resulting in induction of ER stress and UPR. Depending on these observations, to test the hypothesis that endoplasmic reticulum stress (ER stress) might affect the expression of FAM134B gene encoding for a ER resident protein, FAM13B4 expressions were tested in response to induction of ER stress with distinct ER stress inducers.

4.5.1 Tunicamycin treatment increases FAM134B expression in Huh7 cells

Tunicamycin is a mixture of antibiotics used as an agent for ER stress induction. It prevents the synthesis of N-linked glycoproteins in the ER, resulting in insufficient modifications leading to accumulation of these proteins and ER stress.

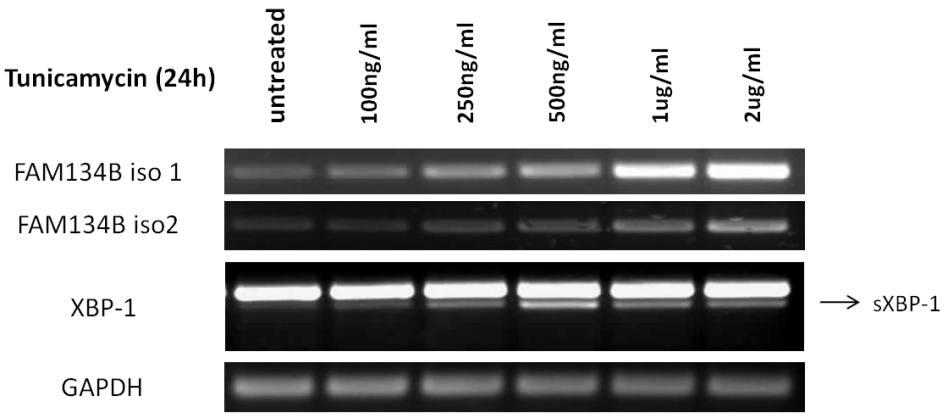

Figure 4.14: Tunicamyin treatment causes an increase in FAM134B expression

According to the semi-quantitative RT-PCR results shown above, tunicamycin-induced ER stress stimulates FAM134B expression in Huh7 cells. In this experiment, tunicamycin treatment was done for 24 h with different concentrations, ranging from 100ng/ml to 2ug/ml. As seen in the figure, both isoforms 1 and isoform 2 expressions of FAM134B are increased in response to the treatment, with a gradual amplification in correlation with the concentration of the tunicamycin. Here, XBP-1 was used as a marker for ER stress. Under unstressed conditions XBP-1 mRNA is found in unspliced form, whereas, induction of ER stress results on splicing of XBP-1, producing a 26 bp shorter mRNA, which is used as a marker for ER stress (Lee et al., 2002). GAPDH was used as an internal control for this semi-quantitative RT-PCR experiment.

4.5.2 Dithiothreitol (DTT) treatment increases FAM134B expression in Huh7 cells

DTT is a common reducing agent, targeting disulfide bonds on proteins. Thanks to its reducing activity, DTT is also used as a common ER stress inducer (Li et al., 2011). Therefore, in addition to tunicamycin treatment, DTT treatment was also tested as a different type of ER stress induction method in Huh7 cells. In this experiment, Huh7 cells were treated with the given concentration of DTT for 2 days. Cells were collected, total RNAs were extracted and cDNAs were synthesized from DTT treated samples. The figure below shows the RT-PCR results of the experiment.

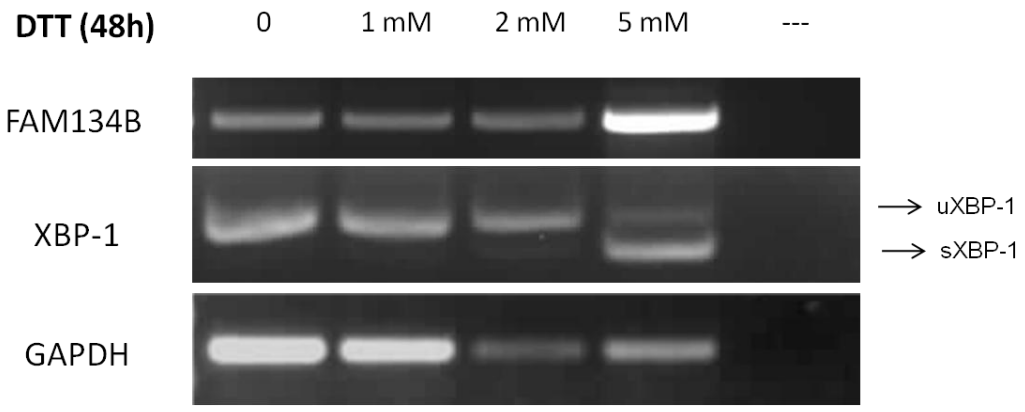

Figure 4.15: DTT treatment causes an increase in FAM134B expression

According to these results, DTT treatment causes an increase in total FAM134B expression in Huh7 cells. This results is promising if it is considered with the previous results showing that tunicamycin induced ER stress increases FAM134B expression. Detection of increased FAM134B expression upon DTT treatment, further supported the findings that FAM134B gene expression is responsive to ER stress, induced by distinct factors.

4.5.3 Thapsigargin treatment increases FAM134B expression in Huh7 cells

Thapsigargin is a reagent targeting SERCA pumps on the ER membrane. Therefore, thapsigargin treatment is a cause of ER stress through the mechanism affecting the calcium ion content of the ER (Denmeade and Isaacs, 2005). In order to test the effect of a different type of ER stress induction on FAM134B experiment, thapsigargin treatment was done Huh7 cells for 48 hours. Total mRNAs were isolated, cDNAs were synthesized and qRT-PCR analysis was done with total FAM13B4 primers.

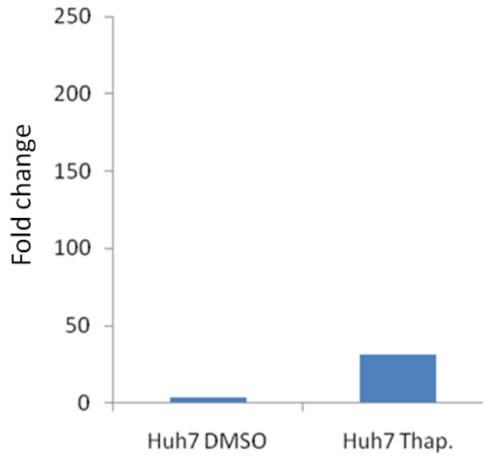

Figure 4.16: Thapsigargin treatment increases FAM134B expression in Huh7 cells

According to this qRT-PCR result, FAM134B expression is increased more than 20 fold in response to thapsigargin treatment for 48 hours, with a thapsigargin concentration of 2µM in DMSO. This result indicates that FAM134B expression is also up-regulated in response to calcium dependent ER stress in Huh7 cells.

4.5.4 Detection of changes at protein levels of FAM134B in response to ER stress

Previous results indicated increased FAM134B mRNA levels in response to ER stress induction by tunicamycin, DTT or thapsigargin. Since these agents can induce ER stress through different mechanism, it is possible to state that FAM134B mRNA levels are up-regulated as a result of general ER stress, independent of the basis of stress induction. In order to detect changes at protein levels of FAM134B in response to ER stress induction, western blot experiments were done following ER stress induction in a few cell lines. Snu387 is a poorly-differentiated cell line with high FAM134B protein isoform 1 level, while Huh7 is a well-differentiated cell line with very low FAM134B protein compared to Snu387 (see Figure 4.10). These cell lines were treated with 500 ng/ml tunicamycin for different time points and changes in FAM134B protein levels were detected with immunoblotting experiments.

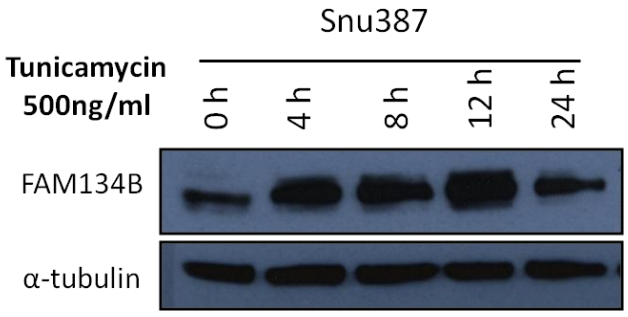

Figure 4.17: Tunicamycin increases FAM134B protein levels in Snu387 cells

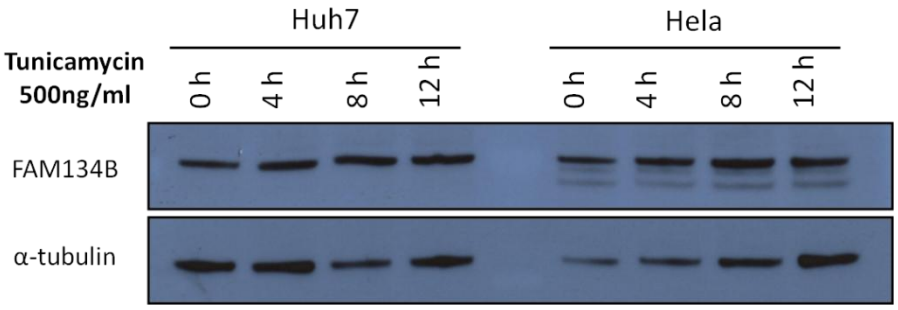

Figure 4.18: Tunicamycin treatment does not affect FAM134B protein levels in Huh7 and Hela cells

Western blot results showed that in response to tunicamycin induced ER stress cannot induce up-regulation of FAM134B protein in all cell types. While FAM13B4 protein levels were detected to be increased in Snu387 cells, in Huh7 and Hela cells, tunicamycin treatment did not cause a significant change in FAM134B at protein level. Similar different responses to ER stress induction at the level of FAM134B protein were also observed in Huh7 and FAM134B overexpressing Huh7 cells (see Figure 4.30).

4.5.5 Change in FAM134B expression at G2-M and G1 stages of cell cycle

In order to test whether FAM134B expression varies between stages of cell cycle, cell synchronization analysis was done using Huh7 cells. In brief, Huh7 cells were treated with nocadozole for 18 hours. After 18 hours, nocadozole was removed and samples were collected at every 5 hours. Semi-quantitative RT-PCR experiment was done to detect changes in the expression on FAM134B.

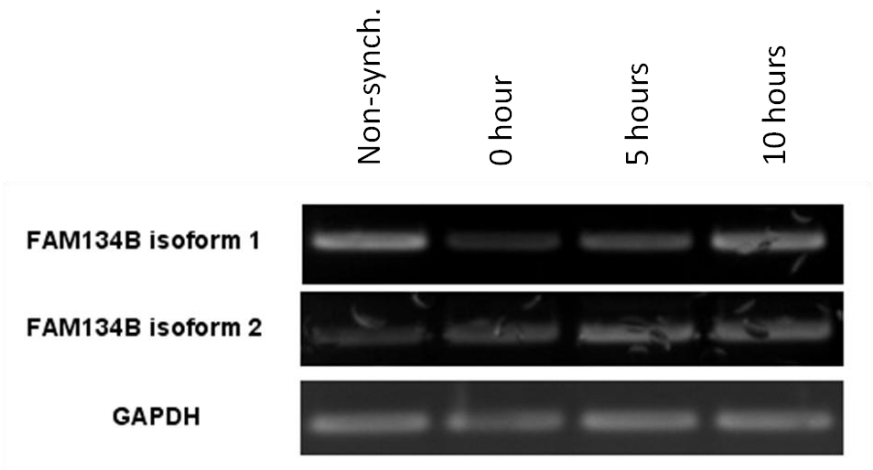

Figure 4.19: FAM134B expression in synchronized Huh7 cells, detected by RT-PCR

According to the synchronization results, FAM134B isoform 1 expression is considerably decreased in G2-M stage (0 hour) of Huh7 cells, compared to non-synchronized Huh7 cells. And also, its expression is gradually increased following the removal of nocadozole, at 5^{th} and 10^{th} hours corresponding to G1 stage. On the

other hand, isoform 2 expression does not change as significant as isoform 1, only slightly increasing at 5th hour compared to time 0. There is no change at expression level of FAM134B isoform 2 between non-synchronized Huh7 cell and G2-M phase synchronized cells.

4.6 Differential expression of FAM134B in well- and poorly-differentiated cell lines might be linked to their ER stress status

Analysis of FAM134B expression in Chen and Wurmbach data sets showed that FAM134B expression is down-regulated in HCC compared to normal liver. Furthermore, within the subgroups of HCC, samples with higher grade have low levels of FAM134B expression in comparison with low grade samples (see Figures 4.12 and 4.13). On the other hand, previous experiment showing FAM134B protein levels in rat tissues is likely to further support these findings, because FAM134B protein was detected in the liver of rat. Nevertheless, tissue results and microarray data results are not seem to be correlated with the results obtained from the detection of FAM134B in HCC cell line panel. According to these results, FAM134B was detected to be highly expressed in almost all poorly-differentiated cell lines, while expressions were low in well-differentiated HCCs. These controversial results showing that poorly-differentiated group (representing advanced stage of HCC) have higher FAM13B4 expression than that of well-differentiated group (representing early HCC) were actually explained by their status of ER stress.

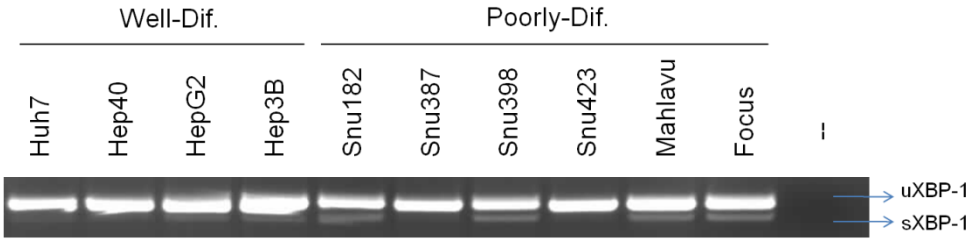

Figure 4.20: ER stress status of HCC cells, detected by sXBP-1 RT-PCR

Figure 4.20 shows semi-quantitative RT-PCR results of XBP-1, which is an ER stress marker, in well- and poorly-differentiated cell lines. According to these results,

most of poorly-differentiated cells have an active UPR at basal level, without any treatment. However, well-differentiated HCC cells do not have an activated UPR, indicated by lack of sXBP-1.

This observation is further supported by detection of ER stress response in these cell lines at the protein level. Other ER stress markers, phospho-PERK and phospho-eIF2α were used as ER stress markers in this experiment.

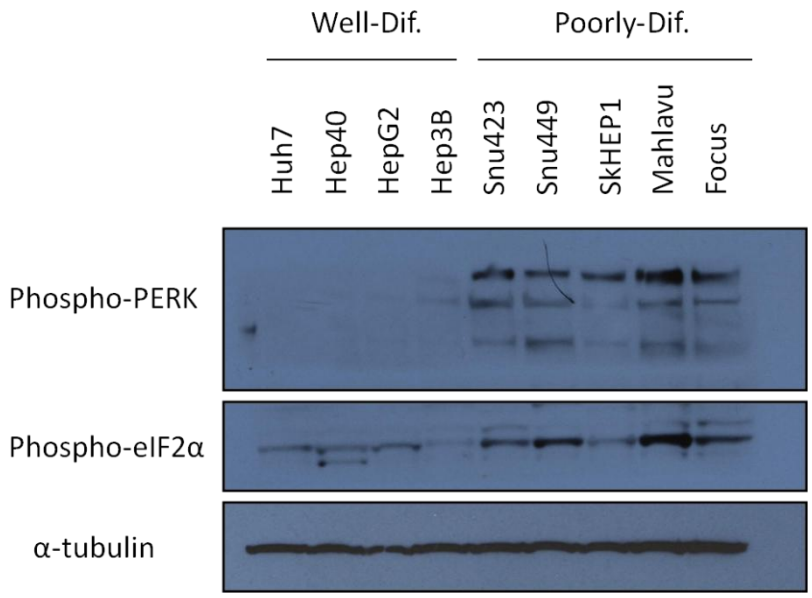

Figure 4.21: ER stress status of HCC cell lines, detected by western blot

According to the western blot results, both of PERK branch ER stress markers, phospho-PERK and phospho-eIF2α are active in poorly-differentiated cell lines, while only a slight eIF2α phosphorylation is detected in well-differentiated cell lines. Unlike poorly-differentiated cell lines, well-differentiated cell lines do not show PERK phosphorylation at basal level, under untreated conditions. In this experiment α-tubulin was used as a loading control for the western blot experiment.

4.7 FAM134B overexpression in Huh7 cells

Our group previously produced stable clones of Huh7 cell lines overexpressing FAM134B isoform 1. In order for overexpression studies, Huh7 cells were preferred

because both of FAM134B transcript variants are low in this cell line. Stable ectopic overexpression of isoform 1 was done using CT-3XFLAG-FAM134B-iso1 (C-terminal Flag tagged) and NT-3XFLAG-FAM134B-iso1 (N-terminal Flag tagged), and p3XFLAG-CMV10 vector as a control (Tasdemir et al. unpublished data).

4.7.1 Testing FAMB134 overexpressing stable Huh7 clones

Stable Huh7 clones overexpressing FAM134B isoform 1 and one control clone (CMV10-11) were tested with western blot using antibodies against FAM134B and Flag tag. Western blot results are given below.

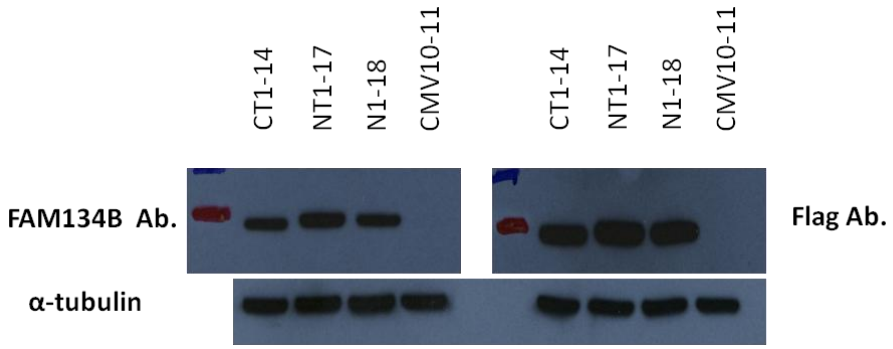

Figure 4.22: Testing FAM134B overexpressing clones, detected by western blot

Figure 4.22 shows that all three clones are positive isoform 1 overexpressing clones of Huh7. Detection of the same band with Flag antibody shows that the band do not represent endogenous FAM134B protein but instead Flag-tagged FAM134B isoform 1 expressed form the vector construct.

4.7.2 FAM134B overexpression does not induce ER stress

FAM134B expression is regulated by induction of ER stress. Treatments with tunicamycin, DTT or thapsigargin result in up-regulation of FAM134B expression in Huh7 cell lines (see Figures 4.14, 4.15, 4.16). These results contributed to the establishment of a new hypothesis that FAM134B overexpression itself might induce

a ER stress response, and activate UPR without any treatment. This hypothesis was tested by detecting ER stress marker XBP-1 in FAM134B overexpressing Huh7 cells (Huh7-FAM134B) and in control CMV10-11 Huh7 clones (Huh7-Control).

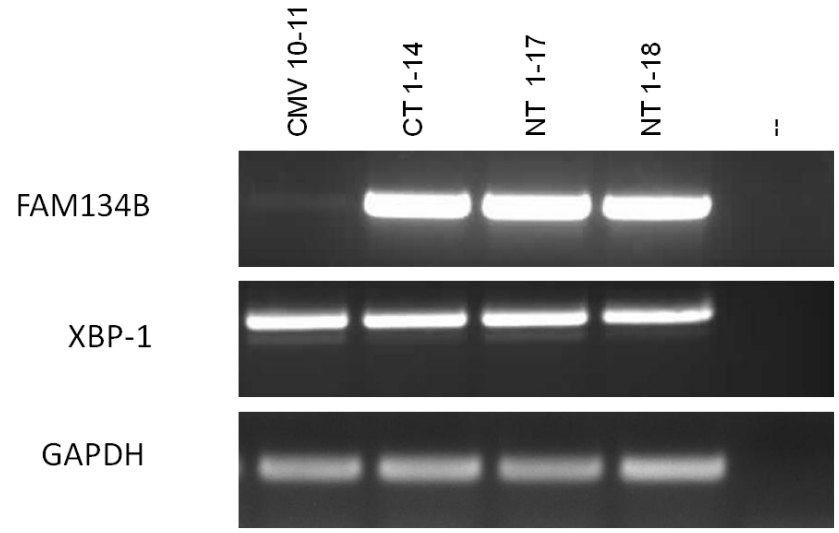

Figure 4.23: Testing ER stress in Huh7-FAM134B clones, detected by RT-PCR

This RT-PCR experiment showed that even though FAM134B expression is correlated with the ER stress response, overexpression of FAM13B4 does not contribute to induction of ER stress response under untreated conditions. In other words, FAM134B itself is not sufficient to activate IRE1 branch of UPR, functioning in the transduction of UPR signaling.

4.7.3 FAM134B overexpression does not promote epithelial-to-mesenchymal transition in Huh7 cells

Huh7 cells are categorized as well-differentiated cells, possessing epithelial like characteristics, such as E-cadherin expression, and hepatocyte markers (Yuzugullu et al., 2009). Epithelial like characteristic of Huh7 cells can be observed in in vitro culture. However, FAM134B overexpressing Huh7 clones were observed to be dissimilar to parental and Huh7-Control clones, having more spiked cell shape and

fibroblast like morphology (data not shown). On the other hand, studies of Ulianich et al. showed that tunicamycin and thapsigargin treatment to PC Cl3 thyroid epithelial cells triggers dedifferentiation, resulting a epithelial-to-mesenchymal (EMT) transition of these cells. This was found to be associated with downregulation of E-cadherin, upregulation of vimentin, alpha-smooth muscle actin (Ulianich et al., 2008). In order to test such an EMT phenotype occurs in our FAM134B overexpressing Huh7 clones, epithelial and mesenchmal markers were aimed to be detected in these clones by immunofluorescence (IF) and RT-PCR experiments.

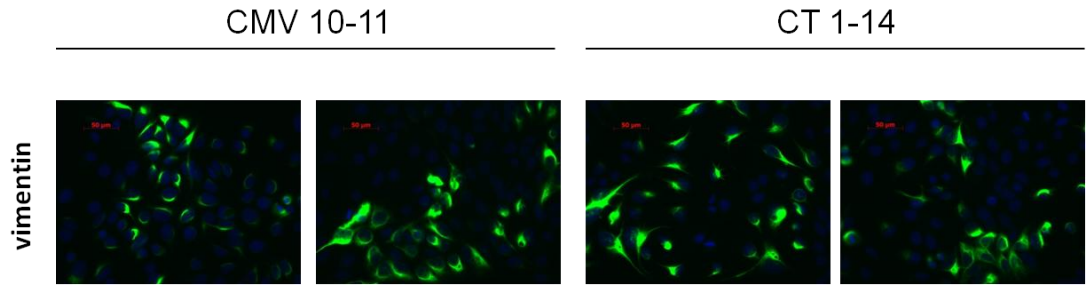

Figure 4.24: Detection of EMT marker vimentin in Huh7-FAM134B cells by IF

Results of IF experiment showed that vimentin expression is not considerably changed in Huh7-FAM134B (CT 1-14) cells compared to Huh7-Control (CMV 10-11) cells, detected by low heterogeneous vimentin staining in both cases.

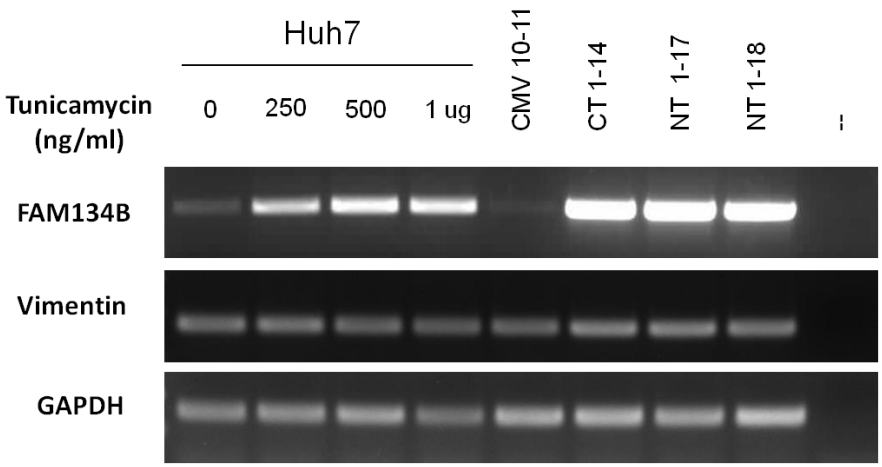

Figure 4.25: Neither tunicamycin treatment, nor FAM134B expression induces EMT in Huh7

In addition to the immunofluorescence experiment, possible change in vimentin expression was tested by semi-quantitative RT-PCR experiment. According to the results shown above, FAM134B overexpression does not induce vimentin expression in Huh7 cells. Besides, unlike thyroid epithelial cells, Huh7 epithelial like cells does not undergo epithelial-to-mesenchymal transition upon tunicamycin treatment.

4.7.4 FAM134B overexpression does not induce autophagy in Huh7 cells

Dysregulation of ER homeostasis might cause induction of autophagy in order to facilitate the removal of unfolded proteins. Induction of ER stress by inducers, such as tunicamycin and DTT, also triggers autophagic response that can be detected by autophagy markers (Qin et al., 2010). In our Huh7 HCC model, activation of autophagy upon ER stress induction by tunicamycin was shown with a western blot experiment.

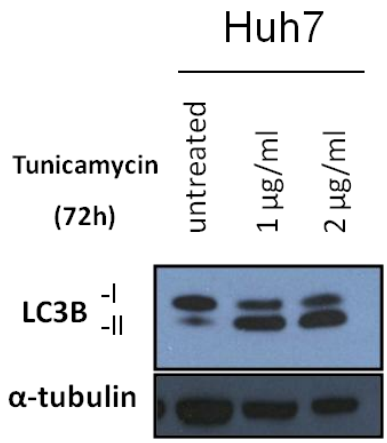

Figure 4.26: Tunicamycin induces autophagy in Huh7 cells

Figure 4.26 shows western blot results of autophagy induction upon tunicamycin treatment to Huh7 cells for 72 hours. Here, LC3B is a commonly used autophagy marker, making transition from its longer form I to shorter form II in the autophagic response (Barth et al., 2010). As seen in the figure, both 1µg/ml and 2µg/ml tunicamycin treatment induces autophagy in Huh7 cells. α-tubulin was used as an equal loading control for the western blot experiment.

Tunicamycin induces autophagy in Huh7 cells. This fact made us hypothesize that FAM134B might be related to the induction of autophagy in response to ER stress. In order to test if FAM134B overexpression on Huh7 cells might affect autophagy in the lack of any ER stress induction, autophagy marker LC3B was checked in the Huh7-FAM134B clones and their control counterpart.

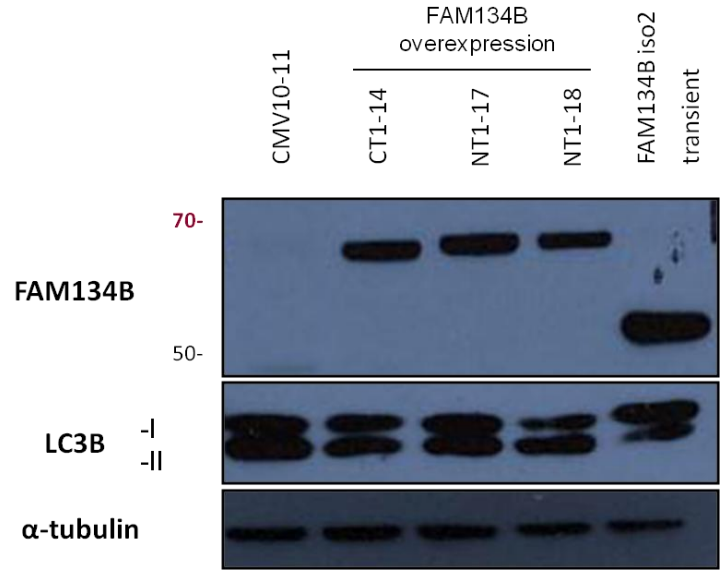

Figure 4.27: FAM134B overexpression does not induce autophagy in Huh7 cells

According to the results shown in Figure 4.27, FAM134B overexpressing Huh7 clones, CT1-14, NT1-17 and NT1-18, does not differ in their autophagic response when compared to Huh7-Control (CMV10-11). On the other hand, in order to test if FAM134B protein isoform 2 can affect on autophagy, this form was overexpressed by transient transfection into Huh7 cells. According to the results, overexpression of FAM134B isoform 2 does not induce autophagy in Huh7 under untreated conditions.

4.8 Induction of ER stress impairs proliferation of Huh7 cells

Accumulation of unfolded proteins in the ER as a result of various factors described before damages ER homeostasis. Impaired homeostasis is signaled downstream through UPR to make cells undertake precautions against risky fates of the cells. Apart from triggering a signal to overcome the stress at the initial response, extended

and persistent stress is likely to be prevented by directing stressed cells to death. On the other hand, studies of Chiang et al. showed that N-glycosylation inhibitor tunicamycin treatment to Hep3B and HepG2 cells inhibits cell proliferation of these cells, resulting in the G1 arrest. This effect was further identified as associated with the decreases in the expression of key effectors of cell cycle, cyclin D1 and cyclin A (Chiang et al., 2008b). In order to test the effect of ER stress induction on Huh7 cells, BrdU incorporation assay was performed and followed by detection of BrdU positivity with immunofluorescence experiment.

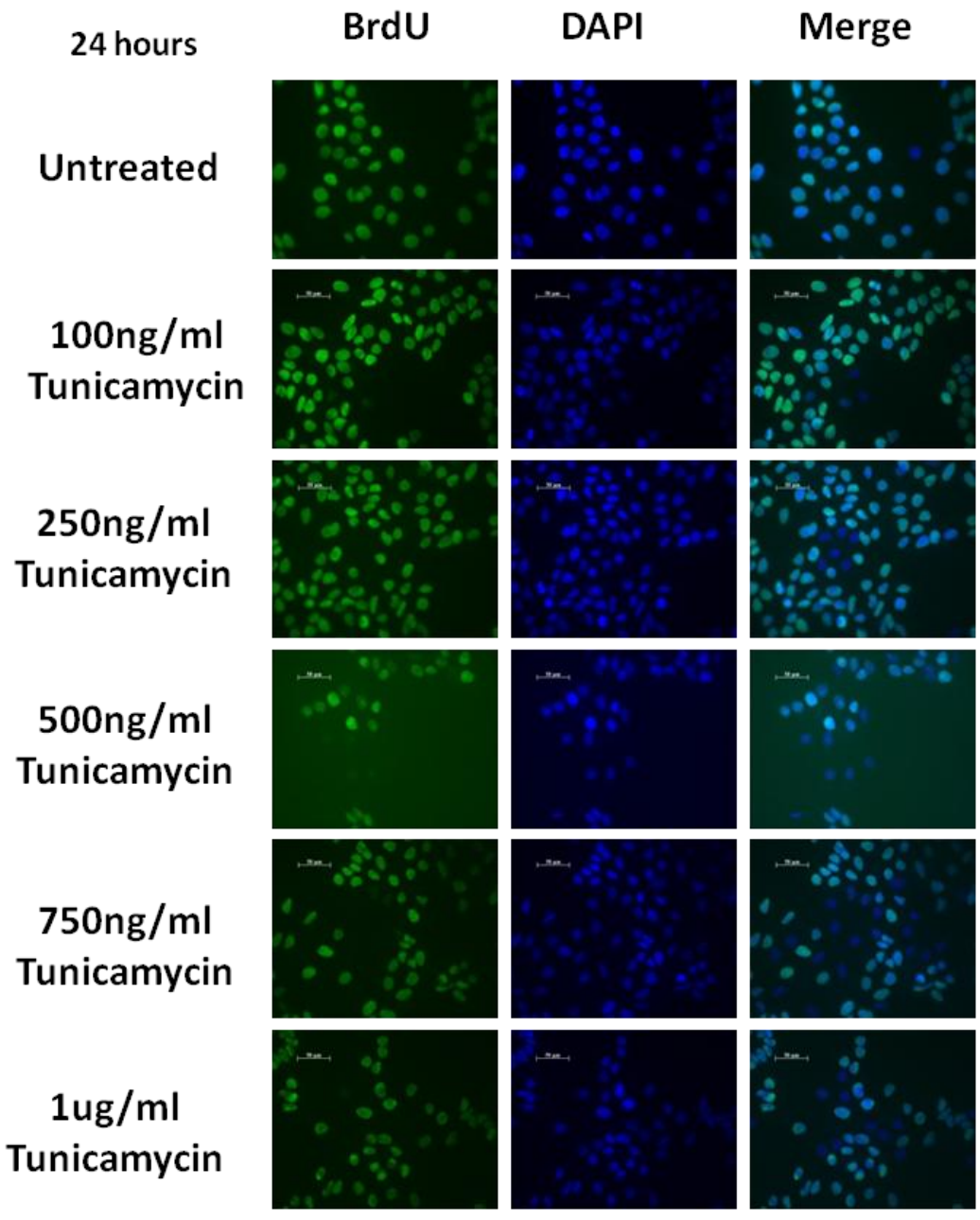

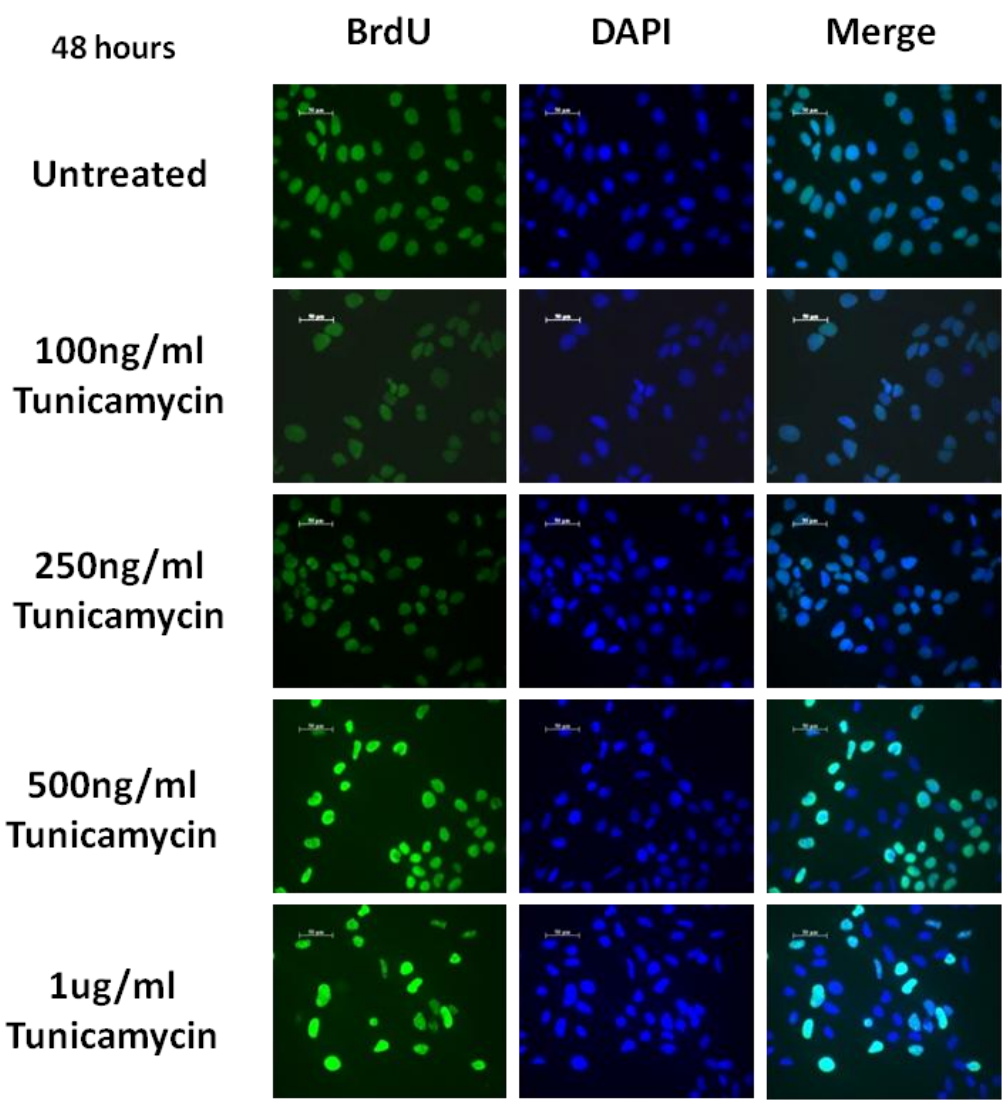
48 hours
BrdU
DAPI
Merge
Untreated
100ng/ml Tunicamycin
250ng/ml Tunicamycin
500ng/ml Tunicamycin
1ug/ml Tunicamycin

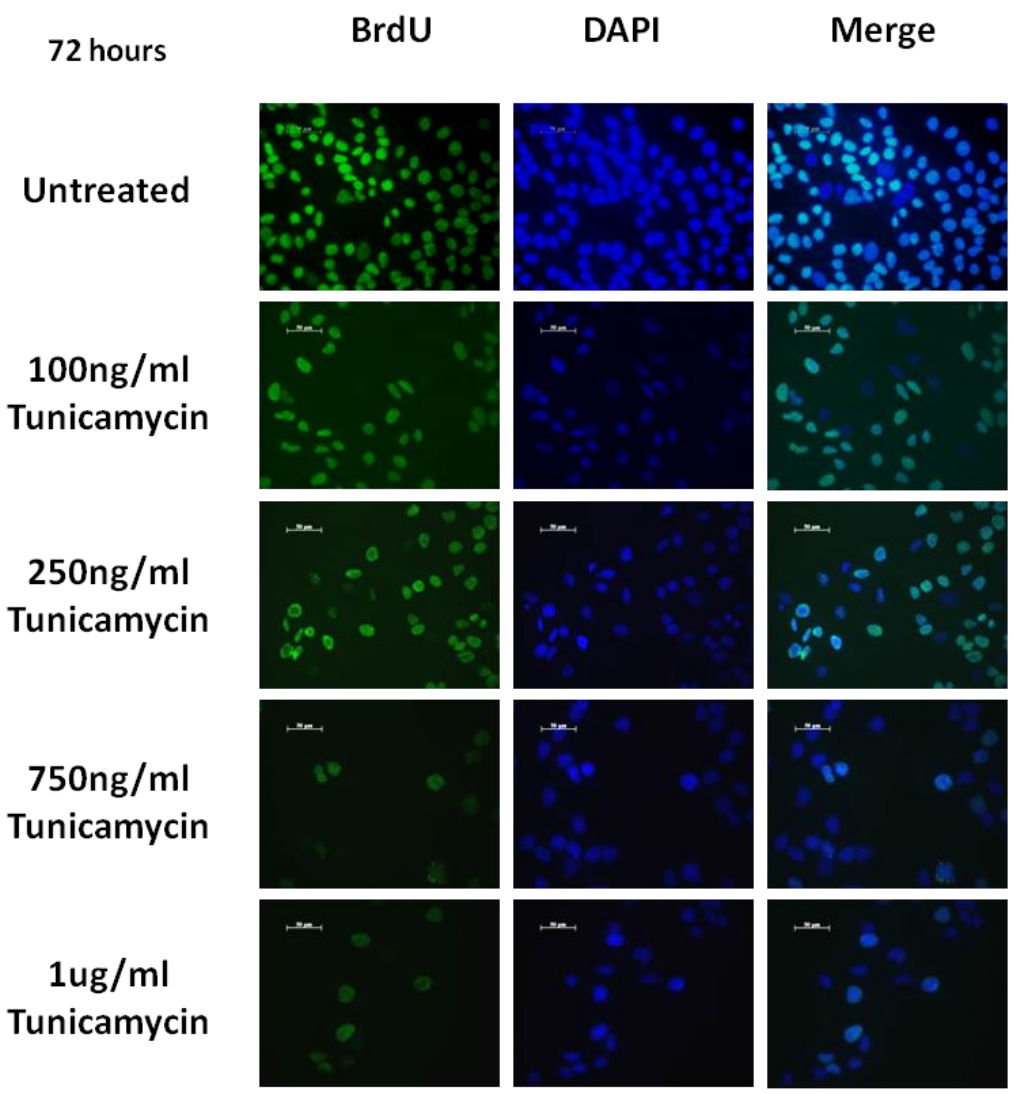

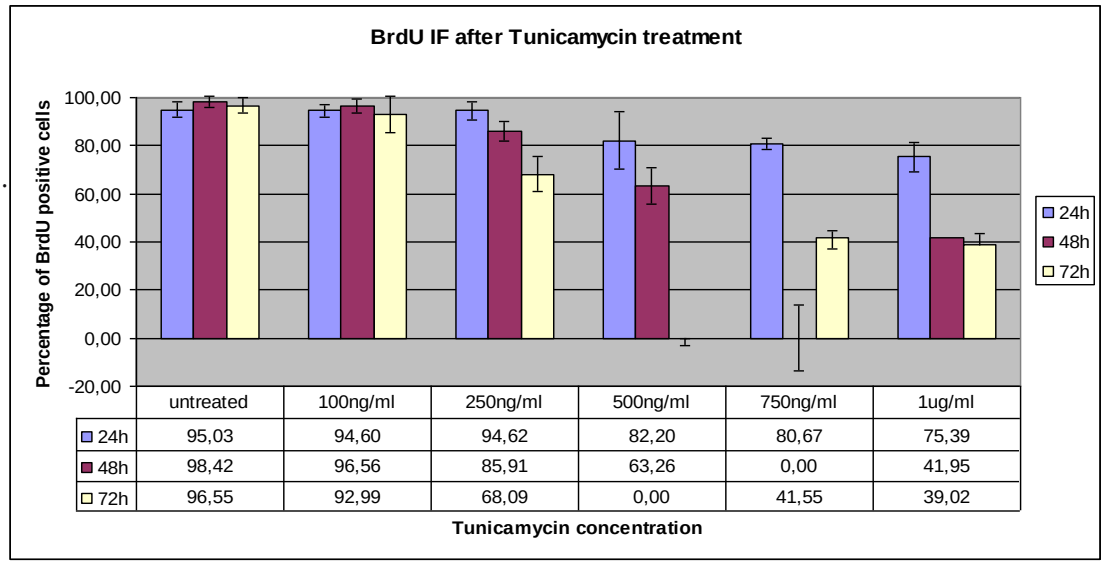

	untreated	100ng/ml	250ng/ml	500ng/ml	750ng/ml	1ug/ml
24h	95,03	94,60	94,62	82,20	80,67	75,39
48h	98,42	96,56	85,91	63,26	0,00	41,95
72h	96,55	92,99	68,09	0,00	41,55	39,02

Figure 4.28: Tunicamycin inhibits proliferation of Huh7 cells, detected by BrdU IF

According to the results of BrdU incorporation assay following tunicamycin treatment to Huh7 cells, tunicamycin induced ER stress has an effect on proliferation capacity of Huh7 cells. Various concentrations of tunicamycin treatment showed that BrdU incorporation percentage is inversely proportional to the concentration of tunicamycin treatment, less BrdU positivity in response to higher tunicamycin treatment. Concentrations of 750ng/ml and 1µg/ml can decrease BrdU positivity of Huh7 cells by 60% after 48h or 72h treatments. On the other hand, these results showed that long term (48h or more) tunicamycin treatment is much more effective in comparison to 24 h treatment, with a difference of almost 40% more reduction. Furthermore, 100ng/ml concentration is not sufficient to decrease proliferation of Huh7 considerably, possibly due to the fact that Huh7 liver cancer cells are resistant to ER stress to some extent.

Effects of tunicamycin on proliferation of Huh7 cells were also shown by detection of a key regulator of cell cycle. Retinoblastoma protein (pRb) is an important tumor suppressor, which is active when hypophosphorylated and able to inhibit cell cycle progression. Phosphorylation of Rb inactivates retinoblastoma protein resulting in the promotion of cell cycle (Vietri et al., 2006). Therefore, in order to determine the effect of tunicamycin treatment to cell cycle and proliferation of Huh7 cells, changes in pRb phosphorylation were showed by immunoblotting. Tunicamycin treatments were done with different concentrations and at different time point.

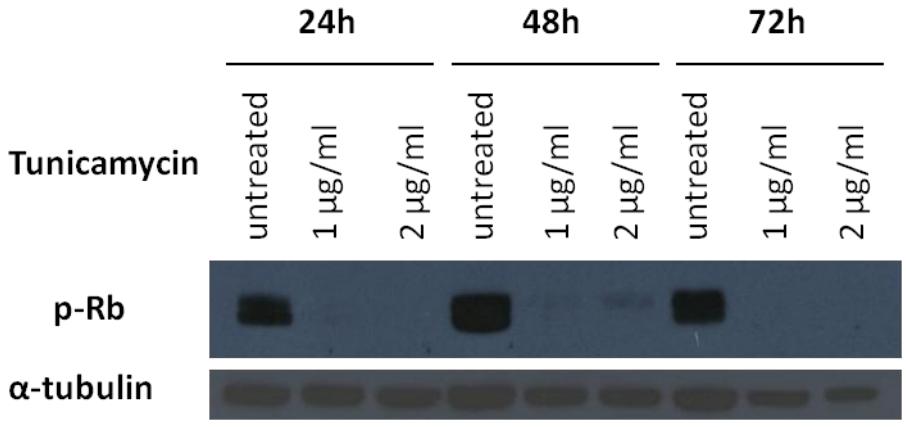

Figure 4.29: Tunicamycin induces pRb activation and cell cycle arrest in Huh7 cells

As seen in Figure 4.29, tunicamycin treatment results in pRb dephosphorylation even after 24 hours. This result shows that following tunicamycin exposure, Huh7 cells try to stop cell cycle by activating pRb. pRb dephosphorylation is directly correlated with the inhibition of cell proliferation as detected in Figure 4.28 by BrdU incorporation assay.

4.9 FAM134B increases sensitivity to thapsigargin induced apoptosis in Huh7 cells

4.9.1 Western blot experiment

Severe and prolonged ER stress causes induction of apoptotic response. The elements of UPR having role in apoptosis induction are reviewed at the introduction part (see Sec. 1.3.4). To test possible role of FAM134B protein in thapsigargin induced apoptosis response, experiments on detection of the apoptotic response were done, comparing responses of Huh7-FAM134B (CT1-14) and Huh7-Control (CMV10-11) clones.

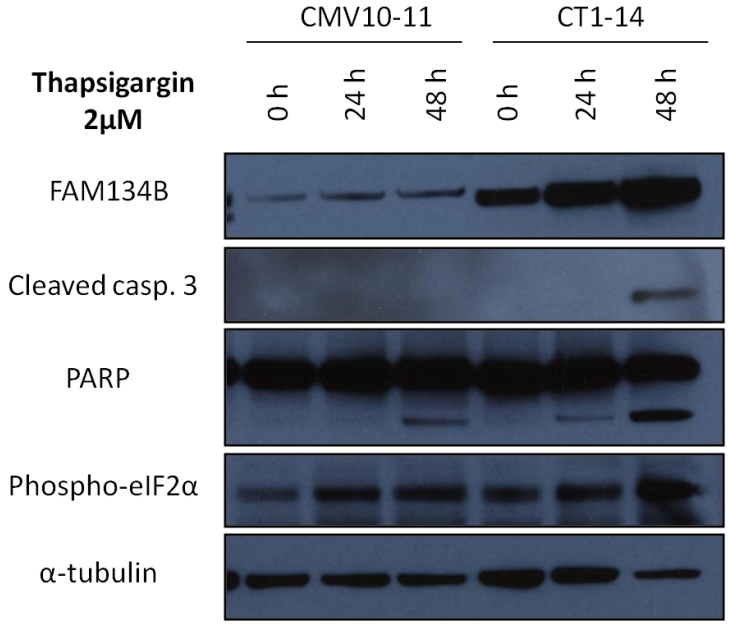

Figure 4.30: FAM134B increases sensitivity to thapsigargin induced apoptosis in Huh7 cells, detected by western blot

According the results shown in the Figure 4.30, FAM13B4 overexpressing Huh7 cells (CT1-14) are more sensitive to thapsigargin induced apoptosis compared to control Huh7 cells under the same conditions. Upon thapsigargin treatment with the concentration of 2μM, PARP cleavage was detected after 24h in Huh7-FAM134B cells while it was not detected in control cells. Furthermore, at 48 hour, executioner caspase 3 is cleaved and activated in Huh7-FAM134B cells while this activation is not observed in Huh7 control cells. On the other hand, eIF2α phosphorylation levels also differ between these two clones. Its phosphorylation in Huh7-FAM134B cells is higher than that of Huh7-Control cells at 48h, indicating that PERK branch activation is more intense in FAM13B4 overexpressing Huh7 cells.

Another critical observation obtained from this western blot results is that thapsigargin treatment to Huh7-Control cells slight increases the FAM134B protein level; whereas, treatment to Huh7-FAM134B cells causes a considerable upregulation at FAM134B protein level upon treatment with the same concentration and duration. According to this western blot result, and results obtained in Figures 4.17 and 4.18, FAM134B protein level is amplified more significantly in cells that already have high FAM134B protein level, in response to ER stress induction. Put another way, if FAM134B protein level is low in a cell, ER stress induction does not substantially provide an increase at protein level of FAM134B. This might indicate a possible auto-regulation dependent control of FAM134B protein.

4.9.2 Cell cycle analysis with flow cytometry

In addition to western blot experiment, effects of FAM134B overexpression on thapsigargin induced apoptosis sensitivity was experimented by cell cycle analysis using propidium iodide. Propidium iodide is an intercalating reagent with a fluorescent activity. It can be used for detection of the DNA content due to its ability to bind DNA. In this study, propidium iodide staining of DNA was used for cell cycle analysis depending on the idea that fluorescent signal obtained from the dye corresponds to particular phase of cell cycle. Propidium iodide measurements and percentages of cell cycle analysis following thapsigargin treatment to Huh7-FAM134B and Huh7-Control cells are shown below.

Huh7-Control, DMSO+

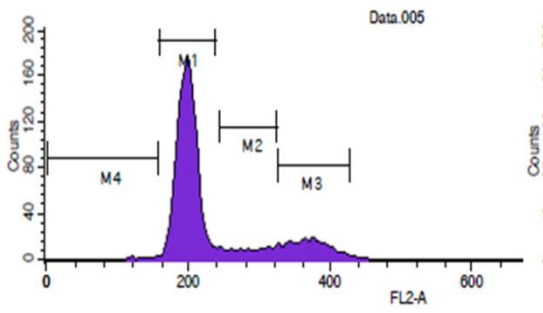

Histogram Statistics

File: Data.005 Acquisition Date: 07-Mar-11
Gate: G2 Gated Events: 7771
Total Events: 10000 X Parameter: FL2-A (Linear)

Marker	Left, Right	Events	% Gated	% Total	CV
All	0, 1023	7771	100.00	77.71	28.88
M1	159, 239	5732	73.76	57.32	6.63
M2	245, 325	685	8.81	6.85	8.45
M3	327, 428	1212	15.60	12.12	6.76
M4	2, 157	43	0.55	0.43	11.29

Huh7-Control, Thapsigargin+

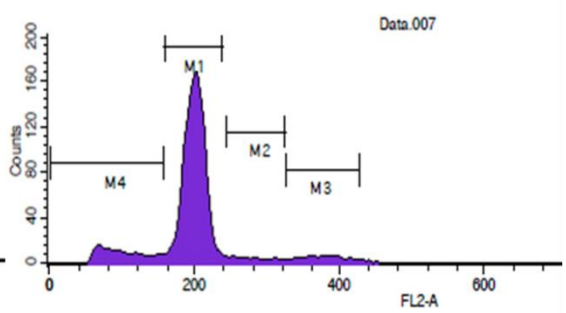

Histogram Statistics

File: Data.007 Acquisition Date: 07-Mar-11
Gate: G2 Gated Events: 7344
Total Events: 10000 X Parameter: FL2-A (Linear)

Marker	Left, Right	Events	% Gated	% Total	CV
All	0, 1023	7344	100.00	73.44	30.32
M1	159, 239	5693	77.52	56.93	6.71
M2	245, 325	284	3.87	2.84	8.35
M3	327, 428	418	5.69	4.18	7.11
M4	2, 157	889	12.11	8.89	27.96

Huh7-FAM134B, DMSO+

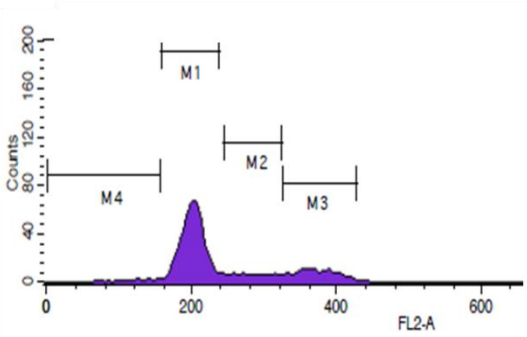

Histogram Statistics

File: Data.013 Acquisition Date: 07-Mar-11
Gate: G2 Gated Events: 3824
Total Events: 5000 X Parameter: FL2-A (Linear)

Marker	Left, Right	Events	% Gated	% Total	CV
All	0, 1023	3824	100.00	76.48	30.20
M1	159, 239	2459	64.30	49.18	7.45
M2	245, 325	456	11.92	9.12	8.13
M3	327, 428	749	19.59	14.98	6.80
M4	2, 157	96	2.51	1.92	22.95

Huh7-FAM134B, Thapsigargin+

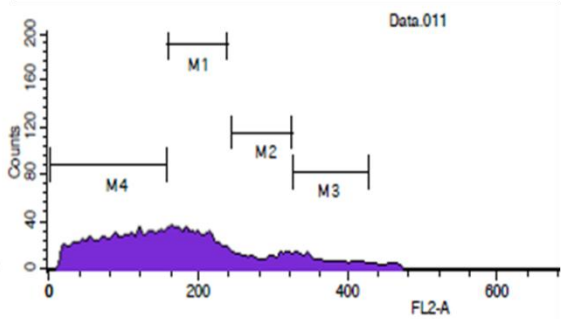

Histogram Statistics

File: Data.011 Acquisition Date: 07-Mar-11
Gate: G2 Gated Events: 7854
Total Events: 10000 X Parameter: FL2-A (Linear)

Marker	Left, Right	Events	% Gated	% Total	CV
All	0, 1023	7854	100.00	78.54	57.70
M1	159, 239	2335	29.73	23.35	11.53
M2	245, 325	845	10.76	8.45	8.72
M3	327, 428	723	9.21	7.23	8.15
M4	2, 157	3683	46.89	36.83	43.05

Figure 4.31: FAM134B increases sensitivity to thapsigargin induced apoptosis in Huh7 cells, detected by propidium iodide based cell cycle analysis

Figure 4.31 shows the flow cytometry results of propidium iodide staining in FAM134B overexpressing Huh7 and control huh7 cells after 2µM thapsigargin treatment for 48 hours. In these figures, M4 represents sub-G1 phase corresponding to apoptotic cells, while M1 represents G1, M2 represents S, and M3 represents G2 phases of cell cycle. According to these results, thapsigargin treatment results in 12.11% apoptotic cells in Huh7-Control cells. However, thapsigargin treatment to FAM134B overexpressing cells resulted in 46.89% apoptotic cells. On the other hand, thapsigargin treatment drastically decreases the percentage of cells at G2 phase; whereas, percentage of cells at G1 phase was slightly increased in Huh7-Control cells. These results indicate that Huh7-FAM134B cells are much more sensitive to the same concentration and duration of thapsigargin treatment.

4.10 FAM134B overexpression impairs cell proliferation during thapsigargin induced ER stress

Such an effect of FAM134B in apoptosis sensitivity was aimed to be further supported by possibly similar effect on cell proliferation. In order to test this hypothesis, real-time cell proliferation analysis was done with Huh7-Control and Huh7-FAM134B cells in response to thapsigargin treatment by using xCELLigence.

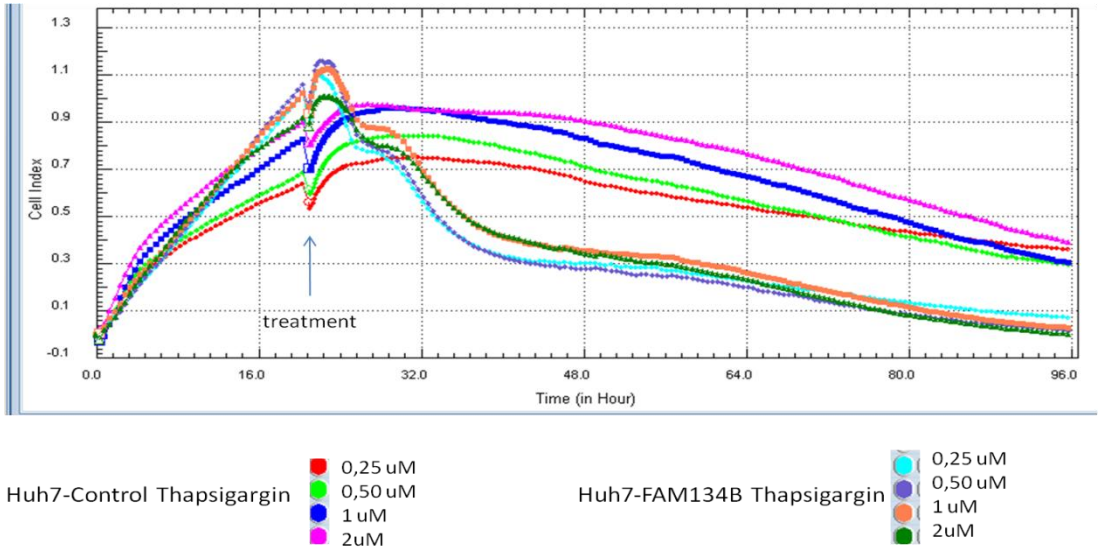

Figure 4.32: FAM134B overexpression impairs proliferation of Huh7 cells during thapsigargin induced ER stress

Real-time cell proliferation assay showed that FAM134B overexpressing Huh7 cells are more sensitive to thapsigargin treatment, detected by immediate reduction in the cell index even 5 hours after treatment. Thapsigargin treatment starts affecting cell proliferation of Huh7-Control cells after approximately 10 hours following the treatment.

These results come up with the interpretation that FAM134B protein increases the effectiveness of thapsigargin treatment, in ways that early and amplified apoptosis response, in addition to early and more significant decrease in proliferative capacity of the cells.

4.11 FAM134B increases sensitivity to tunicamycin induced apoptosis in Huh7 cells

4.11.1 Western blot experiment

The findings that FAM134B overexpression affects both thapsigargin induced apoptosis and cell proliferation response led to experiment similar effect with a different ER stress inducer, tunicamycin. Therefore, Huh7-Control and Huh7-FAM134B cells were treated with 5μg/ml tunicamycin for 48hours to compare their apoptotic responses to the same dose and duration.

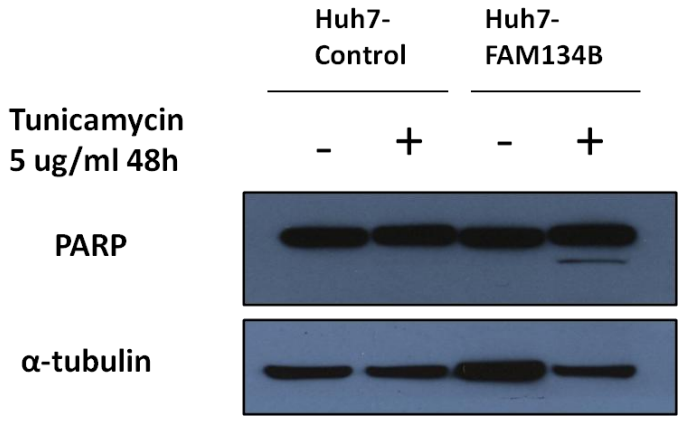

Figure 4.33: FAM134B increases sensitivity to tunicamycin induced apoptosis in Huh7 cells, detected by western blot

Western blot result revealed that FAM134B overexpression also increases sensitivity to tunicamycin induced apoptosis in Huh7 cells. Here, apoptosis is detected with cleaved PARP protein, while α-tubulin was used as a loading control.

4.11.2 Cell cycle analysis with flow cytometry

Increased sensitivity to tunicamycin induced apoptosis was shown using flow cytometry for cell cycle analysis of propidium iodide staining.

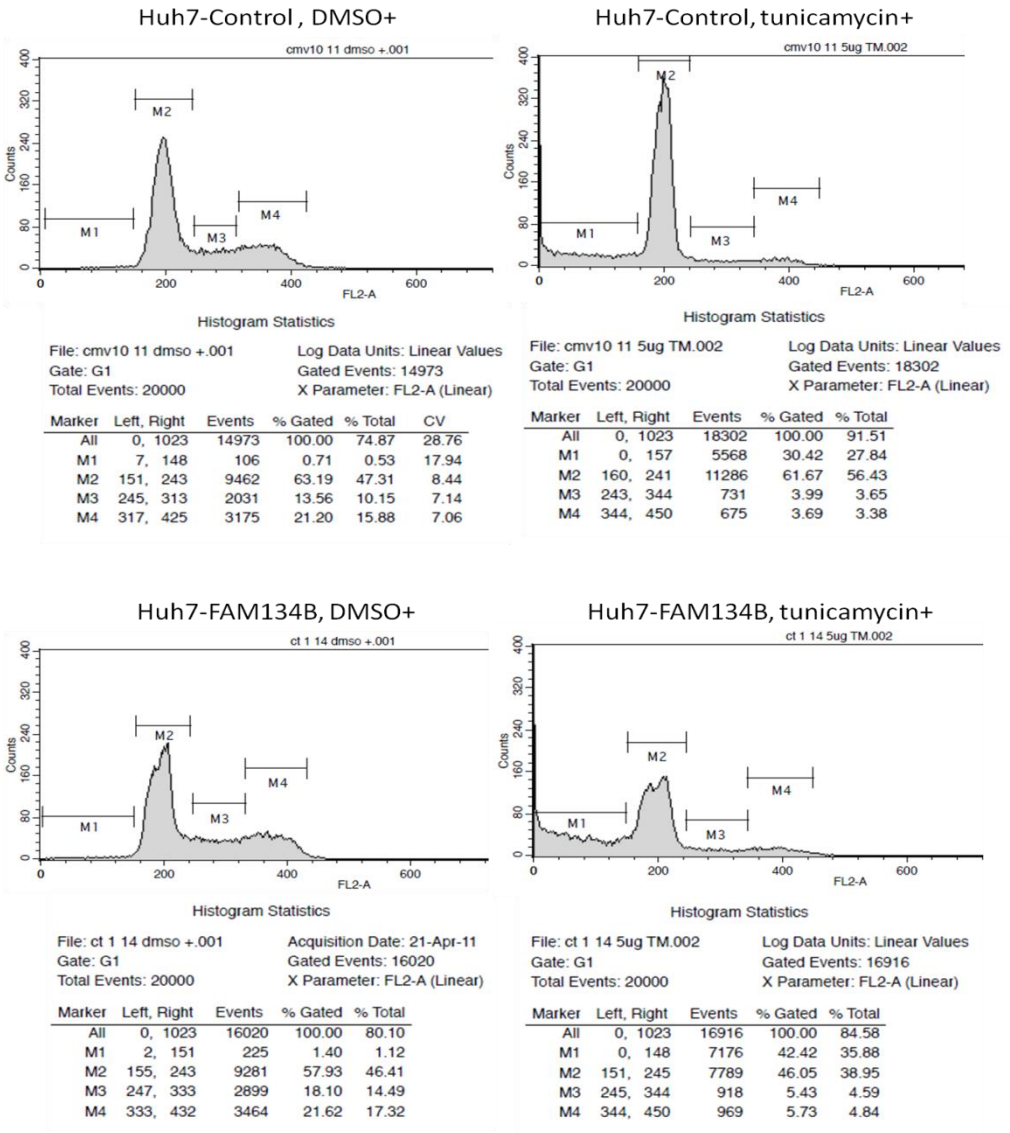

Figure 4.34: FAM134B increases sensitivity to thapsigargin induced apoptosis in Huh7 cells, detected by propidium iodide based cell cycle analysis

According to the results given in Figure 4.34, M1 region corresponds to sub-G1 cells, which are considered as apoptotic cells. Results showed that 5 µg/ml tunicamycin treatment caused 30% of Huh7-Control cells to follow apoptosis, while 42% of Huh7-FAM134B cells entered apoptosis in response to the same treatment condition. Hence, it is possible to state that FAM134B also increases sensitivity to tunicamycin induced apoptosis in Huh7 cells, even though the difference of their percentages is not as great as difference detected in thapsigargin treatment.

4.12 FAM134B overexpression impairs cell proliferation during tunicamycin induced ER stress

Effect of FAM134B in tunicamycin treatment was further tested in a way that these cells are possibly influenced in terms of their proliferation efficiency during tunicamycin induced ER stress. Proliferative responses of Huh7-Control and Huh7-FAM134B cells were experimented using xCELLigence real time system.

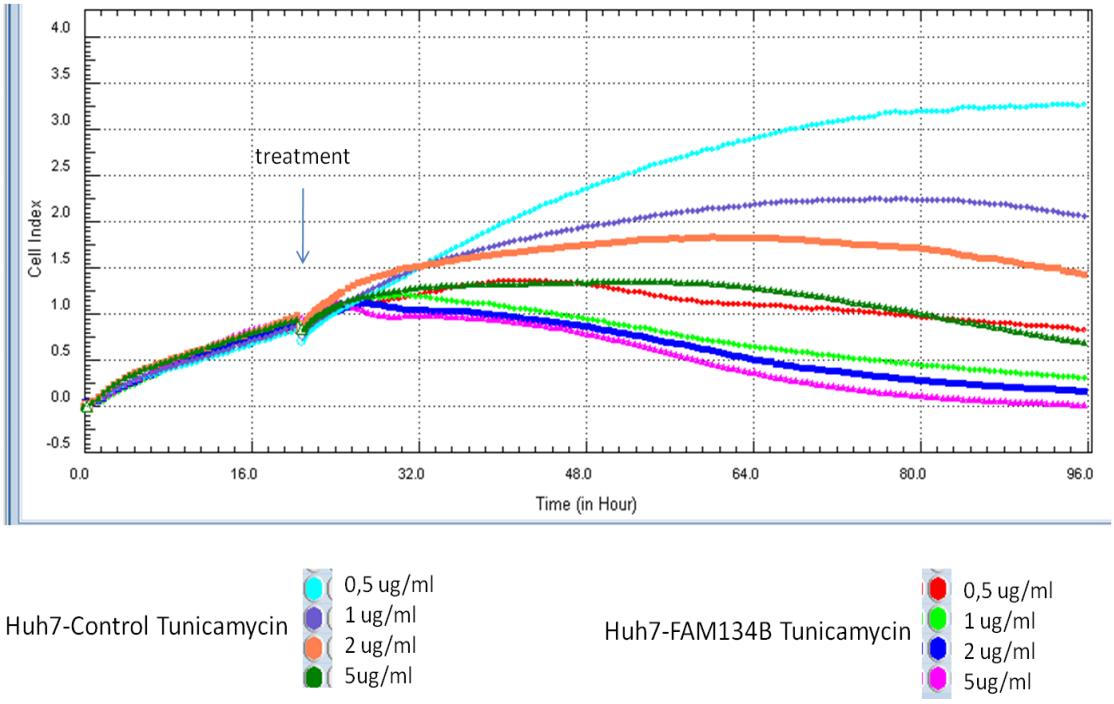

Figure 4.35: FAM134B overexpression impairs proliferation of Huh7 cells during thapsigargin induced ER stress

Figure 4.35 shows real time proliferation of Huh7-FAM134B and Huh7-Control cells after treatment with various concentrations of tunicamycin. According to the results, cell indexes are the same at the time when treatments are done. Soon after treatments, Huh7-FAM134B cells' cell indexes start decreasing, while that of Huh7-Control cells still increases for a while. In brief, proliferation analysis indicated that not only in terms of apoptosis response, but also FAM134B is associated with the impairment of cell proliferation during tunicamycin induced ER stress response in Huh7 cells.

4.13 FAM134B is likely to increase the severity of ER stress response

Previous experiments showing stronger effects of thapsigargin on FAM134B overexpressing cells come up with questioning why these cells are more susceptible to thapsigargin treatment. It was shown that FAM134B overexpression itself does not suffice to induce an ER stress response (see Figure 4.23). However, abundant FAM134B protein might affect the influence of ER stress response if these cells are treated with a stress inducer. This hypothesis was tested by semi-quantitative RT-PCR experiment following the treatment of Huh7-FAM134B and Huh7-Control cells with 2 μM thapsigargin for 48 hours.

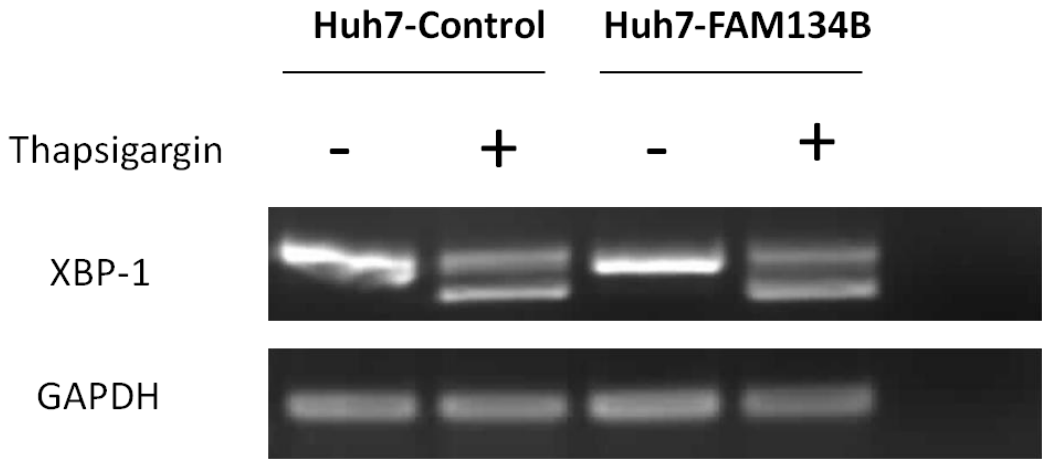

Figure 4.36: FAM134B increases the intensity of UPR following thapsigargin treatment

As seen in Figure 4.36, thapsigargin treatment to FAM134B overexpressing Huh7 cells brings about increased activation of XBP-1 transcription factor compared to Huh7-Control cells, detected by more intense sXBP-1 band. This is at least a clue about the differential activation of IRE1 branch of UPR in the presence of abundant FAM134B protein. Hence, FAM134B overexpressing cells might trigger stronger UPR signaling, eventually leading to amplified cellular response in terms of apoptosis and proliferation. This hypothesis is further supported by the result showing that eIF2α phosphorylation is more intense in Huh7-FAM134B cells compared to Huh7-Control cells (see Figure 4.30).

5. DISCUSSION AND CONCLUSION

This study primarily focused on the characterization of FAM134B in the contexts of hepatocellular carcinoma and endoplasmic reticulum stress. Starting from the originating point that FAM134B was found to be associated with senescence response (Ozturk et al. unpublished data), its relationships between replicative senescence, premature senescence, and endoplasmic reticulum stress were aimed to be experimented.

5.1 FAM134B in the context of senescence

After it was shown that immortal Huh7 HCC cells can be reprogrammed into spontaneous replicative senescence (Ozturk et al., 2006), the idea that tumorigenesis might be inhibited through induction of such a senescence phenotype became more plausible. On the other hand, analysis of significantly upregulated gene in response to spontaneous replicative senescence resulted in identification of FAM134B (Ozturk et al., unpublished data). First experiments on the identification of the relationship between FAM134B and replicative senescence came up with the understanding that FAM134B itself might not be a cause of senescence induction, detected by overexpression analysis (Tasdemir et al., unpublished data). Therefore, FAM134B is possibly associated with the senescence phenotype acquired as a result of spontaneous senescence response (Ozturk et al., 2006). However, in this study we aimed to find out if there is a direct correlation with the senescence phenotype of Huh7 cells and FAM134B expression. Thence, a possible change in FAM134B expression was tested in response to induction of a different type of senescence: premature senescence.

Experiments on induction of premature senescence by adriamycin or TGF-β revealed that FAM134B expression detected to be upregulated in spontaneous replicative senescence is not directly associated with the senescence phenotype. Acquiring premature senescence by adriamycin treatment does not cause a significant change in

FAM134B expression. Additionally, induction of premature senescence by TGF-β treatment in Huh7 cells resulted in repression of FAM134B expression. These results firstly indicated that upregulation of FAM134B expression in replicative senescence of Huh7 is not related to the senescence phenotype, instead, possibly another cellular response appeared at this stage might have caused an increased FAM134B expression in these spontaneously replicative senescent clones of Huh7. Secondly, according to these results FAM134B is somehow a target of TGF-β signaling. TGF-β treatment resulted in a considerable decrease in FAM134B expression. This can be explained by a mechanism involving TGF-β pathway elements and control of FAM134B expression.

On the other hand, this study provided the significant observations that FAM134B is associated with ER stress. Therefore, another explanation for the upregulation of FAM134B gene expression in spontaneous replicative senescence might be linked to stressed ER and activation of UPR in senescent clones. It has been known that chaperones and folding enzymes are negatively affected during aging, may be resulting in promotion of stress response (Naidoo, 2009). Because cellular senescence is associated with aging, increase in FAM134B expression might be linked to the dysregulated ER function as a result of aging. In addition, possibly not premature senescent cells but cells in replicative senescent stage obtain a characteristic of senescence associated secretory phenotype, causing secretion of massive amounts of cytokines (Davalos et al., 2010). Secretion of these cytokines demands their production and modification of in the ER, consequently leading to accumulation of a heavy load in the ER and triggering UPR as a result.

5.2 Differential expression of FAM134B in tissues

Our studies on detection of FAM134B protein levels in organs resulted in detection of FAM134B protein primarily in the brain, and also in liver and testis (see Figure 4.11). This was not an unexpected result due to the fact that studies of Kurth et al. showed that FAM134B is predominantly expressed in neurons, detected by in situ hybridization (Kurth et al., 2009). Neurons and hepatocytes are cell types that are kept at quiescent G0 stage under normal circumstances. Together with these result,

especially considering neurons and hepatocytes, it is likely to interpret that FAM134B expression is mainly observed in cells with low proliferative capacity. One other significant support for this idea is the increased expression of FAM134B in replicative senescent clones of a cancer cell line, Huh7. As Huh7 cells lose their proliferative capacity, FAM134B expression is increased, in a concurrence with the high expression and low proliferative capacity in neurons and hepatocytes.

5.3 Characterization of FAM134B in the context of hepatocellular carcinoma

Characterization of FAM134B in the context of hepatocellular carcinoma refers to two different implications. One is characterization of FAM134B in the pathogenesis and distinct stages of HCC progression in vivo, and the other one is characterization in term of the differentiation status of HCC cell lines in vitro.

Protein level analysis of FAM134B in the tissues (see Figure 4.11), and expression analysis in Chen and Wurmbach microarray data revealed that FAM134B is expressed in the normal liver (see Figures 4.12 and 4.13) (Chen et al., 2002; Wurmbach et al., 2007). However, according to these microarray data, expression of FAM134B is decreased as molecular pathogenesis of HCC progresses. In other words, expression is greater in normal liver than in cirrhotic liver and dysplasia, whereas, expression is lower in HCC compared to previous stages of pathogenesis. On the other hand, expression is also decreased in late stages of HCC, compared to early stages of HCC. These data propose that FAM134B is not associated with the carcinogenic characteristic of HCC. In fact, previous findings showing that FAM134B expression is associated with low proliferative capacity, are directly correlated with this statement.

At the cellular level, our experiments showed that especially isoform 1 of FAM134B is expressed in poorly-differentiated cell lines, but not in well-differentiated cell lines, except in Hep40 (see Figures 4.8 and 4.9). This data does not seem to be correlated with the data obtained from molecular pathogenesis stages of HCC. Well-differentiated HCC cell lines are considered as epithelial or hepatocyte like cell lines

characterized as being positive for hepatocyte and epithelial markers; whereas, poorly-differentiated cell lines are categorized as mesenchymal-like cell lines that are positive for mesenchymal markers and have more metastatic characteristics (Yuzugullu et al., 2009). Therefore, poorly-differentiated cells lines are expected to represent late stages of hepatocarcinogenesis in vitro, while well-differentiated cells represent early stages of hepatocellular carcinoma. When these characteristics are taken into consideration, it is possible to state that in vivo and in vitro data are contradictory.

Even though poorly-differentiated HCC cell lines are expected to represent later stages of HCC and they are not characterized with low proliferative capacity, FAM134B mRNA and protein levels are high in these cells. In this study, this contradiction was aimed to be solved by explaining this case not as a matter of differentiation or stage of pathogenesis, but in terms of possible other cellular factors affecting these cells. As a matter of fact, what was observed is that most of the poorly-differentiated cell lines have an active ER stress response at a basal level under untreated conditions (see Figures 4.20 and 4.21). Detection of basal spliced XBP-1 in some of the poorly-differentiated cells as well as the presence of basal level PERK and eIF2α phosphorylations are the indicators of, at least to some extent, active PERK and IRE1 branches of UPR in these cells. Our results showing that ER stress induction results in upregulation of FAM134B expression possibly serves for the most reasonable explanation for the link between high FAM134B expression and active ER stress response in these cells.

5.4 Describing FAM134B in the context of ER stress

Previous studies resulted in the detection of FAM134B localization on the endoplasmic reticulum membrane, co-localized with calnexin (Tasdemir et al., unpublished data); or on the cis-Golgi membrane, co-localized with giantin (Kurth et al., 2009). Considering these findings, FAM134B was aimed to be identified in terms of its response to ER stress. Thus, our results showed that induction of ER stress with diverse stress inducers, such as tunicamycin, dithiothreitol, or thapsigargin, provides increased FAM134B expression in Huh7 cells.

Increase in FAM134B expression in response to ER stress induction has also provided further support for other hypotheses. As being an ER stress responsive gene, its high expression pattern in poorly-differentiated HCC cell lines could be, and increased expression in replicative senescent Huh7 cells is likely to be explained by the presence of active ER stress response in these cells. Put in another way, the presence of FAM134B expression in these cells are due to the presence of an active ER stress response at basal level.

FAM134B was detected to be associated with ER stress response. However, increased expression of FAM134B was identified only as a result of ER stress induction. Overexpression of FAM134B did not result in triggering a UPR in Huh7 cells (see Figure 4.23). This shows that FAM134B is not a key factor in signal transduction from stressed ER to the downstream elements of UPR, unlike IRE1, ATF6 and PERK. However, as being an ER stress responsive gene, its expression is possibly regulated at transcription level by one of the downstream elements of UPR signaling.

At the transcription level, FAM134B is regulated by UPR, showed by increased expression in response to ER stress induction. However, western blot experiments provided interesting results on protein levels of FAM134B in response to ER stress induction. According to these results, FAM134B protein levels are significantly upregulated in response to ER stress induction only in cells with high FAM134B protein levels. For instance, in Snu387 cell line, with high FAM134B protein level, tunicamycin treatment results in an increase of FAM134B protein level (see Figure 4.17). However, tunicamycin treatment to Huh7 or HeLa cells does not cause an increase in protein levels of FAM134B in these cells (see Figure 4.18). This observation is further supported by another western blot result showing that thapsigargin treatment results in a drastic increase in the protein level of FAM134B in FAM134B overexpressing Huh7 clone CT1-14, while there is only a slight increase in protein level of FAM134B in Huh7 control clone CMV10-11 (see Figure 4.30). These results might indicate that FAM134B is involved in a type of auto-regulation loop, providing amplified protein production only in the case that the initial protein level is substantially high. Another possibility is that apart from control

of FAM134B at the transcription level, FAM134B protein levels are further controlled at the protein degradation level, which is inhibited when an ER stress is induced in a cell, resulting in the accumulation of FAM134B protein in response to ER stress.

5.5 FAM134B and morphology of Huh7 cells

In in vitro culture, FAM134B overexpressing Huh7 cells were detected in an altered morphology, having spiky shapes on the cell membrane, a bit elongated cytoplasm and slightly separated colonization, in comparison with the parental Huh7 and control Huh7 cells. These phenotypic changes seemed to be associated with mesenchymal-like characteristics. Therefore, this hypothesis was tested by detection of a mesenchymal marker vimentin by immunofluorescence and semi-quantitative RT-PCR experiments (see Figures 4.24 and 4.25). In addition, previously reported data of Ulianich et al., showing that ER stress induction by tunicamycin or thapsigargin in thyroid epithelial cells triggers EMT of these cells, was also tested using epithelial-like HCC cell line Huh7 (Ulianich et al., 2008). However, results revealed that there is no significant change in vimentin expression, when the cell overexpresses FAM134B. This result suggested that the cause of different cellular morphology of FAM134B overexpressing Huh7 cells is possibly due to unexpected changes during production of these stable clones.

5.6 FAM134B and autophagic response

It has been known that induction of ER stress leads to activation of autophagic response (Qin et al., 2010). In this study, firstly, we detected induction of autophagy in Huh7 HCC cells in response to tunicamycin treatment. Results showed that tunicamycin treatment for 72 hours triggers an autophagic response, observed by conversion of the autophagy marker LC3B, from its LC3B-I form to LC3B-II form (see Figure 4.26). Since FAM134B is responsive to ER stress induction, a possible relationship between FAM134B and autophagic response was tested. Comparison of autophagy in FAM134B overexpressing Huh7 clones and their control counterparts showed that FAM134B overexpression does not affect autophagy in Huh7 cells.

However, this experiment was done under untreated conditions. Therefore, rate of autophagic response in FAM134B overexpressing cells might change in response to ER stress induction by tunicamycin or thapsigargin.

5.7 FAM134B as a mediator of ER stress induced apoptosis

After detecting FAM134B as an ER stress responsive gene, we searched for a role of FAM134B in the context of ER stress response in Huh7 HCC cells. Thapsigargin and tunicamycin induced apoptosis responses of FAM134B overexpressing Huh7 cells and Huh7-Control cells were detected by western blot experiment, showing that Huh7-FAM134B cells are more sensitive to the same tunicamycin or thapsigargin treatments (see Figures 4.30 and 4.33). Propidium iodide based cell cycle analysis following these treatments also indicated significant differences between these clones in terms of rate of apoptotic cells in the population (see Figures 4.31 and 4.34). On the other hand, it was shown that triggering ER stress in Huh7 cells impairs cell proliferation (see Figure 4.28). Treatment of Huh7-FAM134B clones with tunicamycin or thapsigargin resulted in increased loss of proliferative capacity in these cells, in comparison with the Huh7-Control cells (see Figures 4.32 and 4.35). All these results pointed out a significant role of FAM134B protein in cells' response to ER stress induction with chemicals.

FAM134B increases sensitivity to ER stress induced apoptosis of Huh7 cells, at least when ER stress is induced by tunicamycin or thapsigargin. This might be further supported by apoptosis induction with other ER stress inducers. However, being sensitive to more than one chemical suggests that the mediator role of FAM134B in this response is not associated with a particular type of ER stress, such as calcium ion deprivation induced by thapsigargin, or lack of glycoprotein synthesis induced by tunicamycin. Therefore, it is possible to state that FAM134B has a general role affecting the response of the cell to the stressed ER. Increased stress response in FAM134B overexpressing Huh7 cells is further supported by detection of increased XBP-1 splicing following thapsigargin treatment (see Figure 4.36). This result suggested that, at least activation of IRE1 branch of UPR might be influenced by the abundance of FAM134B protein. However, not only IRE1 arm of UPR, but also

activation of the PERK arm of UPR is also affected by the overexpression of FAM134B protein in Huh7 cells, detected by increased eIF2α phosphorylation in FAM134B overexpressing cell compared to control cells (see Figure 4.30).

Increased sensitivity to ER stress in FAM134B overexpressing cells might be explained by its possible function in ER structure. FAM134B structure is predicted to have two hydrophobic segments flanked by hydrophilic loop, similar to the structure of reticulon proteins (Kurth et al., 2009; Voeltz et al., 2006). Reticulons undertake a role in shaping the ER membrane by inserting their hydrophobic domains into the ER membrane, shaping the curvature of ER membrane (Voeltz et al., 2006). On the other hand, studies of Shuck et al. showed that UPR signaling controls the expansion of ER membrane via generation of ER sheets. Furthermore, expansion of ER membrane relieves the stress in the ER independent of chaperone protein levels (Schuck et al., 2009). Based on these findings, one hypothesis is that after induction of ER stress with tunicamycin or thapsigargin, cells try to expand their ER membrane and increase ER size in order to relieve the stress in the ER. However, overexpression of a reticulon-like protein FAM134B in the ER membrane might inhibit expansion of ER size following stress induction, thereby preventing the alleviation of the ER stress. This is likely to result in sensing increased ER stress. This might also explain why Huh7-FAM134B cells are more sensitive to ER stress induced apoptosis. Due to the prevention of ER size expansion, UPR response is amplified, triggering more severe stress response and eventually apoptosis.

Another hypothesis might be related to the direct involvement of some reticulon proteins in apoptosis. Studies of Tagami et al. suggested that Reticulon 4B (RTN4B) protein is able to interact with anti-apoptotic protein Bcl-2. This interaction results in the localization of Bcl-2 on the ER membrane, resulting in the prevention of its anti-apoptotic activity (Tagami et al., 2000). As being a reticulon-like protein, FAM134B might have such a function on the ER membrane, causing accumulation of Bcl-2 protein on the ER membrane, thereby, inhibiting its anti-apoptotic activity on mitochondria. In this case, FAM134B overexpression itself might not be sufficient to trigger apoptosis; whereas, the help of an ER stress inducer and prolonged exposure might facilitate the apoptotic response in FAM134B overexpressing cells.

5.8 FAM134B in the pathogenesis of HCC

The basis of HCC is the accumulation of excess tissue damage in hepatocytes, and later on, the acquisition of proliferation capacity. Our results showed that FAM134B is associated with ER stress induced apoptosis, and that FAM134B is expressed in normal liver. When these are taken into consideration, FAM134B might have a role in the accumulation of tissue damage in liver, especially in response to the ER stress. Therefore, FAM134B might be linked to the pathogenesis of hepatocellular carcinoma.

It is known that at least two of the major risk factors of hepatocellular carcinoma are associated with ER stress. One of them is the hepatitis C virus infection. HCV infection is a major cause of chronic hepatitis, which is likely to result in cirrhosis and HCC. HVC infection causes abundant expression of NS5A in the ER, leading to ER stress and activation of STAT-3 and NF-κB in hepatocytes (Waris et al., 2002). Another risk factor, diabetes, is also associated with ER stress in the liver. The link is primarily due to the accumulation of free fatty acids in the liver and acquisition of insulin resistance in the liver (Maclaren et al., 2007). Studies of Ozcan et al. showed that ER stress is a key characteristic of insulin resistance and type 2 diabetes at both cellular and organismal levels (Ozcan et al., 2004). Taken together, our results indicating that FAM134B is a factor in ER stress induced apoptosis can be interpreted in a way that FAM134B contributes to the liver pathogenesis during the early stages of HCC. Even though HCV and diabetes are the main factors resulting in ER stress in hepatocytes, hepatocytes expressing FAM134B might become more susceptible for accumulation of tissue damage at these stages, due to the fact that FAM134B amplifies the apoptotic response in ER stress conditions.

6. FUTURE PERSPECTIVES

This study has primarily revealed that FAM134B is a significant ER stress response gene, and it is associated with apoptosis response resulting from the ER stress. Even though results given in this study have provided preliminary data for the establishment of this information, further studies are still required to support the hypotheses suggested here, and to further examine the role of FAM134B in the context of ER stress and hepatocellular carcinoma.

First of all, the findings showing that FAM134B is an ER stress response gene could be additionally supported by inducing ER stress with other chemicals such as Brefeldin A. On the other hand, this study only involves experiments with thapsigargin and tunicamycin induced apoptosis detection in Huh7 cells. Apoptosis induction and sensitivity to ER stress induced apoptosis experiments in Huh7-FAM134B and Huh7-Control cells could be done using different ER stress inducers such as DTT and Brefeldin A. Moreover, apoptosis sensitivity could be further detected by other apoptosis detection methods, such as TUNEL or Annexin V immunofluorescence assays.

Furthermore, studies on ER stress related characterization of FAM134B should be supported by knock down experiments. This might involve downregulation of FAM134B expression by shRNA or siRNA approaches. The fact that FAM134B increases the sensitivity to ER stress induced apoptosis should be shown in terms of its vice versa effect, when FAM134B protein level is decreased in a cell line, which has a high endogenous FAM134B protein level.

FAM134B is an ER or cis-Golgi membrane protein. Its knockdown results in reduced cis-Golgi size in N2a cells (Kurth et al., 2009). These findings suggest that FAM134B might have a structural role in endoplasmic reticulum membrane too. This hypothesis could be tested by knock down studies of FAM134B, followed by detection of changes in ER size by confocal microscopy. On the other hand, ER size changes should be experimented in these cells in response to ER stress induction.

Besides, changes in the ER size of FAM134B overexpressing and control Huh7 cells should be detected following the ER stress induction by thapsigargin or tunicamycin. Studies of Schuck et al. showed that alleviation of ER stress in response to chemical treatment is also related to the expansion of ER size (Schuck et al., 2009). If FAM134B is somehow able to inhibit the ER membrane expansion, it is possible to detect a deficiency in expansion of ER size in FAM13B4 overexpressing Huh7 cells.

FAM134B is a reticulon like protein. It was shown that reticulon 4 B protein has a role of binding to Bcl-2 anti-apoptotic protein, causing it to localize on the ER membrane and inhibiting its anti-apoptotic function on the mitochondria (Tagami et al., 2000). FAM134B may also have a similar function. Therefore, interating partners of FAM134B should be detected by immunoprecipitation experiments. On the other hand, detection of interacting partner may result in identification of a differetn role of FAM134B on the ER, such as transport between ER and Golgi.

Our results showed that FAM134B is expressed in normal liver. And, according to the results of other studies, FAM134B expression decreases during the pathological stages of HCC in the liver (see Figures 4.12 and 4.13). These findings should be further supported by detection of FAM134B in the tissue samples of different pathological stages. These experiments can be done by immunohistochemistry or by western blot techniques in order to detect the changes at the protein level.

Mutation in FAM134B gene is associated with a neurodegenrative disease (Kurth et al., 2009). However, in vivo effects of FAM134B deficiency has not been experimented in mouse models. Therefore, it might be worth to study mouse knock out model of FAM134B and its relationship with the development of liver pathogenesis. According to the results we obtained in our studies, FAM134B knock out mouse might be less susceptible for development of HCC under the effect of same risk factors, such a HCV infection.

Here, we only used in vitro HCC model in this study. Similar effects of FAM134B might be associated with the other cancer types too. Therefore, such overexpression analysis and also knock down analysis could be done in different cancer types.

7. REFERENCES

Adams, L.A., and Angulo, P. (2005). Recent concepts in non-alcoholic fatty liver disease. Diabet Med *22*, 1129-1133.

Ahn, J., and Flamm, S.L. (2004). Hepatocellular carcinoma. Dis Mon *50*, 556-573.

Badvie, S. (2000). Hepatocellular carcinoma. Postgrad Med J *76*, 4-11.

Barth, S., Glick, D., and Macleod, K.F. (2010). Autophagy: assays and artifacts. J Pathol *221*, 117-124.

Beasley, R.P., Hwang, L.Y., Lin, C.C., and Chien, C.S. (1981). Hepatocellular carcinoma and hepatitis B virus. A prospective study of 22 707 men in Taiwan. Lancet *2*, 1129-1133.

Bertolotti, A., Zhang, Y., Hendershot, L.M., Harding, H.P., and Ron, D. (2000). Dynamic interaction of BiP and ER stress transducers in the unfolded-protein response. Nat Cell Biol *2*, 326-332.

Block, T.M., Mehta, A.S., Fimmel, C.J., and Jordan, R. (2003). Molecular viral oncology of hepatocellular carcinoma. Oncogene *22*, 5093-5107.

Bowen, D.G., and Walker, C.M. (2005). Adaptive immune responses in acute and chronic hepatitis C virus infection. Nature *436*, 946-952.

Bressac, B., Kew, M., Wands, J., and Ozturk, M. (1991). Selective G to T mutations of p53 gene in hepatocellular carcinoma from southern Africa. Nature *350*, 429-431.

Bruix, J., and Sherman, M. (2005). Management of hepatocellular carcinoma. Hepatology *42*, 1208-1236.

Calfon, M., Zeng, H., Urano, F., Till, J.H., Hubbard, S.R., Harding, H.P., Clark, S.G., and Ron, D. (2002). IRE1 couples endoplasmic reticulum load to secretory capacity by processing the XBP-1 mRNA. Nature *415*, 92-96.

Campisi, J. (2005). Senescent cells, tumor suppression, and organismal aging: good citizens, bad neighbors. Cell *120*, 513-522.

Chen, X., Cheung, S.T., So, S., Fan, S.T., Barry, C., Higgins, J., Lai, K.M., Ji, J., Dudoit, S., Ng, I.O., *et al.* (2002). Gene expression patterns in human liver cancers. Mol Biol Cell *13*, 1929-1939.

Chiang, D.Y., Villanueva, A., Hoshida, Y., Peix, J., Newell, P., Minguez, B., LeBlanc, A.C., Donovan, D.J., Thung, S.N., Sole, M., *et al.* (2008a). Focal gains of VEGFA and molecular classification of hepatocellular carcinoma. Cancer Res *68*, 6779-6788.

Chiang, P.C., Hsu, J.L., Yeh, T.C., Pan, S.L., and Guh, J.H. (2008b). Elucidation of susceptible factors to endoplasmic reticulum stress-mediated anticancer activity in human hepatocellular carcinoma. Naunyn Schmiedebergs Arch Pharmacol *377*, 167-177.

Cox, J.S., Shamu, C.E., and Walter, P. (1993). Transcriptional induction of genes encoding endoplasmic reticulum resident proteins requires a transmembrane protein kinase. Cell *73*, 1197-1206.

Cox, J.S., and Walter, P. (1996). A novel mechanism for regulating activity of a transcription factor that controls the unfolded protein response. Cell *87*, 391-404.

Credle, J.J., Finer-Moore, J.S., Papa, F.R., Stroud, R.M., and Walter, P. (2005). On the mechanism of sensing unfolded protein in the endoplasmic reticulum. Proc Natl Acad Sci U S A *102*, 18773-18784.

Davalos, A.R., Coppe, J.P., Campisi, J., and Desprez, P.Y. (2010). Senescent cells as a source of inflammatory factors for tumor progression. Cancer Metastasis Rev *29*, 273-283.

Davila, J.A., Morgan, R.O., Shaib, Y., McGlynn, K.A., and El-Serag, H.B. (2005). Diabetes increases the risk of hepatocellular carcinoma in the United States: a population based case control study. Gut *54*, 533-539.

Denmeade, S.R., and Isaacs, J.T. (2005). The SERCA pump as a therapeutic target: making a "smart bomb" for prostate cancer. Cancer Biol Ther *4*, 14-22.

Diehl, A.M. (2005). Recent events in alcoholic liver disease V. effects of ethanol on liver regeneration. Am J Physiol Gastrointest Liver Physiol *288*, G1-6.

Faloppi, L., Scartozzi, M., Maccaroni, E., Di Pietro Paolo, M., Berardi, R., Del Prete, M., and Cascinu, S. (2011). Evolving strategies for the treatment of hepatocellular carcinoma: from clinical-guided to molecularly-tailored therapeutic options. Cancer Treat Rev *37*, 169-177.

Farazi, P.A., and DePinho, R.A. (2006). Hepatocellular carcinoma pathogenesis: from genes to environment. Nat Rev Cancer *6*, 674-687.

Farazi, P.A., Glickman, J., Jiang, S., Yu, A., Rudolph, K.L., and DePinho, R.A. (2003). Differential impact of telomere dysfunction on initiation and progression of hepatocellular carcinoma. Cancer Res *63*, 5021-5027.

Farrell, G.C., and Larter, C.Z. (2006). Nonalcoholic fatty liver disease: from steatosis to cirrhosis. Hepatology *43*, S99-S112.

Ferber, M.J., Montoya, D.P., Yu, C., Aderca, I., McGee, A., Thorland, E.C., Nagorney, D.M., Gostout, B.S., Burgart, L.J., Boix, L., *et al.* (2003). Integrations of the hepatitis B virus (HBV) and human papillomavirus (HPV) into the human telomerase reverse transcriptase (hTERT) gene in liver and cervical cancers. Oncogene *22*, 3813-3820.

Fornari, F.A., Randolph, J.K., Yalowich, J.C., Ritke, M.K., and Gewirtz, D.A. (1994). Interference by doxorubicin with DNA unwinding in MCF-7 breast tumor cells. Mol Pharmacol *45*, 649-656.

Gomaa, A.I., Khan, S.A., Toledano, M.B., Waked, I., and Taylor-Robinson, S.D. (2008). Hepatocellular carcinoma: epidemiology, risk factors and pathogenesis. World J Gastroenterol *14*, 4300-4308.

Groopman, J.D., Scholl, P., and Wang, J.S. (1996). Epidemiology of human aflatoxin exposures and their relationship to liver cancer. Prog Clin Biol Res *395*, 211-222.

Harding, H.P., Zhang, Y., and Ron, D. (1999). Protein translation and folding are coupled by an endoplasmic-reticulum-resident kinase. Nature *397*, 271-274.

Haze, K., Yoshida, H., Yanagi, H., Yura, T., and Mori, K. (1999). Mammalian transcription factor ATF6 is synthesized as a transmembrane protein and activated by proteolysis in response to endoplasmic reticulum stress. Mol Biol Cell *10*, 3787-3799.

Hitomi, J., Katayama, T., Eguchi, Y., Kudo, T., Taniguchi, M., Koyama, Y., Manabe, T., Yamagishi, S., Bando, Y., Imaizumi, K., *et al.* (2004). Involvement of

caspase-4 in endoplasmic reticulum stress-induced apoptosis and Abeta-induced cell death. J Cell Biol *165*, 347-356.

Hussain, S.P., Schwank, J., Staib, F., Wang, X.W., and Harris, C.C. (2007). TP53 mutations and hepatocellular carcinoma: insights into the etiology and pathogenesis of liver cancer. Oncogene *26*, 2166-2176.

Ji, C., and Kaplowitz, N. (2006). ER stress: can the liver cope? J Hepatol *45*, 321-333.

Kozutsumi, Y., Segal, M., Normington, K., Gething, M.J., and Sambrook, J. (1988). The presence of malfolded proteins in the endoplasmic reticulum signals the induction of glucose-regulated proteins. Nature *332*, 462-464.

Kurth, I., Pamminger, T., Hennings, J.C., Soehendra, D., Huebner, A.K., Rotthier, A., Baets, J., Senderek, J., Topaloglu, H., Farrell, S.A., *et al.* (2009). Mutations in FAM134B, encoding a newly identified Golgi protein, cause severe sensory and autonomic neuropathy. Nat Genet *41*, 1179-1181.

Lee, K., Tirasophon, W., Shen, X., Michalak, M., Prywes, R., Okada, T., Yoshida, H., Mori, K., and Kaufman, R.J. (2002). IRE1-mediated unconventional mRNA splicing and S2P-mediated ATF6 cleavage merge to regulate XBP1 in signaling the unfolded protein response. Genes Dev *16*, 452-466.

Lei, K., and Davis, R.J. (2003). JNK phosphorylation of Bim-related members of the Bcl2 family induces Bax-dependent apoptosis. Proc Natl Acad Sci U S A *100*, 2432-2437.

Li, B., Yi, P., Zhang, B., Xu, C., Liu, Q., Pi, Z., Xu, X., Chevet, E., and Liu, J. (2011). Differences in endoplasmic reticulum stress signalling kinetics determine cell survival outcome through activation of MKP-1. Cell Signal *23*, 35-45.

Liu, C.J., and Kao, J.H. (2007). Hepatitis B virus-related hepatocellular carcinoma: epidemiology and pathogenic role of viral factors. J Chin Med Assoc *70*, 141-145.

Liu, C.Y., Xu, Z., and Kaufman, R.J. (2003). Structure and intermolecular interactions of the luminal dimerization domain of human IRE1alpha. J Biol Chem *278*, 17680-17687.

Llovet, J.M., and Bruix, J. (2008). Molecular targeted therapies in hepatocellular carcinoma. Hepatology *48*, 1312-1327.

Llovet, J.M., Burroughs, A., and Bruix, J. (2003). Hepatocellular carcinoma. Lancet *362*, 1907-1917.

Ma, K., Vattem, K.M., and Wek, R.C. (2002). Dimerization and release of molecular chaperone inhibition facilitate activation of eukaryotic initiation factor-2 kinase in response to endoplasmic reticulum stress. J Biol Chem *277*, 18728-18735.

Maclaren, N.K., Gujral, S., Ten, S., and Motagheti, R. (2007). Childhood obesity and insulin resistance. Cell Biochem Biophys *48*, 73-78.

Marciniak, S.J., Yun, C.Y., Oyadomari, S., Novoa, I., Zhang, Y., Jungreis, R., Nagata, K., Harding, H.P., and Ron, D. (2004). CHOP induces death by promoting protein synthesis and oxidation in the stressed endoplasmic reticulum. Genes Dev *18*, 3066-3077.

McCullough, K.D., Martindale, J.L., Klotz, L.O., Aw, T.Y., and Holbrook, N.J. (2001). Gadd153 sensitizes cells to endoplasmic reticulum stress by down-regulating Bcl2 and perturbing the cellular redox state. Mol Cell Biol *21*, 1249-1259.

McKillop, I.H., and Schrum, L.W. (2005). Alcohol and liver cancer. Alcohol *35*, 195-203.

Michielsen, P.P., Francque, S.M., and van Dongen, J.L. (2005). Viral hepatitis and hepatocellular carcinoma. World J Surg Oncol *3*, 27.

Mori, K., Kawahara, T., Yoshida, H., Yanagi, H., and Yura, T. (1996). Signalling from endoplasmic reticulum to nucleus: transcription factor with a basic-leucine zipper motif is required for the unfolded protein-response pathway. Genes Cells *1*, 803-817.

Naidoo, N. (2009). ER and aging-Protein folding and the ER stress response. Ageing Res Rev *8*, 150-159.

Nakagawa, T., and Yuan, J. (2000). Cross-talk between two cysteine protease families. Activation of caspase-12 by calpain in apoptosis. J Cell Biol *150*, 887-894.

Nakagawa, T., Zhu, H., Morishima, N., Li, E., Xu, J., Yankner, B.A., and Yuan, J. (2000). Caspase-12 mediates endoplasmic-reticulum-specific apoptosis and cytotoxicity by amyloid-beta. Nature *403*, 98-103.

Ozcan, U., Cao, Q., Yilmaz, E., Lee, A.H., Iwakoshi, N.N., Ozdelen, E., Tuncman, G., Gorgun, C., Glimcher, L.H., and Hotamisligil, G.S. (2004). Endoplasmic reticulum stress links obesity, insulin action, and type 2 diabetes. Science *306*, 457-461.

Ozturk, M. (1991). p53 mutation in hepatocellular carcinoma after aflatoxin exposure. Lancet *338*, 1356-1359.

Ozturk, M. (1999). Genetic aspects of hepatocellular carcinogenesis. Semin Liver Dis *19*, 235-242.

Ozturk, M., Arslan-Ergul, A., Bagislar, S., Senturk, S., and Yuzugullu, H. (2009). Senescence and immortality in hepatocellular carcinoma. Cancer Lett *286*, 103-113.

Ozturk, N., Erdal, E., Mumcuoglu, M., Akcali, K.C., Yalcin, O., Senturk, S., Arslan-Ergul, A., Gur, B., Yulug, I., Cetin-Atalay, R., *et al.* (2006). Reprogramming of replicative senescence in hepatocellular carcinoma-derived cells. Proc Natl Acad Sci U S A *103*, 2178-2183.

Paradis, V., Youssef, N., Dargere, D., Ba, N., Bonvoust, F., Deschatrette, J., and Bedossa, P. (2001). Replicative senescence in normal liver, chronic hepatitis C, and hepatocellular carcinomas. Hum Pathol *32*, 327-332.

Parfrey, H., Mahadeva, R., and Lomas, D.A. (2003). Alpha(1)-antitrypsin deficiency, liver disease and emphysema. Int J Biochem Cell Biol *35*, 1009-1014.

Parikh, S., and Hyman, D. (2007). Hepatocellular cancer: a guide for the internist. Am J Med *120*, 194-202.

Parkin, D.M., Bray, F., Ferlay, J., and Pisani, P. (2005). Global cancer statistics, 2002. CA Cancer J Clin *55*, 74-108.

Pietrangelo, A. (2009). Iron in NASH, chronic liver diseases and HCC: how much iron is too much? J Hepatol *50*, 249-251.

Qin, L., Wang, Z., Tao, L., and Wang, Y. (2010). ER stress negatively regulates AKT/TSC/mTOR pathway to enhance autophagy. Autophagy *6*, 239-247.

Rao, R.V., and Bredesen, D.E. (2004). Misfolded proteins, endoplasmic reticulum stress and neurodegeneration. Curr Opin Cell Biol *16*, 653-662.

Reaper, P.M., di Fagagna, F., and Jackson, S.P. (2004). Activation of the DNA damage response by telomere attrition: a passage to cellular senescence. Cell Cycle *3*, 543-546.

Ron, D., and Walter, P. (2007). Signal integration in the endoplasmic reticulum unfolded protein response. Nat Rev Mol Cell Biol *8*, 519-529.

Rutkowski, D.T., and Kaufman, R.J. (2004). A trip to the ER: coping with stress. Trends Cell Biol *14*, 20-28.

Schlaeger, C., Longerich, T., Schiller, C., Bewerunge, P., Mehrabi, A., Toedt, G., Kleeff, J., Ehemann, V., Eils, R., Lichter, P., *et al.* (2008). Etiology-dependent molecular mechanisms in human hepatocarcinogenesis. Hepatology *47*, 511-520.

Schuck, S., Prinz, W.A., Thorn, K.S., Voss, C., and Walter, P. (2009). Membrane expansion alleviates endoplasmic reticulum stress independently of the unfolded protein response. J Cell Biol *187*, 525-536.

Scorrano, L., Oakes, S.A., Opferman, J.T., Cheng, E.H., Sorcinelli, M.D., Pozzan, T., and Korsmeyer, S.J. (2003). BAX and BAK regulation of endoplasmic reticulum Ca2+: a control point for apoptosis. Science *300*, 135-139.

Senturk, S., Mumcuoglu, M., Gursoy-Yuzugullu, O., Cingoz, B., Akcali, K.C., and Ozturk, M. (2010). Transforming growth factor-beta induces senescence in hepatocellular carcinoma cells and inhibits tumor growth. Hepatology *52*, 966-974.

Shen, J., Chen, X., Hendershot, L., and Prywes, R. (2002). ER stress regulation of ATF6 localization by dissociation of BiP/GRP78 binding and unmasking of Golgi localization signals. Dev Cell *3*, 99-111.

Sherwood, S.W., Rush, D., Ellsworth, J.L., and Schimke, R.T. (1988). Defining cellular senescence in IMR-90 cells: a flow cytometric analysis. Proc Natl Acad Sci U S A *85*, 9086-9090.

Soussi, T. (2007). p53 alterations in human cancer: more questions than answers. Oncogene *26*, 2145-2156.

Stickel, F., and Hellerbrand, C. (2010). Non-alcoholic fatty liver disease as a risk factor for hepatocellular carcinoma: mechanisms and implications. Gut *59*, 1303-1307.

Sun, A.Y., Ingelman-Sundberg, M., Neve, E., Matsumoto, H., Nishitani, Y., Minowa, Y., Fukui, Y., Bailey, S.M., Patel, V.B., Cunningham, C.C., *et al.* (2001). Ethanol and oxidative stress. Alcohol Clin Exp Res *25*, 237S-243S.

Suruki, R.Y., Mueller, N., Hayashi, K., Harn, D., DeGruttola, V., Raker, C.A., Tsubouchi, H., and Stuver, S.O. (2006). Host immune status and incidence of hepatocellular carcinoma among subjects infected with hepatitis C virus: a nested case-control study in Japan. Cancer Epidemiol Biomarkers Prev *15*, 2521-2525.

Tagami, S., Eguchi, Y., Kinoshita, M., Takeda, M., and Tsujimoto, Y. (2000). A novel protein, RTN-XS, interacts with both Bcl-XL and Bcl-2 on endoplasmic reticulum and reduces their anti-apoptotic activity. Oncogene *19*, 5736-5746.

Tang, W.K., Chui, C.H., Fatima, S., Kok, S.H., Pak, K.C., Ou, T.M., Hui, K.S., Wong, M.M., Wong, J., Law, S., *et al.* (2007). Oncogenic properties of a novel gene JK-1 located in chromosome 5p and its overexpression in human esophageal squamous cell carcinoma. Int J Mol Med *19*, 915-923.

Tellinghuisen, T.L., and Rice, C.M. (2002). Interaction between hepatitis C virus proteins and host cell factors. Curr Opin Microbiol *5*, 419-427.

Thorgeirsson, S.S., and Grisham, J.W. (2002). Molecular pathogenesis of human hepatocellular carcinoma. Nat Genet *31*, 339-346.

Ulianich, L., Garbi, C., Treglia, A.S., Punzi, D., Miele, C., Raciti, G.A., Beguinot, F., Consiglio, E., and Di Jeso, B. (2008). ER stress is associated with dedifferentiation and an epithelial-to-mesenchymal transition-like phenotype in PC Cl3 thyroid cells. J Cell Sci *121*, 477-486.

Urano, F., Wang, X., Bertolotti, A., Zhang, Y., Chung, P., Harding, H.P., and Ron, D. (2000). Coupling of stress in the ER to activation of JNK protein kinases by transmembrane protein kinase IRE1. Science *287*, 664-666.

Vietri, M., Bianchi, M., Ludlow, J.W., Mittnacht, S., and Villa-Moruzzi, E. (2006). Direct interaction between the catalytic subunit of Protein Phosphatase 1 and pRb. Cancer Cell Int *6*, 3.

Voeltz, G.K., Prinz, W.A., Shibata, Y., Rist, J.M., and Rapoport, T.A. (2006). A class of membrane proteins shaping the tubular endoplasmic reticulum. Cell *124*, 573-586.

Waris, G., and Siddiqui, A. (2003). Regulatory mechanisms of viral hepatitis B and C. J Biosci *28*, 311-321.

Waris, G., Tardif, K.D., and Siddiqui, A. (2002). Endoplasmic reticulum (ER) stress: hepatitis C virus induces an ER-nucleus signal transduction pathway and activates NF-kappaB and STAT-3. Biochem Pharmacol *64*, 1425-1430.

Wei, M.C., Zong, W.X., Cheng, E.H., Lindsten, T., Panoutsakopoulou, V., Ross, A.J., Roth, K.A., MacGregor, G.R., Thompson, C.B., and Korsmeyer, S.J. (2001). Proapoptotic BAX and BAK: a requisite gateway to mitochondrial dysfunction and death. Science *292*, 727-730.

Wiemann, S.U., Satyanarayana, A., Tsahuridu, M., Tillmann, H.L., Zender, L., Klempnauer, J., Flemming, P., Franco, S., Blasco, M.A., Manns, M.P., *et al.* (2002).

Hepatocyte telomere shortening and senescence are general markers of human liver cirrhosis. FASEB J *16*, 935-942.

Wurmbach, E., Chen, Y.B., Khitrov, G., Zhang, W., Roayaie, S., Schwartz, M., Fiel, I., Thung, S., Mazzaferro, V., Bruix, J., *et al.* (2007). Genome-wide molecular profiles of HCV-induced dysplasia and hepatocellular carcinoma. Hepatology *45*, 938-947.

Xu, C., Bailly-Maitre, B., and Reed, J.C. (2005). Endoplasmic reticulum stress: cell life and death decisions. J Clin Invest *115*, 2656-2664.

Yamamoto, K., Ichijo, H., and Korsmeyer, S.J. (1999). BCL-2 is phosphorylated and inactivated by an ASK1/Jun N-terminal protein kinase pathway normally activated at G(2)/M. Mol Cell Biol *19*, 8469-8478.

Ye, J., Rawson, R.B., Komuro, R., Chen, X., Dave, U.P., Prywes, R., Brown, M.S., and Goldstein, J.L. (2000). ER stress induces cleavage of membrane-bound ATF6 by the same proteases that process SREBPs. Mol Cell *6*, 1355-1364.

Yoneda, T., Imaizumi, K., Oono, K., Yui, D., Gomi, F., Katayama, T., and Tohyama, M. (2001). Activation of caspase-12, an endoplastic reticulum (ER) resident caspase, through tumor necrosis factor receptor-associated factor 2-dependent mechanism in response to the ER stress. J Biol Chem *276*, 13935-13940.

Yoshida, H., Matsui, T., Yamamoto, A., Okada, T., and Mori, K. (2001). XBP1 mRNA is induced by ATF6 and spliced by IRE1 in response to ER stress to produce a highly active transcription factor. Cell *107*, 881-891.

Yoshida, H., Oku, M., Suzuki, M., and Mori, K. (2006). pXBP1(U) encoded in XBP1 pre-mRNA negatively regulates unfolded protein response activator pXBP1(S) in mammalian ER stress response. J Cell Biol *172*, 565-575.

Yu, M.W., Yeh, S.H., Chen, P.J., Liaw, Y.F., Lin, C.L., Liu, C.J., Shih, W.L., Kao, J.H., Chen, D.S., and Chen, C.J. (2005). Hepatitis B virus genotype and DNA level and hepatocellular carcinoma: a prospective study in men. J Natl Cancer Inst *97*, 265-272.

Yuzugullu, H., Benhaj, K., Ozturk, N., Senturk, S., Celik, E., Toylu, A., Tasdemir, N., Yilmaz, M., Erdal, E., Akcali, K.C., *et al.* (2009). Canonical Wnt signaling is antagonized by noncanonical Wnt5a in hepatocellular carcinoma cells. Mol Cancer *8*, 90.

Zhou, J., Liu, C.Y., Back, S.H., Clark, R.L., Peisach, D., Xu, Z., and Kaufman, R.J. (2006). The crystal structure of human IRE1 luminal domain reveals a conserved dimerization interface required for activation of the unfolded protein response. Proc Natl Acad Sci U S A *103*, 14343-14348.